British Geological Survey

Mineral Reconnaissance Programme

Gold in the Ochil Hills, Scotland

Department of Trade and Industry

MRP Report 116
Technical Report WF/91/1

Gold in the Ochil Hills, Scotland

J S Coats, M H Shaw, M J Gallagher,
M Armstrong, P G Greenwood,
B C Chacksfield, J P Williamson
and N J Fortey

BRITISH GEOLOGICAL SURVEY

Technical Report WF/91/1

Mineral Reconnaissance Programme Report 116

Gold in the Ochil Hills, Scotland

J S Coats, M H Shaw, M J Gallagher, M Armstrong, P G Greenwood, B C Chacksfield, J P Williamson and N J Fortey

Contributors

M N Ingham, A S Robertson, P H A Nancarrow, D J Bland, S Redwood and A D Evans

Authors

Geochemistry
J S Coats and M H Shaw

Geology
M J Gallagher and M Armstrong

Geophysics
P G Greenwood, B C Chacksfield and J P Williamson

Mineralogy
N J Fortey

Trace-element analysis
M N Ingham and A S Robertson

XRD and electron microprobe
P H A Nancarrow and D J Bland

Geology
S Redwood

Borehole geophysics
A D Evans

This report was prepared for the Department of Trade and Industry

Maps and diagrams in this report use topography based on Ordnance Survey mapping

Bibliographical reference

Coats, J S, Shaw, M H, Gallagher, M J, Armstrong, M, Greenwood, P G, Chacksfield, B C, Williamson, J P, and Fortey, N J. 1991. Gold in the Ochil Hills, Scotland. *British Geological Survey Technical Report* WF/91/1 (*BGS Mineral Reconnaissance Programme Report* 116).

Keyworth, Nottingham 1991

BRITISH GEOLOGICAL SURVEY

The full range of Survey publications is available through the Sales Desks at Keyworth and at Murchison House, Edinburgh, and in the BGS London Information Office in the Natural History Museum Earth Galleries. The adjacent bookshop stocks the more popular books for sale over the counter. Most BGS books and reports are listed in HMSO's Sectional List 45, and can be bought from HMSO and through HMSO agents and retailers. Maps are listed in the BGS Map Catalogue and the Ordnance Survey's Trade Catalogue, and can be bought from Ordnance Survey agents as well as from BGS.

The British Geological Survey carries out the geological survey of Great Britain and Northern Ireland (the latter as an agency service for the government of Northern Ireland), and of the surrounding continental shelf, as well as its basic research projects. It also undertakes programmes of British technical aid in geology in developing countries as arranged by the Overseas Development Administration.

The British Geological Survey is a component body of the Natural Environment Research Council.

Keyworth, Nottingham NG12 5GG
☎ Plumtree (06077) 6111 Telex 378173 BGSKEY G
Fax 06077-6602

Murchison House, West Mains Road, Edinburgh EH9 3LA
☎ 031-667 1000 Telex 727343 SEISED G
Fax 031-668 2683

London Information Office at the Natural History Museum Earth Galleries, Exhibition Road, South Kensington, London SW7 2DE
☎ 071-589 4090 Fax 071-584 8270
☎ 071-938 9056/57

19 Grange Terrace, Edinburgh EH9 2LF
☎ 031-667 1000 Telex 727343 SEISED G

St Just, 30 Pennsylvania Road, Exeter EX4 6BX
☎ Exeter (0392) 78312 Fax 0392-437505

Bryn Eithyn Hall, Llanfarian, Aberystwyth, Dyfed SY23 4BY
☎ Aberystwyth (0970) 611038 Fax 0970-624822

Windsor Court, Windsor Terrace, Newcastle upon Tyne NE2 4HB
☎ 091-281 7088 Fax 091-281 9016

Geological Survey of Northern Ireland, 20 College Gardens, Belfast BT9 6BS
☎ Belfast (0232) 666595 Fax 0232-662835

Maclean Building, Crowmarsh Gifford, Wallingford, Oxfordshire OX10 8BB
☎ Wallingford (0491) 38800 Telex 849365 HYDROL G
Fax 0491-25338

Parent Body
Natural Environment Research Council
Polaris House, North Star Avenue, Swindon, Wiltshire SN2 1EU
☎ Swindon (0793) 411500 Telex 444293 ENVRE G
Fax 0793-411501

Printed in England for the British Geological Survey by Saxon Printing Limited, Derby

CONTENTS

FIGURES

TABLES

SUMMARY

Mineral reconnaissance drainage sampling in the late 1970s identified gold in heavy mineral concentrates collected from a number of localities in the Ochil Hills. Subsequent detailed sampling of these localities showed that alluvial gold is present over a large area of the central Ochils and extends eastwards to the Firth of Tay. The most anomalous catchment, Borland Glen, near Glen Devon, was the focus for further integrated geological, geochemical, and geophysical studies.

The geology of Borland Glen comprises a series of Lower Devonian andesitic lavas and pyroclastics intruded by a diorite body and porphyry dykes. Minor hydrothermal alteration is visible at surface. A large induced polarisation anomaly was found near the watershed between Borland Glen and Coul Burn and was interpreted as a steep-sided zone of disseminated pyrite with associated hydrothermal alteration. Overburden sampling proved gold and mercury anomalies over the same area.

Seven boreholes were drilled to a maximum depth of 102 m to investigate the source of the IP and overburden geochemical anomalies. Intense hydrothermal alteration and brecciation were found to have affected the lavas and pyroclastics in the central, IP-anomalous zone and were accompanied by major pyritisation with associated minor base metal sulphides. Gold values in the drillcore reach a maximum of 505 ppb Au and it is concluded that the bedrock source of the alluvial gold has not been proved. However, the intense hydrothermal alteration in the setting of an evolved calc-alkaline volcanic complex is indicative of a large epithermal system, and a more fertile source may yet be discovered in the area. Other gold sources are indicated in the central Ochils and further detailed investigations are thought to be warranted.

INTRODUCTION

Mineral exploration carried out in 1976-7 by the British Geological Survey in the Kilmelford area of Argyll, Scotland led to the discovery of a mineralised, sub-volcanic, porphyry intrusion which had many of the characteristics of the copper-porphyry model (Ellis et al., 1977). The metal concentrations discovered in the boreholes at Kilmelford were of low economic potential and it was postulated that the cap or more mineralised, upper portion of the intrusion had been removed by erosion along with the cover of Devonian lavas. The Kilmelford intrusion and the similar Lagalochan body investigated a decade later (Harris et al., 1988 and Zhou, 1988) are both considered to have been covered by a pile of andesite lavas and formed as breccia pipes and subvolcanic intrusions, perhaps 1 km below the Lower Devonian ground surface.

After BGS had completed the work at Kilmelford, several other intrusive bodies in the Scottish Highlands were investigated for disseminated sulphide mineralisation. The intrusions at Garbh Achadh (Ellis et al., 1978), Tomnadashan (Fortey, 1980), Comrie, Ballachulish (Haslam and Kimbell, 1981) and Etive (Haslam and Cameron, 1985) were studied, but drilling was carried out only at Ballachulish. A search for similar late Caledonian intrusions at a higher structural level and covered by subaerial lavas was then initiated, using drainage geochemistry to detect outlying sulphide-bearing vein systems which might indicate the presence of buried, mineralised porphyry intrusions.

One area covered by this search was the Ochil Hills, an extensive area underlain by Lower Devonian lavas stretching from Stirling to the coast near St Andrews. Reconnaissance drainage sampling was completed in 1978 and detailed stream sediment sampling of a limited number of anomalies was carried out in the following year. At this time a number of boreholes were drilled in the Alva area (Hall et al., 1982) to study the silver-copper-cobalt mineralisation which had been mined from the seventeenth century to the nineteenth. The drainage survey and the limited follow-up did not discover any unusual concentrations of base metals; most of the copper and barium anomalies were related to known veins. As the emphasis of mineral exploration at that time was trending away from copper and molybdenum porphyry-style mineralisation, the exploration in the Ochils was discontinued.

During the 1978 drainage survey, heavy mineral concentrates were routinely examined in the field and the minerals identified noted on the field cards. The student field collectors were instructed on how to identify gold in the pan, and from the 818 concentrates collected in that survey 29 gold occurrences were noted on the field cards. These occurrences are listed with grid references in Appendix 1. At the time, gold was not one of the metals that formed part of the remit of the Mineral Reconnaissance Programme, but when exploration for gold started in 1986 two areas that had earlier been identified as having alluvial gold were put forward as exploration targets. One of them, the Aberfeldy - Glen Almond area, was already of active exploration interest to a mining company. The other was the Ochils (Figure 1), and a decision was taken to carry out a limited appraisal there in 1987. This report stems from that reappraisal and emphasises the value of recording and archiving information, such as gold occurrences in pans, that is outside the main remit of an exploration programme.

Gold had not previously been recorded from this part of the Ochil Hills, apart from one reference to gold at Alva given by Collins (1976), who does not quote the original source. Gold is recorded further west at the Airthry copper mine in a memorandum written by Robert Seton in the reign of James V of Scotland (quoted in Cochran-Patrick, 1878). The same source also notes the presence of cinnabar on the Perthshire side of the water of Alqwharry, which is probably Old Wharry Burn [28507020] west of Glen Devon. Local prospectors have known of alluvial gold occurrences in the central Ochils, but this information was kept relatively secret. A neighbouring area, the East Lomond Hills, also showed visible gold in the reconnaissance survey and there is a record of a "gold rush" here in 1852 quoted by Adamson (1979).

Details of the mineral workings in the Ochils are given by Francis et al. (1970), Dickie and Forster (1974) and Hall et al. (1982). The mineralisation is dominantly Ba-Cu-As-Ag-Pb-Co. The metals are thought to have been derived from the Lower Devonian lavas, and the hydrothermal fluids were of Carboniferous age (Robinson et al., 1989; Jassim et al., 1983). Parnell (1988) has recently recorded minor inclusions of mercury and silver-bismuth selenides in bitumens from Alva.

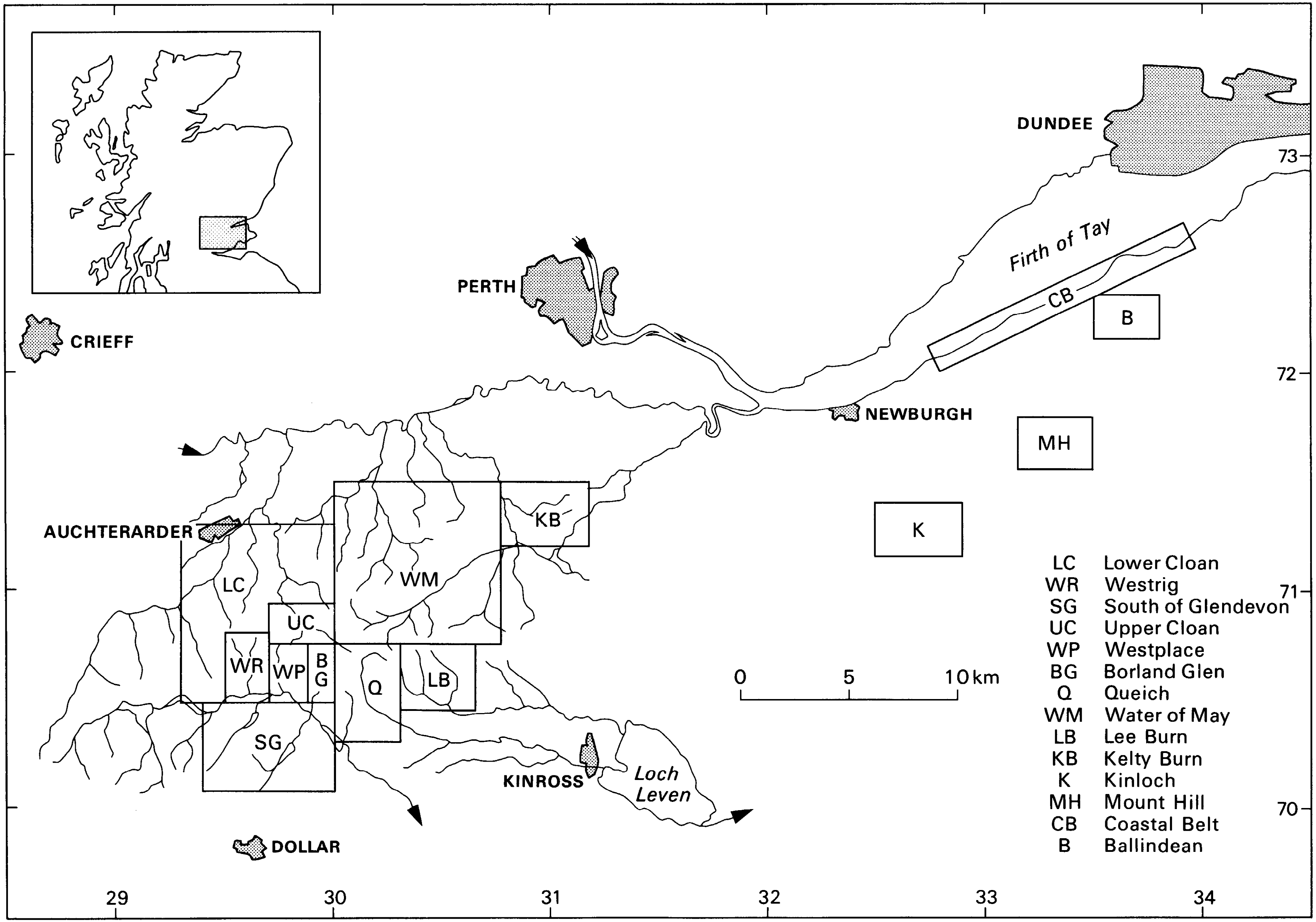

Figure 1 Location map showing the area studied and the sub-areas selected for comparison of drainage geochemistry.

DRAINAGE GEOCHEMISTRY

Introduction and sampling methods

A programme of detailed geochemical sampling was conducted between September 1987 and June 1989 to investigate observations of gold recorded in the 1978 regional survey.

In the regional survey stream sediment, water and panned concentrate samples were collected. The concentrates were prepared by panning approximately 3 litres of -2 mm sediment down to 25 g. This technique was subsequently modified for precious metal exploration to produce a 150 ml concentrate from 4 litres of sieved sediment (Gunn, 1989) and this method was adopted in the later, detailed survey. Here, -150 micron sediments were not collected, as orientation work indicated that much of the gold was coarser than this mesh size.

Care was taken to avoid winnowed, surficial sediment depleted in gold and to dig below the open framework gravels. Sieved sediment was washed by careful agitation under water to reduce the risk of fine gold loss due to surface tension effects.

Regional drainage survey

In the 1978 reconnaissance survey, 29 occurrences of visible gold were noted out of 818 panned concentrates. Most of these sites were resampled in 1987 and visible gold was recorded at 40% of them, confirming the value of the earlier study. The sites where gold was not identified in the 1987 sample were normally in drift covered areas where a single flake of gold may be of erratic occurrence. This resampling highlighted the central Ochils and north Fife areas as of special interest.

The regional geochemistry of the Ochils is not discussed in detail here as it forms part of the forthcoming Tay-Forth sheet of the Geochemical Survey Programme. The analyses of panned concentrates and stream sediments can be obtained from the MRP database. There is little spatial correlation between the area of alluvial gold in the Central Ochils and any of the elements associated with sulphide mineralisation, such as Cu, Pb, Zn or Ba. Extensive Ba mineralisation in the western Ochils is well shown by the maps of Ba in panned samples. However, there is no concentration of high Ba values in the Borland Glen area, even though baryte was visually recorded in the pan and pieces of baryte up to 1 cm across can be panned from Creich Burn. Cu shows few anomalies in those areas with the highest concentrations of alluvial gold. For example, the samples from Borland Glen do not exceed 30 ppm in either panned concentrate or stream sediment. Most high Cu values in panned concentrate (>250 ppm) relate to artificial contamination.

However, detailed examination of the geochemistry of the Borland Glen catchment for the gold pathfinder elements As, Bi and Sb identified the area as enriched. This geochemical signature was then applied to other areas, using a selection criteria of Bi >4 ppm in stream sediment and, As >19 ppm and Sb >4 ppm in panned concentrate. Twenty-two anomalous sites were identified within seven main areas: Borland Glen and Coul Burn, Gleneagles House and Cloan area, Glen Devon Forest and the adjacent Glendey Burn, Alva Glen, Strawearn and West Bank Burns near Glenfarg, the Lindores area and a coastal belt on the Firth of Tay. Further details of these localities can be retrieved from the MRP database. The detailed sampling described here does not cover three of these areas - Alva, Strawearn and Lindores - as visible gold was not recorded in the 1978 survey. There are records of As, Sb and Bi mineralisation from the Alva Glen area (Dickie and Forster, 1974; Parnell, 1988) but gold has not been recorded from the Alva silver mine, except for an unattributed reference given in Collins (1976).

The conventional pathfinder elements As, Bi and Sb therefore provide guides to the occurrence of alluvial gold and in areas such as Alva, Strawearn and Lindores further follow-up sampling is recommended.

Detailed sampling

The summary statistics for 189 panned concentrates from the (1987-89) survey are shown in Table 1.

Table 1 Summary statistics of follow-up panned concentrate samples

Element	Median	Percentiles		Max.	Min.
		25th	75th		
Au (ppb)	25	0	854	140000	0
Ca	16200	13100	20200	50100	6000
Ti	9950	7120	13475	30210	3960
Mn	2630	1345	4015	9420	460
Fe	95800	70450	130600	205000	31200
V	207	153	261	613	69
Cr	391	302	518	76	1143
Ni	25	19	34	89	9
Cu	15	12	19	322	5
Zn	82	66	97	336	39
Ag	3	1	5	42	0
Sb	1	0	7	532	0
Ba	344	271	458	70034	121
Ce	23	16	30	92	0
As	12	9	17	47	0
Bi	0	0	0	59	0

Notes

1. All elements in ppm except Au in ppb.
2. Au determined by AAS after an aqua regia attack and solvent extraction and the other elements by XRF.

Au, as expected, shows a wide range in concentration between <10 ppb to 140 ppm. A log-probability graph (Figure 2) shows a very large anomalous population, 50% of the samples containing >25 ppb Au. With 25% of the total exceeding 850 ppb Au, the data distribution is biased by extremely elevated values from the follow-up survey. Figure 3 shows Au distribution,

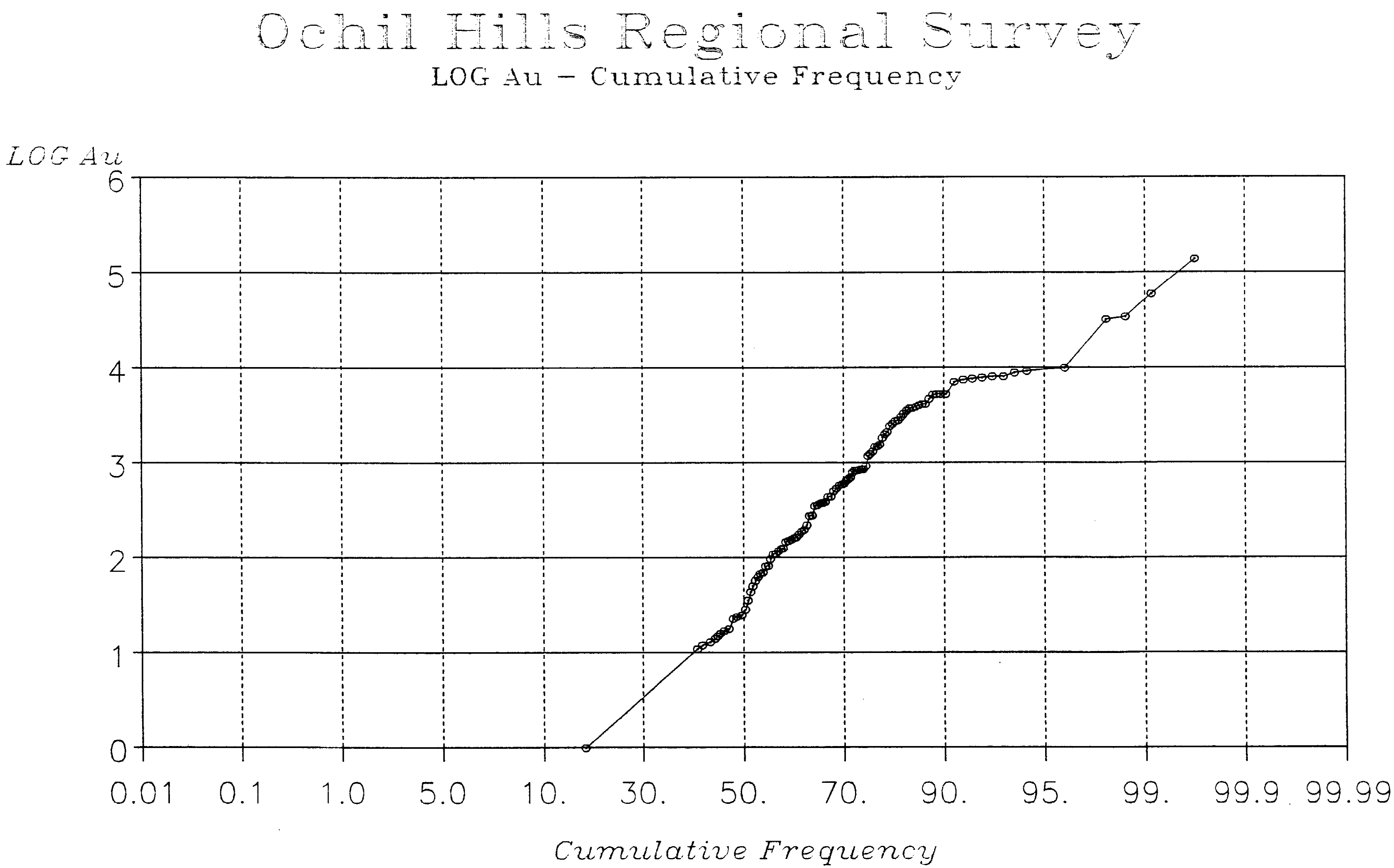

Figure 2 Log-probability graph of Au (ppb) in panned concentrates from the regional survey (0 = <10 ppb, 1 = 10 ppb, 2 = 100 ppb, 3 = 1000 ppb, 4 = 10 ppm, 5 = 100 ppm).

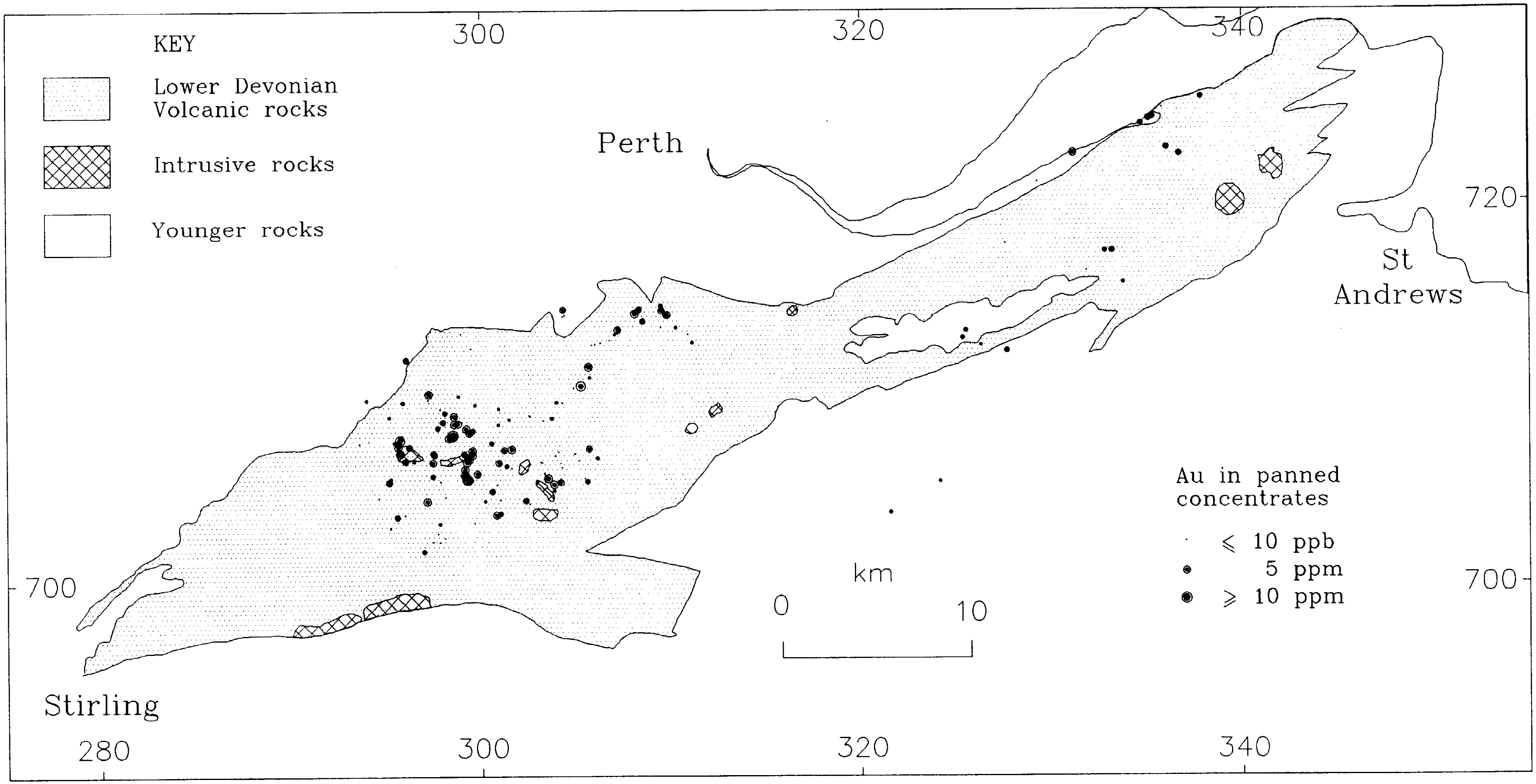

Figure 3 Distribution of volcanic rocks and gold content of panned concentrates in the Ochil Hills.

and indicates the general area covered in the detailed sampling and the concentration of high values centred on Glen Devon.

Gold exhibits few significant correlations with other elements: only Fe, Mn and Ti have significant Spearman rank correlations at the 99% confidence level. This is due to the similar dynamic behaviour of gold and coarser particles of heavy minerals such as magnetite and ilmenite in the fluvial environment. Conventional pathfinder elements such as Sb, As, Bi and the base metals Cu, Pb, Zn are not significantly correlated with Au. Silver shows a slight correlation with Au, an association confirmed by microprobe analyses of the gold grains.

Comparison of sub-areas

The region sampled in detail can be subdivided into fourteen sub-areas (Figure 1), in each of which the Au concentration can be compared on a non-parametric basis using quantile box plots (Figure 4). Those significantly higher in alluvial gold have median and 25th quantile values greater than the overall median. These are Westrig Burn, Borland Glen, and the Firth of Tay coastal belt. The large variability of the gold concentration is also illustrated by this diagram. Levels up to 10 ppm Au (the upper detection limit of most of the analytical results) occur in the majority of sub-areas. The distribution of Au in each sub-area is discussed below.

North Fife Region

The areas sampled were a coastal belt along the southern margin of the Tay Estuary and three areas inland to the south at Ballindean [336 722], Mount Hill [333 716] and Kinloch [327 712]. Glacial and fluvioglacial deposits are widespread over the region forming a thick cover so that outcrops are scarce on the lower ground. The topography ranges from gentle hills (mostly around 200 m in height) to flat or gently undulating stretches of lower ground where the drift thickens considerably. The chief land uses are mixed farming with forestry on the steeper ground and human settlements are small.

Coastal belt. Along the 10 km long coastal belt eight samples were collected. The streams are generally small and their flow sluggish or intermittent. In some of the streams close to the high tide mark gullying of late glacial tills and resultant localised upgrading have occurred; the highest value being 3784 ppb Au at Flisk Point [33118 72250]. The coastal superficial deposits are a potential source for the gold, although its origin is as yet unproven.

Ballindean. Three sites at around 46 m elevation produced values ranging from 197 to 378 ppb Au. Thick superficial deposits again form the cover. The elevation, drainage geometry and distance from the coast rule out recent fluvial processes as the main transporting mechanism.

Mount Hill. Six kilometres to the SW of Ballindean two sites on the lower northern slopes of Mount Hill are anomalous (111 and 507 ppb Au). Three samples from the western hill margin are near or below the detection limit. Further sampling will be needed to deduce a pattern from these observations.

Kinloch. All of five samples taken are weakly anomalous (12 to 190 ppb Au). The drainage here has been modified during land improvement making comparison with other areas difficult.

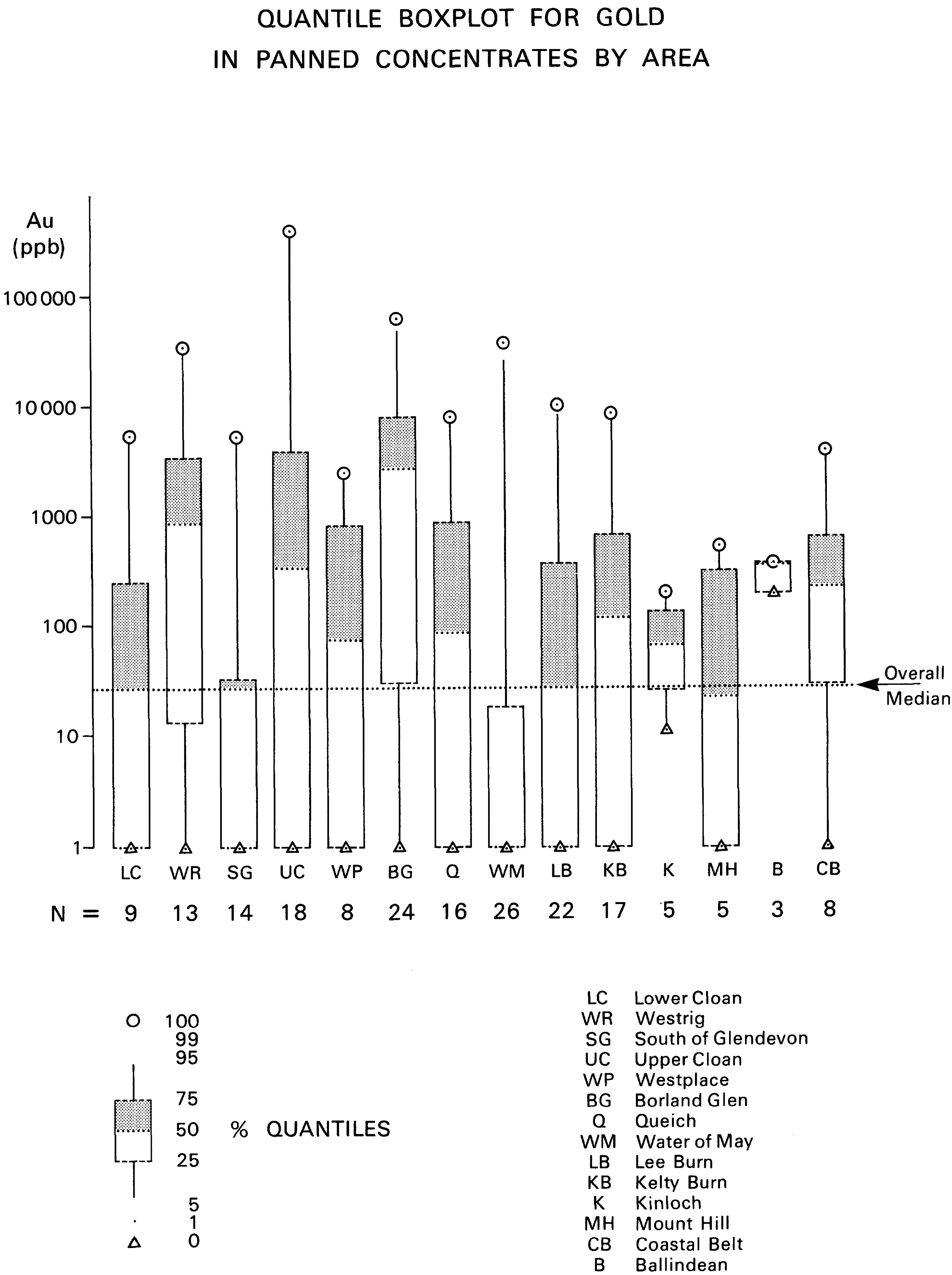

Figure 4 Comparison of Au levels in panned concentrates in the sub-areas using qualitle box plots.

Central Ochils

Panned concentrates were collected from streams over an area between the south side of Glen Devon and the Bridge of Earn, some 20 km in length by 10 km wide (Figure 1).

The relief ranges from undulating to hilly (approaching 500 m in places). Most streams are well-developed, with plentiful well-worked sediment. Late-Devensian glacial till drapes the lower hill slopes and forms extensive cover in main valleys. Fluvioglacial reworking of these deposits has given rise to up to four poorly defined terraces as seen in the south-facing tributary valleys of Glen Devon. Renewed incision of these alluvial terraces has taken place as the result of deforestation. On the highest ground drift cover is thin (1-2 m) and relatively stable with active scree being restricted to only the steepest slopes. Trial pit profiles indicate that solifluction and eluviation processes have also influenced drift development.

The higher and steeper ground is dominated by dry heath species and is given over to rough grazing. Elsewhere mixed farming and forestry are practiced as a result of greater accessibility and improvability of the land.

Alluvial gold is widespread throughout the central Ochils. Localised upgrading occurs in upland areas particularly where the present drainage cuts through fluvioglacial terrace margins. The generally coarse grain size yields a wide range of Au values, necessitating repeat sampling and closely spaced infill work to establish a more meaningful range within each catchment. Sub-areas were defined by observing gold distribution in the field and a summary of Au analyses from these is given in Figure 4. The results are described in detail below.

Borland Glen. Here the original 1978 anomalous site lies on the SE side of White Creich Hill but on first resampling, Creich Burn, which drains Borland Glen, is richer in gold. Most of the gold observed in the pan is 0.05 - 1.0 mm in size and panning of unsieved terrace material in the vicinity of Heart Plantation [29930 70650] revealed gold particles up to 10 mm in size. From 24 panned concentrates levels of over 1000 ppb Au are recorded in 14, of which 4 exceed 10000 ppb (Figure 5). In Creich Burn a general upstream increase in gold was observed, although between-site variation is pronounced because of the coarse grain size of the gold and the 'nugget effect'. Samples must be collected below the armoured, surface layer of the bouldery alluvium. Lower levels of gold in the headwaters of the Creich Burn are attributed to the lack of alluvial upgrading and not necessarily to a scarcity of gold.

The stream east of White Creich Hill that was recorded as containing gold in the original survey in 1978 yielded a value of 2571 ppb gold in the 1987-89 survey.

Rounded grains of cinnabar up to 1.5 mm in size are present in stream sediment and overburden. They are most abundant in the vicinity of the Heart Plantation confluence [29930 70650] where some of the highest Au levels are also found. Only 12 samples were analysed for Hg but these samples yielded the very high levels of 22 ppm Hg in a panned drainage concentrate at [29928 70547], and 46 ppm Hg in a panned till sample at [29928 70639].

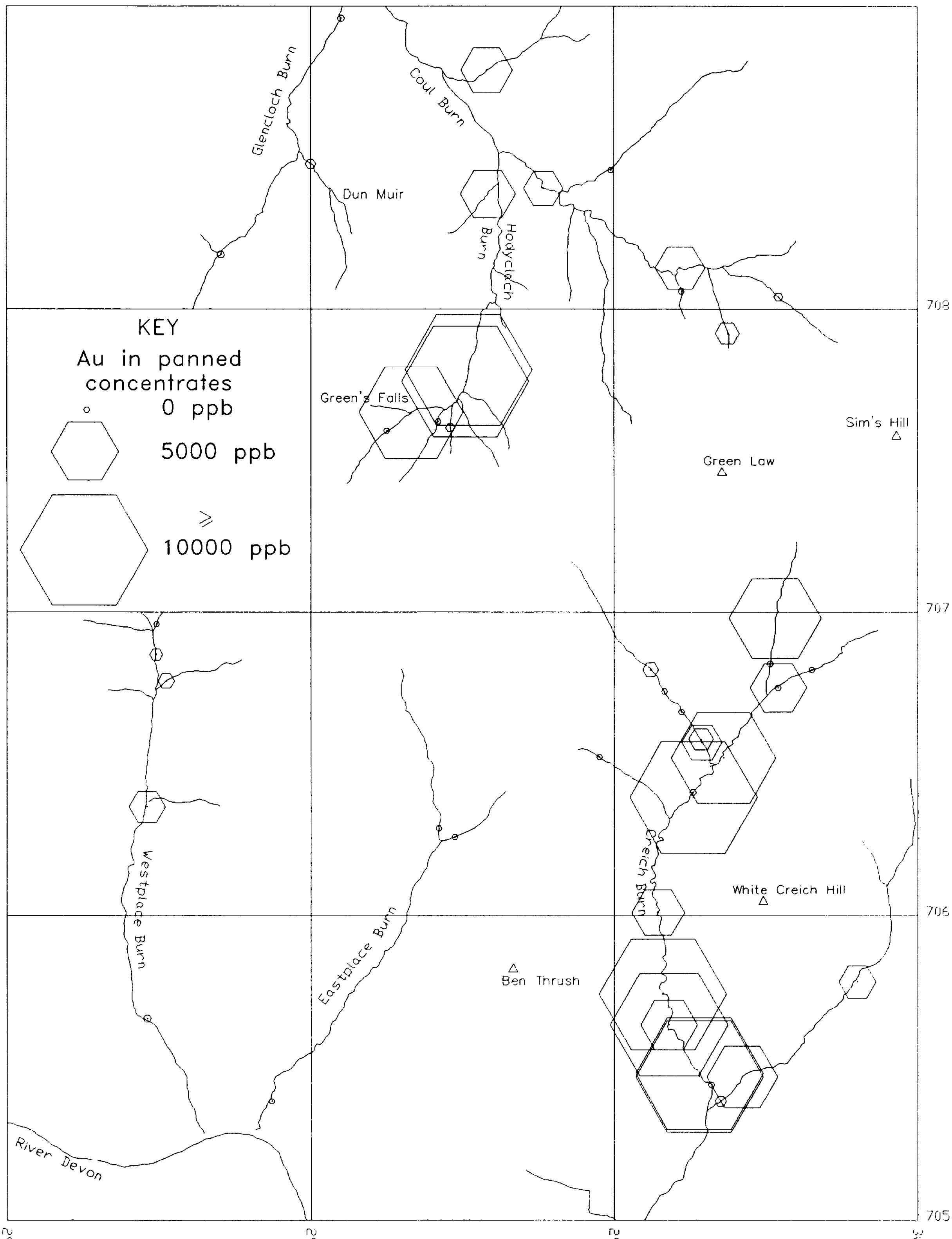

Figure 5 Distribution of Au in panned concentrates in Borland Glen area.

Upper Cloan. To the north of Borland Glen, gold is present in streams draining the northern side of Green Law, most notably the Hodyclach Burn where a peak value of 140 ppm Au [29852 70780] was obtained. Colours (discrete visible gold grains) are less common than in Borland Glen and with the one notable exception analytical values are lower. In the north-west flowing upper reaches of Coul Burn to the north of Green Law [29922 70814 and 29939 70792] gold is also common. The alluvial gold localities in the Upper Cloan district all fall within 1.5 km of Borland Glen.

Lower Cloan. The Lower Cloan subcatchment to the north-west of Upper Cloan contrasts with its neighbour as an area of lower relief and more gentle slopes. Glacial till deposits are widespread, containing clasts of Highland as well as local origin. From the analysis of 15 samples the maximum value of 5328 ppb Au was collected at [29725 70996] but otherwise levels are markedly lower than in the Upper Cloan.

Westplace Burn. Gold appears to be absent from Eastplace Burn, immediately west of Borland Glen, with values below the detection limit. In Westplace Burn, the next stream to the west, one pannned concentrate collected at [29746 70636] has a high content of 2449 ppb Au.

Westrig Burn. Westwards of Westplace Burn, sampling was extended to the Westrig catchment. Gold is commonest in the upper reaches of Westrig Burn and its headwater tributary, Jamie's Grain Burn where the highest level 33 ppm Au was recorded at [29573 70755].

South of Glendevon. Here the larger valleys such as Glensherup and Glenquey are fault controlled and glacial deposits are extensive near to the main valley of Glen Devon. Reworking of these deposits has occurred but overall the drainage morphology appears less favourable to gold concentration than further north. Four of fourteen sites yielded visible gold, and only in Back Burn [29715 70362] close to Borland Glen was the anomaly of significance (5234 ppb Au).

Queich Area. East of Borland Glen, the degree of fluvial reworking is less pronounced and gold distribution is irregular. The highest values are 7489 ppb at Littlerig [30160 70706] and 3300 ppb at Lendrick Hill [30080 70362].

Lee Burn. Superficial deposits increase in thickness and extent towards the south-east margin of the sampled region of the Central Ochils. In the upper Lee Burn [30354 70555] fine-grained gold was found. The initial concentrate exceeeded 10 ppm Au and resampling gave the still anomalous level of 7868 ppb. A gossanous zone was found in the upper part of Lee Burn [30327 70610] and related small sulphidic veins contained up to 0.35% Cu, 1.85% Zn and 1.34% Pb but no detectable Au.

Water of May. Anomalous Au levels were recorded at three of 23 sites sampled in this district. The anomaly at Easter Clow [30567 71137] could not be repeated by two subsequent samples. Single site anomalies occur nearby at [30527 71037] and in the Binzian Burn [30720 71330], where baryte occurs cementing a fault breccia.

Kelty Burn. This stream and its tributaries drain open, rolling hill land with a covering of mixed locally-derived and exotic drift. Ten of 13 samples in the vicinity of Craigowney Hill [3089 7141] yielded analyses in the range 119 to 7712 ppb Au. The presence of vein quartz fragments at sites around [30951 71431] and anomalous Ba levels in the concentrates could be significant. Analysis of concentrates from streams to the south (east-south-east of Rossie Ochil) yielded no more than 18 ppb Au. A source of gold in the upper catchment of Kelty Burn seems probable.

Microprobe analysis of alluvial gold grains

Electron microprobe analysis of gold grains were made using a Cambridge Microscan V, with an electron beam of 15kv, about 5 nA specimen current focused to a nominal 2 micron diameter, with a Link Systems AN10000 energy dispersive X-ray detector. Under these conditions the X-rays detected are from the top 0.5 microns of the specimen. Rough grains from panned concentrates were mounted on a glass slide with double sided tape. The surfaces of the grains were examined on the rough 'virgin' surface where there are often residual layers, probably of clay, which can interfere with the analysis. Thus deliberate scratches were made in the grains and the 'scratch' measurements gave higher silver contents. This is either because the clay is no longer screening the gold from the beam or because the scratch has penetrated through a surface layer of gold with a low silver content.

Thirty one grains from Borland Glen were mounted in epoxy resin on glass slides and polished to reveal a cross section through the grains. Several of the grains showed a variation in colour. Most of the grains displayed the normal pale (?greenish) yellow colour. Several grains showed whiter patches near the outside of the grains. One grain was wholly composed of this whiter gold whilst another had a core of yellow gold and a rim of pale gold. Several grains showed small exterior patches (?partial rims) of reddish gold. A gold alloy colour chart (Butts and Coxe, 1967, p.281) suggests that gold is red-yellow up to a few % Ag, pale (?greenish) yellow up to about 50% and then whitish. Before electron microprobe examination the polished grain surfaces were lightly etched with potassium cyanide/ammonium persulphate solution (Smithells, 1976). In some grains the etch revealed an internal grain structure and showed more reaction with the whitish areas. It was noticed that all the boundaries between the colour shades of gold were sharp indicating either that they had been deposited at different times or that grains of different compositions had been 'welded' together. Groen et al. (1990) have shown that a silver-deficient gold layer is commonly found on alluvial grains of high-silver gold or electrum. These silver-poor rims were probably deposited from solution while the grain was held in sediment.

The chemical compositions of the polished gold grains were determined by electron microprobe. In all, 44 determinations were made, 43 on gold and one on an inclusion. Histograms of the gold and silver contents in 43 determinations on the 31 grains from the upper Borland Glen are given in Figures 6a and 6b. The median composition is 92% Au, 6.3% Ag and a plot of gold versus silver (Figure 7) gives the usual inverse relationship. When the analyses are 'coded' to show whether the gold had reacted to the etch it is seen that the highest silver contents in particular have all reacted (these are the whiter areas). The one inclusion observed (besides quartz) in the gold grains has a composition of 53.7% Au, 6.6% Ag, 15.5% Pb, 4.06% Hg, 2.94% Pd and detectable levels of Te and Bi. However, the majority of the gold grains do not contain detectable Pd, Pb, Cu or Hg.

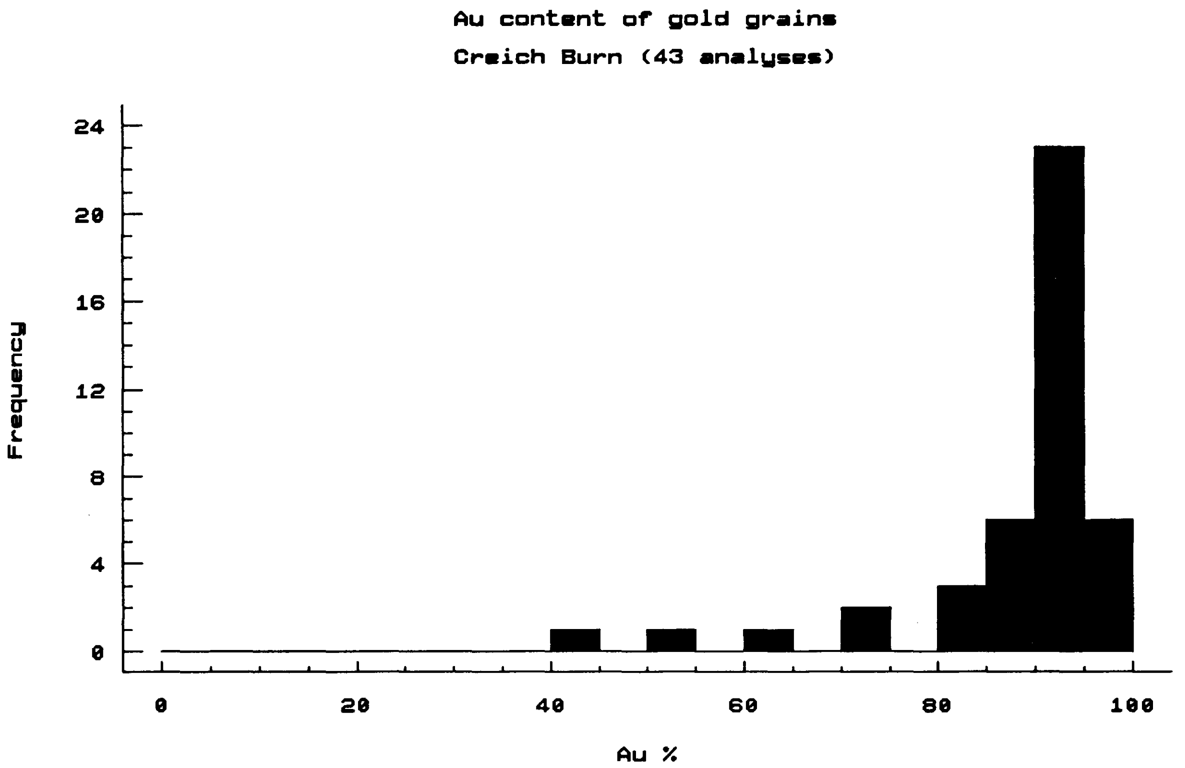

Figure 6a Histogram of Au content in alluvial gold grains in Creich Burn, Borland Glen.

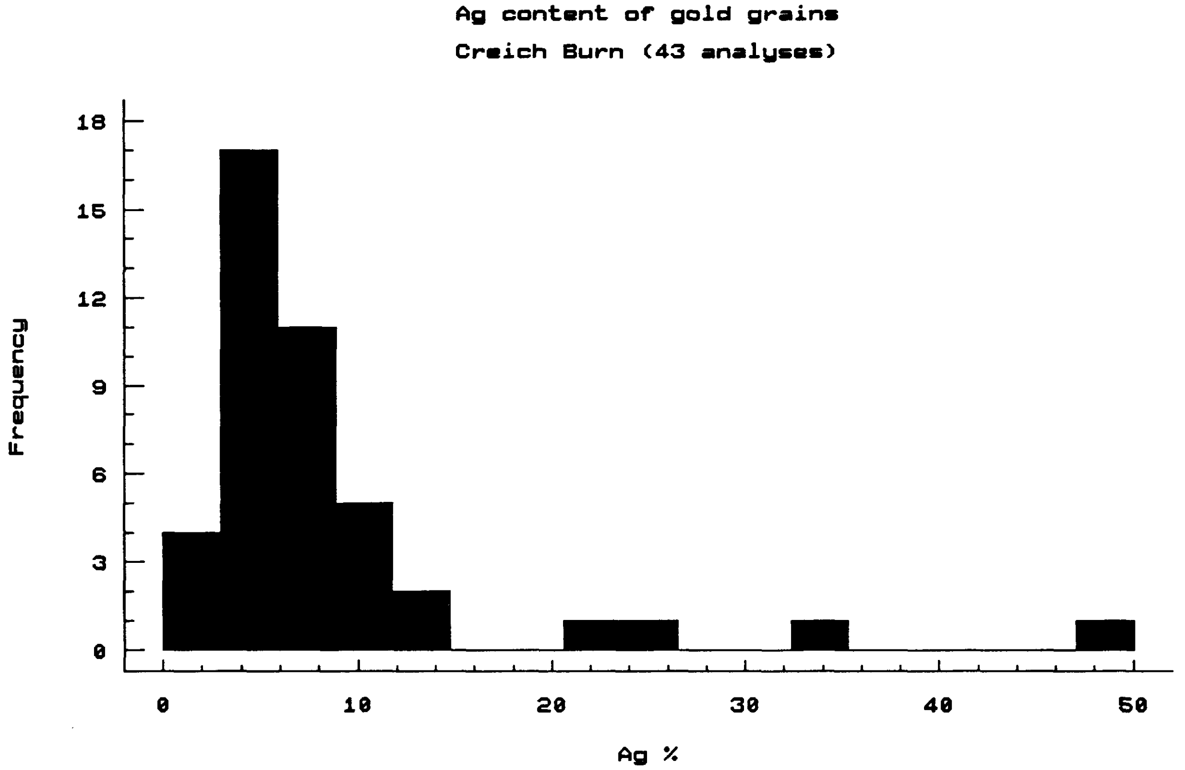

Figure 6b Histrogram of Ag content in alluvial gold grains in Creich Burn, Borland Glen.

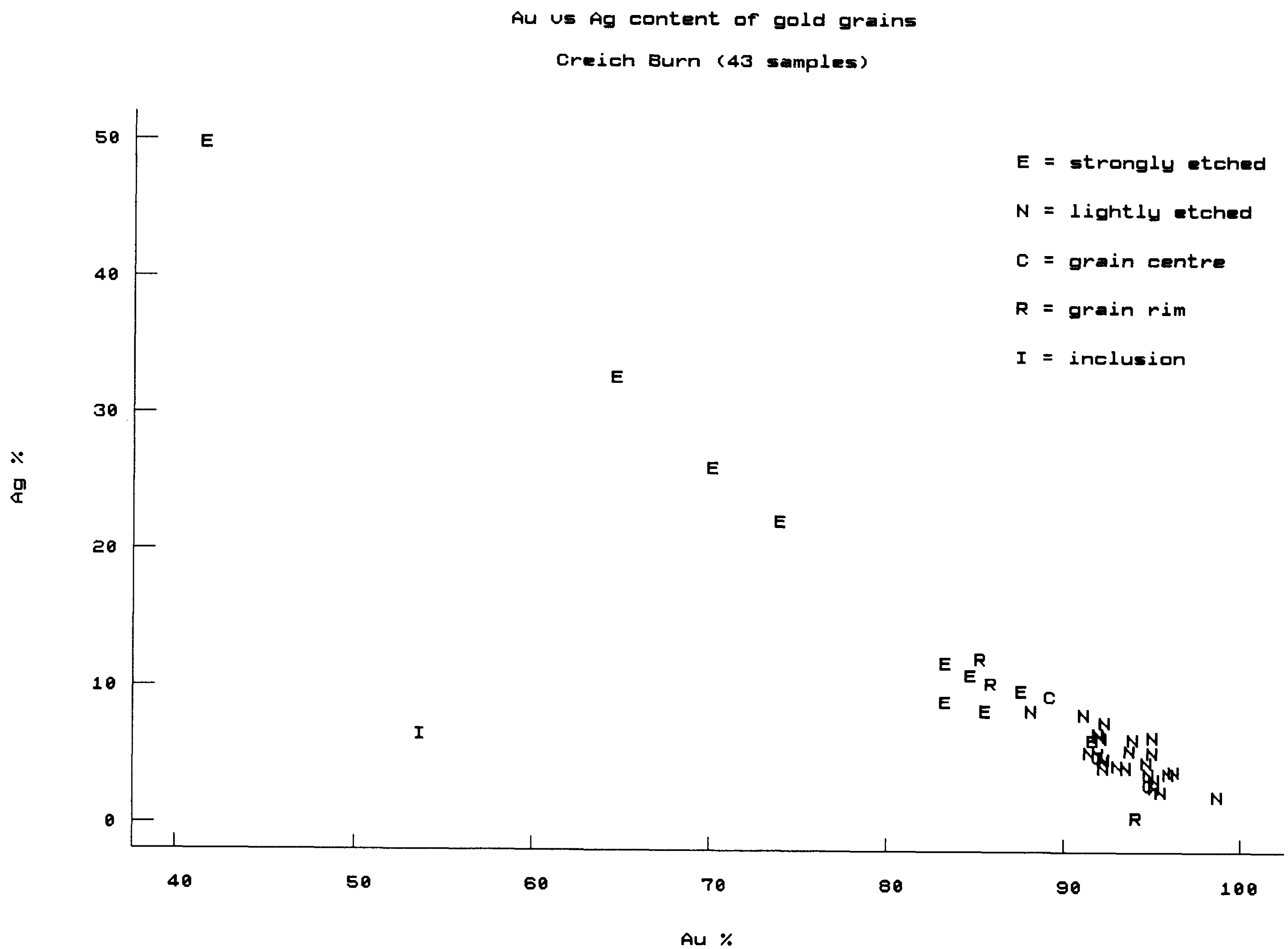

Figure 7 Au vs Ag contents of alluvial gold grains in Creich Burn, Borland Glen.

Summary

Within the Central Ochils the Borland Glen anomaly is part of a broad area containing alluvial gold, stretching westwards to Glen Eagles and eastwards to the Lee Burn catchment. These occurrences are not thought to be derived from a single source but there is a major concentration of high values in the vicinity of Green Law and upper Borland Glen. The Craigowney Hill anomaly is less significant in terms of its areal extent and investigations were therefore focused on the Borland Glen anomaly.

In north Fife gold may be found in a variety of physiographic environments. The thick overburden, lack of exposure and anthropogenic factors are disadvantageous to further investigation. The superficial deposits are thought to be derived from the west, where gold has been found in bedrock; however, the coincident As, Bi, and Sb anomalies at Flisk tend to suggest a local source for the gold.

GEOLOGY

Regional geology of the Ochil Hills

The Ochil Volcanic Formation of Lower Devonian age is situated in the north-east of the Midland Valley graben of Scotland. The lavas and associated volcaniclastic rocks of this thick and variable formation form high ground extending north-eastwards from the western Ochil Hills into the Ochil Hills of Fife and the Sidlaw Hills. In this direction the Ochil Volcanic Formation thins out and passes into the mainly arenaceous Dundee Formation which contains Lower Devonian fossils and which is of fluvial and lacustrine origin. Together these two formations constitute the Arbuthnott Group of the Lower Devonian sequence of Strathmore (Armstrong and Paterson, 1970). The aggregate thickness of the Arbuthnott Group as developed in the Ochil-Sidlaw area is about 2500 m. In the western Ochil Hills this entire thickness is represented by the Ochil Volcanic Formation.

Within the western Ochil Hills (Francis et al., 1970) the Ochil Volcanic Formation is composed predominantly of basic pyroxene-andesite lavas, with a lesser but still important proportion of volcaniclastic rocks, which include material of pyroclastic origin but also much detritus eroded from the contemporaneous volcanic terrain. There are basaltic lavas, hornblende andesites and also distinctive flows of pale-coloured trachyandesite and rhyodacite. The andesite lavas are commonly flow-brecciated (autobrecciated) and in many localities they are traversed by a network of interconnected fissures and voids which were infilled by fine grained sediment after the consolidation of the flow. Markedly autobrecciated lavas are locally difficult to distinguish from the volcaniclastic rocks.

The volcanic rocks of the Ochil Hills are cut by many minor intrusions, mainly in the lower part of the sequence. Most are dykes of acid porphyrite, porphyrite, andesite and basalt. There is a larger intrusion of quartz-feldspar-porphyry in the Borland Glen area. Large intrusions of diorite are emplaced in ground close to the Ochil Fault which forms the southern boundary to the western Ochil Hills. The diorites occur also farther to the north-east in the Glen Devon area. In both areas they are surrounded by wide metamorphic aureoles within which lavas and pyroclastic rocks are hornfelsed with the development of aplitic veins. In the outer parts of the aureoles the contact-altered rocks are in places extensively rotted and appear yellow-weathering (Francis et al., 1970).

Superficial deposits

Although the Ochil Hills have undergone more than one episode of glaciation, the existing drift deposits relate only to events of Late Devensian and Flandrian age. During the Late Devensian an ice-sheet originating in the Highlands traversed the Ochil Hills, as evidenced by erratics of Highland origin stranded on the high ground. Distribution of local erratics, notably those of the distinctive rhyodacite of Craig Rossie, indicates an ice-movement towards the south-east in the ground north of Glen Devon (Francis et al., 1970 p.269).This higher ground has a generally thin cover of lodgement till characterised by boulders set in a purple clay of dominantly local origin.

Valleys in the Ochil Hills are characterised by fills of sandy till, which give rise to sloping terraces commonly with distinct uphill margins against the higher ground of the valley sides. The courses of existing streams are generally cut deeply through these deposits into bedrock. It is evident in places that the deposits shown on the geological maps as till are composite, with intercalations of stratified silt and gravel. In such cases it is probable that deposits of till left behind by the melting ice-sheet were later considerably modified in form and composition by the downhill movement of soliflucted material. These processes were probably especially active during the renewal of arctic conditions in the period of the Loch Lomond Stadial, between 11,000 yrs B.P. and 10,000 yrs B.P., when glaciers were mainly confined to the Highlands of Scotland. Deposits of sand and gravel laid down in contact with glacier ice during deglaciation give rise to a subdued moundy topography in the valley of the Coul Burn. The deposits appear to rest on both till and bedrock.

Geology of Borland Glen

The oldest rocks exposed within the area of Figure 8 are the interbedded lavas and agglomerates in the lower part of Borland Glen south of White Creich Hill. To the north and north-west of Borland Glen, in ground extending to the northern limits of the study area, the dip of the volcanic sequence is to the north-west at an estimated 10 to 15 degrees. West of Borland Glen, however, there is a pronounced general dip to the west and several individual west-south-west dips have been recorded (Francis et al., 1970 p.24). It may be that this divergence of dip relates to the variation of original dips within the accumulating volcanic pile. Another possible explanation is that the changes of dip are associated with a dislocation concealed below poorly exposed ground on the watershed between Glen Devon and the valley of the Coul Burn, (otherwise referred to as Upper Cloan, see Figure 1) although no supporting evidence was forthcoming during the resurvey on which existing Geological Survey maps are based.

The upward sequence from the agglomerates and lavas in Borland Glen consists mainly of flows of basic andesite lava, but includes beds of agglomerate which are exposed in the ground between Ben Trush and the Westplace Burn, with others in the Dun Muir area in the valley of the Coul Burn. There are a number of trachyandesite flows.

A large stock of diorite penetrates the volcanic rocks between Black Creich and White Creich Hill, and extends to the west side of Borland Glen. The diorites, mainly coarse and grey or pink, contain pink aplitic veinlets. An elongate metamorphic aureole, over one kilometre wide and extending in a north-east direction, surrounds the diorite outcrops. Some lavas within the aureole have been

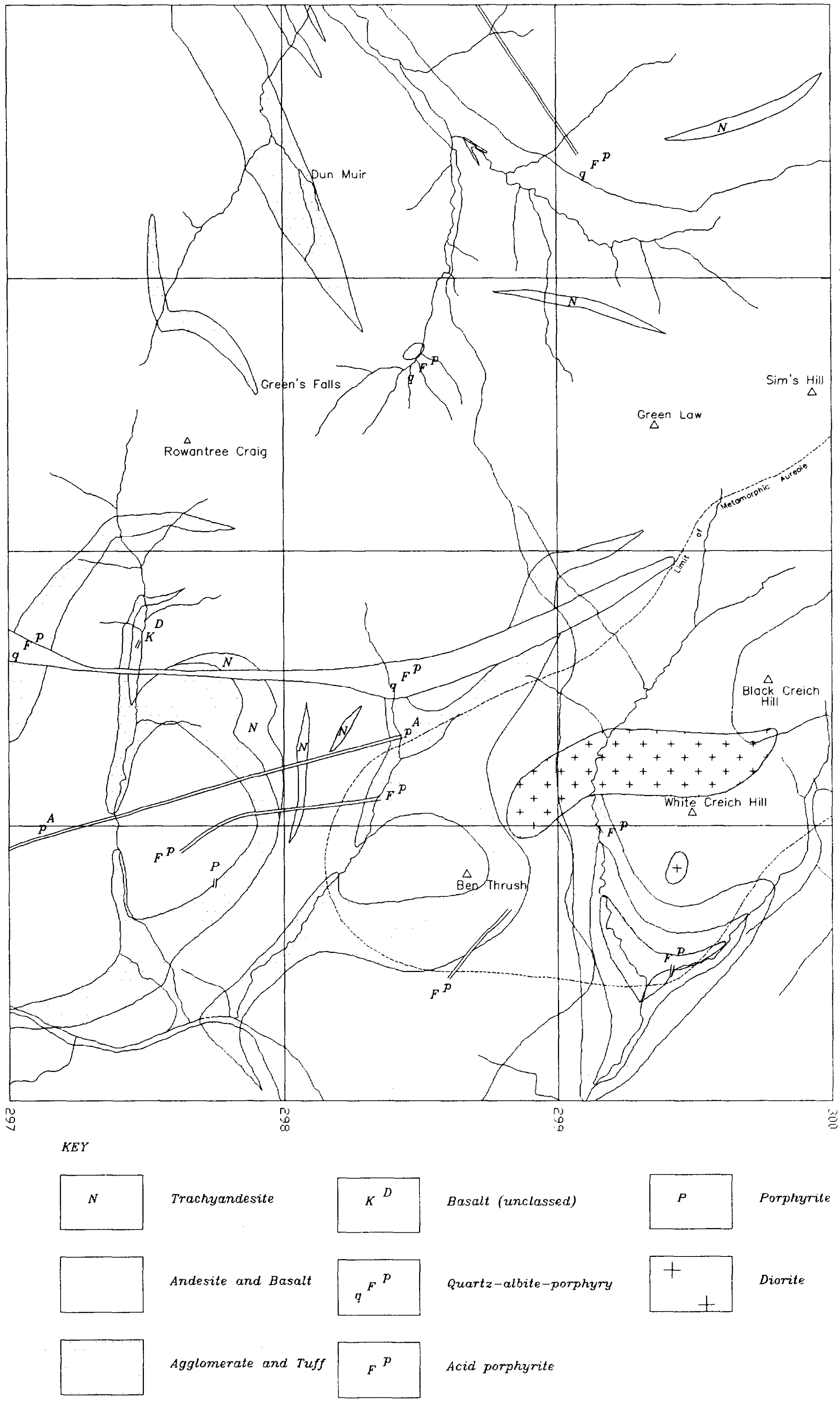

Figure 8 Geological map of Borland Glen.

converted to grey hornfelses with patches of dioritic material of hybrid origin, as on White Creich Hill. Rocks which were originally more heterogeneous, such as amygdaloidal lavas or tuff, show ill-defined pink recrystallised patches. In the outer parts of the aureole the altered rocks are in places rotted and yellow-weathering.

Lava scarps within the aureole on White Creich Hill can be observed to continue into the outcrop of a small boss of diorite on the south side of the hill. Francis et al. (1970 p.38) suggested that this is consistent with the concept that the diorite here represents lavas metasomatised in situ.

Minor intrusions within the study area include dykes of hornblende andesite, basalt, acid porphyrite and quartz-albite-porphyry. A larger intrusion of pink or buff quartz-albite-porphyry extends for over 3 km between the Westrigg Burn and Borland Glen. In the Westplace Burn (south of Rowantree Craig) the intrusion is dyke-like and about 20-25 m wide, broadening both to the east and to the west. A similar rock occurs north of the Glen Devon - Upper Cloan watershed, and is exposed in the Hodyclach Burn east of Green's Falls.

OVERBURDEN SAMPLING

Introduction and sampling methods

Following the recognition of a significant Au anomaly in the drainage of Borland Glen and Hodyclach Burn an overburden sampling programme was commenced in 1988. The initial survey was carried out in April - May 1988 using a 'Minuteman' powered auger to collect a sample of the basal till. The till within 10 cm of the base of the hole was bagged, dried and sieved through 200 micron nylon mesh. The sieved material was ground in a Tema mill and analysed by Acme Analytical Laboratories for Au using an AAS method after a hot aqua regia attack and MIBK extraction, and for Hg by cold vapour AAS after a HCl-HNO3 attack. A panned concentrate sample was also prepared from the basal 1 m of material from the auger hole in the first stage of the till sampling but not extended to the later surveys. The basal till samples were analysed by XRF for Ca, Ti, V, Cr, Mn, Fe, Co, Ni, Cu, Zn, As, Rb, Sr, Y, Nb, Mo, Ag, Sb, Ba, La, Ce, W, Pb, Bi, Th, and U ; the panned concentrates were analysed by XRF for Ca, Ti, Cr, Mn, Fe, Co, Ni, Cu, Zn, As, Rb, Sr, Y, Zr, Nb, Ag, Sb, Ba, Ce, Pb, Bi, Th, and U.

The initial survey was carried out at 25 m intervals along the track from Borland Glen to Upper Cloan, along the forestry track skirting Black Creich Hill and down the small sheep track on the north-west flank of White Creich Hill. This survey was supplemented in September 1988 by five lines on the southern flank of Green Law and Sims Hill covering the main geophysical anomalies (Figure 9).

North of the Borland Glen/Upper Cloan divide, sampling was carried out using a Cobra percussion rig which collects a smaller sized sample but because of its narrow bore probably penetrates nearer to the till/bedrock interface. Three traverses were sampled but the survey not extended to the north because of increasing till thickness and lack of geophysical anomalies.

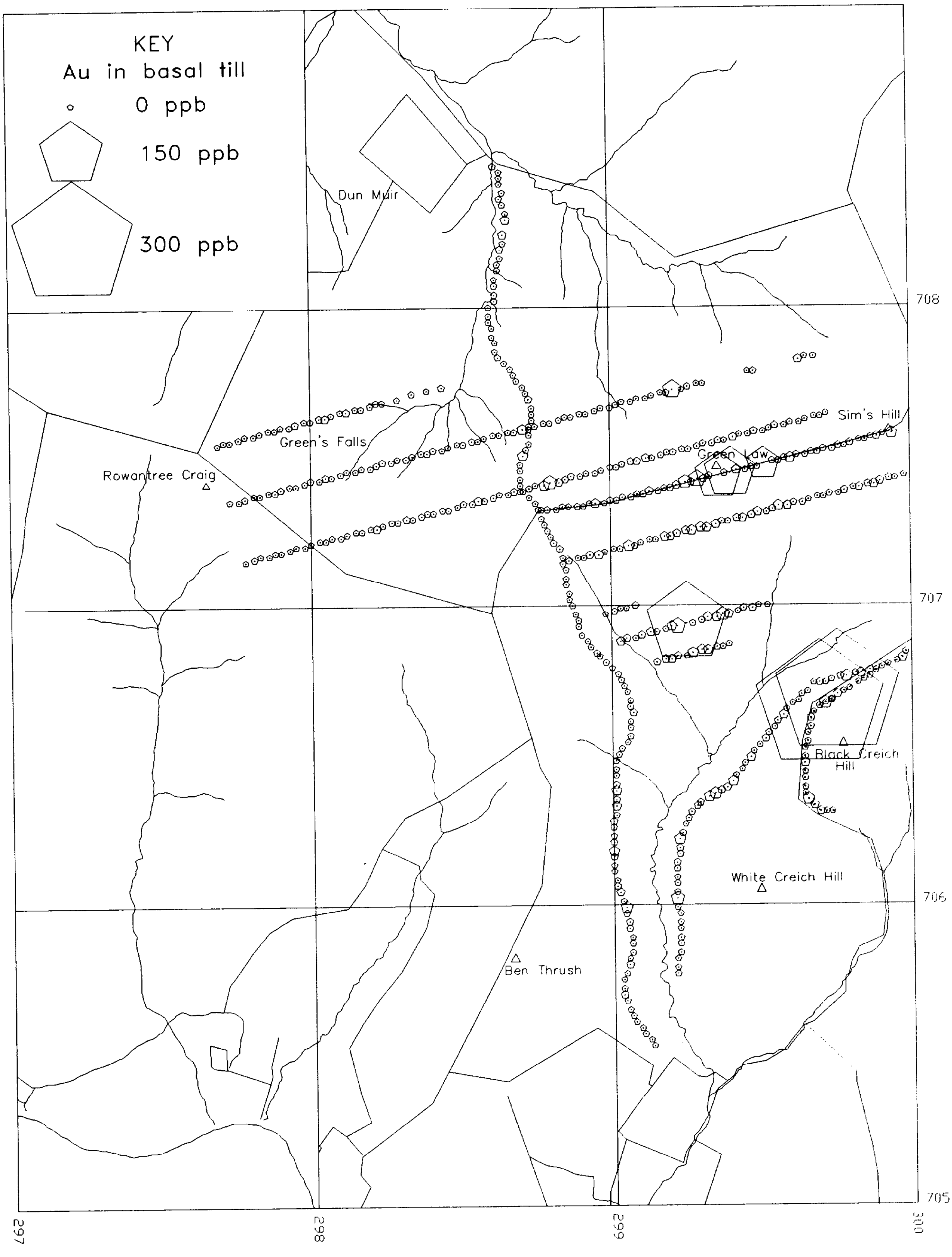

Figure 9 Au distribution in basal overburden, Borland Glen.

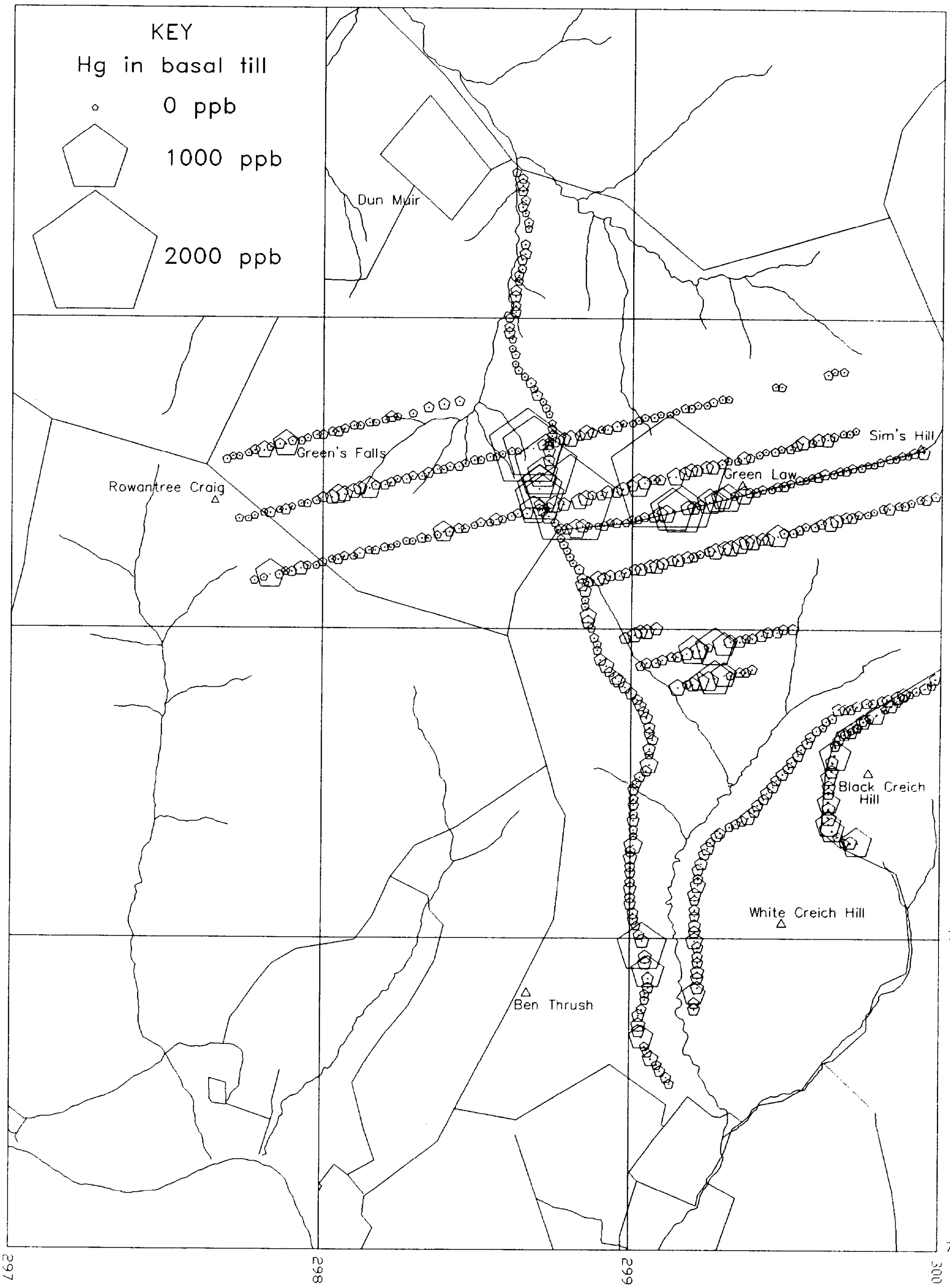

Figure 10 Hg distribution in basal overburden, Borland Glen.

Results

The basal till consists of a stiff, stony clay, pale purple to brown in colour, and containing 1-2 cm clasts of the underlying bedrock. Exotic clasts of Dalradian metamorphic rocks and white quartz pebbles were rare, indicating that the sample is predominantly lodgement till. In stream sections through the till it can be seen that the upper levels contain more exotic, rounded clasts and are probably composed of ablation till. The depth of the overburden varies from 0.2 to 7.2 m with a median of 2.6 m. The thinnest overburden is on the ridge that runs south from Green Law. Details of the clast composition are given in the database but are predominantly of slightly porphyritic andesite or basalt. Pale buff clasts near Green Law may be of an unmapped trachyte lava. Pyroclastic rocks are difficult to identify because of their tendency to be more highly weathered or altered. The main quartz-porphyry dyke that runs east - west across the area was also detected in the clasts and was indicated to extend further east than mapped.

The summary statistics of the elements in the basal till are given in Table 2 and can be compared with the average values for north Midland Valley andesites (Thirlwall, 1981) representing the dominant rock type for this area. Most elements are similar to the average north Midland Valley andesite (Thirlwall, 1981, but see later in the surface rock geochemistry) with the exceptions of Ca and Sr which are significantly lower in the basal tills. This is probably due to leaching of carbonate from the tills or possibly pressure breakdown of the softer carbonate during glaciation.

The distribution of Au in the basal till is shown in Figure 9. The levels are generally low with a median of 2 ppb. A threshold of 10 ppb can be determined from the cumulative frequency distribution. Very anomalous levels (>50 ppb) are found at two sites on the forestry track north-west of Black Creich Hill, on line 00 along the watershed between Borland and Upper Cloan Glens, and on line 450S (Figure 9). The two sites on the forestry track could not be confirmed on resampling and detailed profiling, so that these high values of 300 and 310 ppb may have been caused by contamination in the field or laboratory. The other anomalous sites are believed not to be artifacts because they are associated with lesser anomalies and are surrounded by Hg anomalies. Samples to the north of the watershed are generally lower in Au with the only coherent feature being a small anomaly adjacent to the track, which is associated with the main Hg anomaly.

Mercury behaves similarly to gold in hydrothermal deposits (Boyle, 1979) and has been used as a pathfinder for gold in glacial tills. The presence of cinnabar in the drainage prompted the decision to analyse the basal till for mercury. Mercury levels are higher than gold with a threshold of 100 ppb and 30 % of the samples exceed this level. The peak to background ratio of 27 is, however, lower than the ratio of 160 for Au. The main anomalous zones for Hg (Figure 10) are adjacent to the Borland Glen - Upper Cloan track, near those of Au on the line along the watershed and on line 450S. Detailed examination of the Hg and Au anomalies shows that the Hg forms a 'rabbit's ear' shape, one or two samples displaced (25-50 m) from the Au peak (Figure 11). Gold is correlated with Pb, Zn, and to a lesser extent with Hg and these elements plus As and Sb form a relatively coherent group in the correlation matrix. Copper also appears to be spatially associated with this grouping as shown by Figure 11.

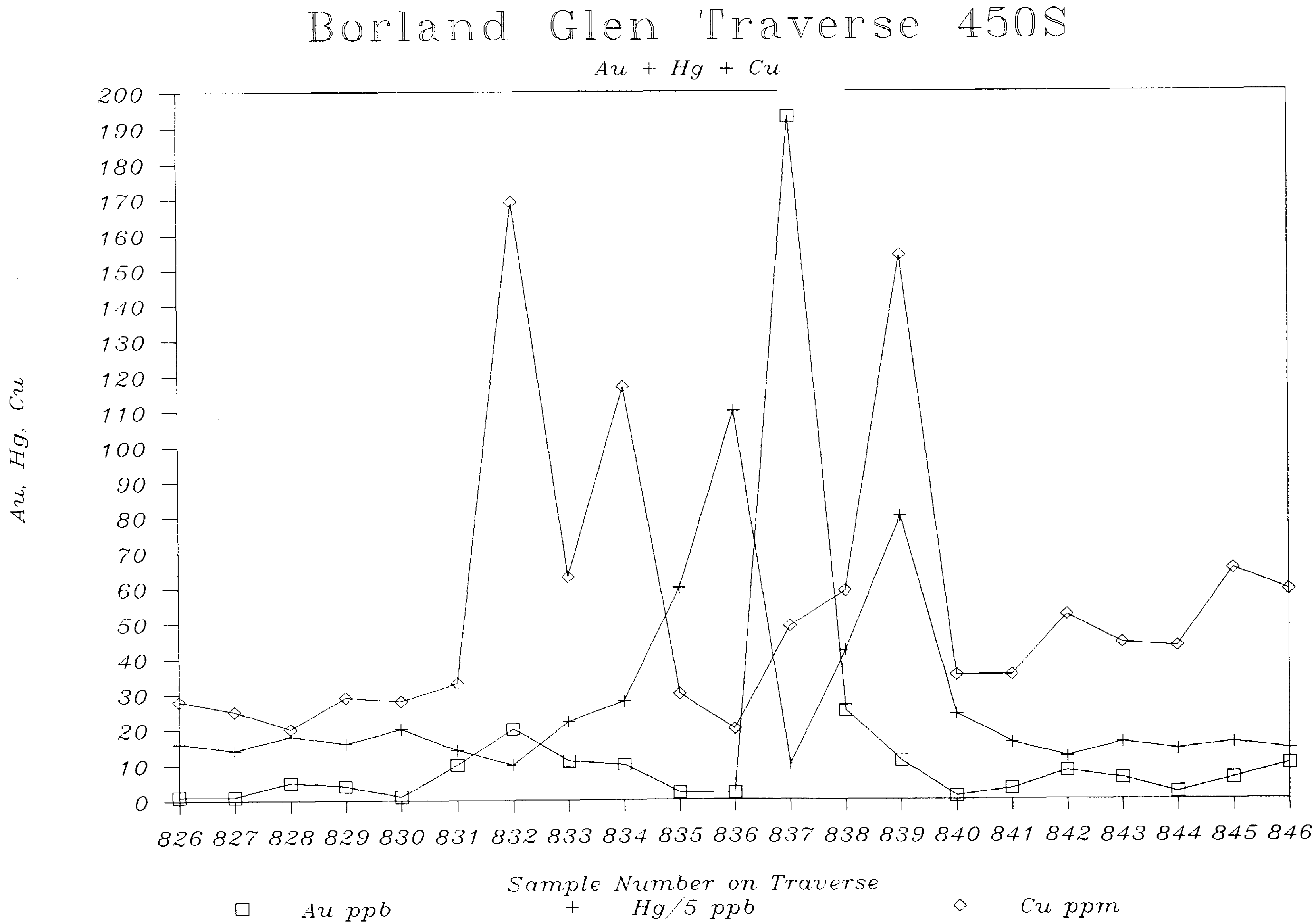

Figure 11 Distribution of Au, Hg and Cu in basal overburden on line 450S.

Table 2 Summary statistics of basal till samples

Element	Median	Percentiles 25th	Percentiles 75th	Maximum	Minimum	NMV lava
Au (ppb)	2	1	4	320	1	
Hg (ppb)	70	50	110	1900	10	
Ca	3950	1675	6050	36700	100	26660
Ti	5305	3125	6050	10800	1070	5216
V	106	66	124	393	13	82
Cr	83	51	112	356	0	31
Mn	1350	1000	1955	19900	90	620
Fe	48000	35850	55600	117400	8600	37370
Ni	29	17	43	135	0	19
Cu	23	13	35	572	0	16
Zn	88	71	125	1852	25	74
As	22	15	34	719	1	
Rb	57	43	82	143	14	78
Sr	266	149	391	860	21	490
Y	16	13	19	32	0	27
Nb	10	9	12	16	5	15
Mo	3	2	5	41	0	
Ag	1	0	2	6	0	
Sb	0	0	2	84	0	
Ba	535	414	660	4957	797	760
La	31	27	36	62	15	38
Ce	40	32	49	103	5	82
W	2	0	4	9	0	
Pb	28	19	45	7451	7	
Bi	1	0	1	22	0	
Th	6	5	7	25	1	12
U	3	1	4	10	0	

Notes

1. All elements in ppm except Au and Hg in ppb.
2. Au and Hg determined by AAS and the other elements by XRF.
3. Number of samples = 546 except V, La, W (366), and Rb, Sr, Y, Nb, Th, U (180).
4. NMV lava is average of north Midland Valley lava (Thirlwall, 1981, Table 4).

Panned till samples

Element distribution in the panned tills follows fairly normal levels for heavy minerals from calc-alkaline rocks (Table 3). High Ti and Fe in many samples indicate a high proportion of magnetite or similar spinels and associated with these two elements are Cr, Ni, Cu and Zn. Zr, Nb, Ce, Y and Th are closely correlated and reflect the incidence of accessory minerals such as zircon and monazite. The chalcophile elements are closely correlated in an As-Sb-Pb-Zn-Cu grouping. The last two elements also show a good correlation with Cr and Ni at low levels, indicating a common substitution for Fe, but a few samples have elevated levels due to sulphide mineralisation. These anomalous samples are concentrated at the margins of the two porphyry dykes crossed by the north - south track.

Table 3 Summary statistics of panned till samples

Element	Median	Percentiles		Maximum	Minimum
		25th	75th		
Ca	6050	3000	9400	32200	500
Ti	6220	4875	7790	24120	1410
Cr	115	65	193	448	0
Mn	980	772	1170	3680	210
Fe	61400	48525	75550	194200	13200
Co	66	46	88	184	11
Ni	24	16	36	125	0
Cu	22	16	34	168	2
Zn	63	45	85	460	26
As	26	18	47	223	7
Rb	39	33	48	107	10
Sr	238	193	300	3346	84
Y	16	13	19	36	7
Zr	265	224	354	1465	96
Nb	12	9	14	27	7
Ag	2	1	3	29	0
Sb	0	0	3	92	0
Ba	418	358	494	17865	63
Ce	26	19	35	108	0
Pb	25	18	35	321	10
Bi	0	0	0	4	0
Th	6	5	7	12	3
U	1	0	2	4	0

Notes

1. All elements in ppm and determined by XRF.
2. Number of samples = 216.

Barium is elevated in a zone adjacent to the larger quartz-porphyry dyke, reaching 1.79 % Ba. Baryte was observed in the pan at this site and at further sites where the panned till was only examined optically and not analysed. Baryte veining is commonly associated with the margins of late-Caledonian acid intrusions as well as being abundant in veins in the Ochils, such as at Alva.

Pyrite is seen in the pans adjacent to the observed mineralisation at [299050 706290] and also on line 450S between KLU 836 at [299273 706943] and KLU 838 at [299224 706931] which covers one of the main geophysical and Au anomalies (Figure 9). No pyrite is visible at outcrop over this zone.

Summary

The overburden sampling indicates that a zone of sulphide mineralisation extends from line 450S to the watershed near Green Law. This zone of mineralisation has elevated Au, Hg, As, Sb, Cu, Pb and Zn values and is believed to be the source of the gold and cinnabar grains found in the Creich Burn drainage. A large Hg anomaly in the overburden adjacent to the Borland Glen - Coul Burn track extends over the watershed into the catchment of Hodyclach Burn, where there are similar Au and Hg anomalies in the drainage. However, there are no anomalous Au values in the basal till extending that far north and the Hg seems to form a halo around the zone of high Au values. There is evidence of extensive baryte mineralisation with minor base metals concentrated at the margins of the quartz-porphyry dyke.

GEOPHYSICAL SURVEYS

Introduction

During September 1988 a geophysical survey was conducted over an area of ca 1 km^2 in Borland Glen, immediately to the south of the principal watershed. The main objective of the survey was to map the zone of sulphide mineralisation indicated by the geochemical data, in order to identify potential drill sites. Geological mapping in the area is difficult because of the lack of exposure, and it was anticipated that the geophysical data would assist in establishing the positions of the major rock units and structures. The geophysical coverage was extended the following year northwards to the Hodyclach Burn area, to test the possibility for a northern extension of the mineralisation.

Borland Glen area

Survey methods

A grid of eight lines measuring 1.4 km in length with 100 m spacings between lines, was established south-west of Sims Hill (483 m). These survey lines (50S to 750S) are shown in Figure 12, together with those covering the Hodyclach Burn area to the north.

Induced polarisation, VLF-EM and magnetic techniques were employed. The field data were obtained with Scintrex digital equipment (IPR-11 and IGS-2), which enabled the data to be captured in solid state memory. It was thus possible to obtain initial plots in the field via a microcomputer to assist the day to day planning of the survey.

Measurements of the magnetic total field were made at 10 m intervals along the traverse lines, simultaneousely with the VLF-EM measurements. The latter comprised measurement of the electric field and the in- and out-of-phase components of the magnetic field. The source of the VLF primary field was the transmitter at Bordeaux, France (FUD, frequency 15.1kHz).

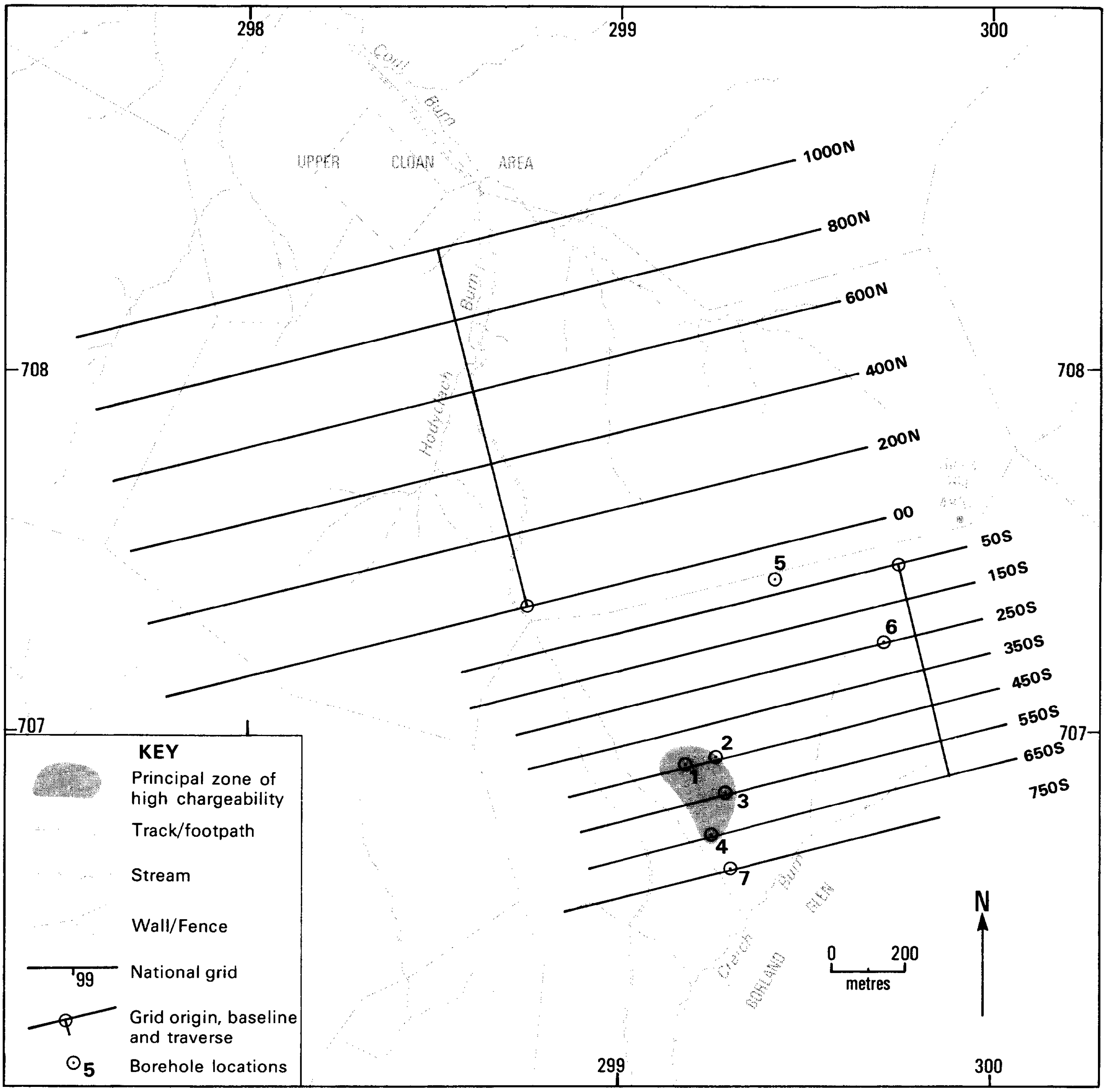

Figure 12 Map showing geophysical survey grids in Borland Glen and Hodyclach Burn areas.

The induced polarisation survey utilised a co-linear dipole-dipole electrode array, with 25m dipoles at centre-to-centre separations from 2 to 7 units of dipole length. A 3.5kW transmitter powered by a motor generator ensured an adequate signal to noise ratio. The decay of the transmitted square-wave voltage was sampled over ten successive periods (or 'slices') and these ten integrated values recorded in a solid state memory. One appropriate integrated value, or 'slice' was then chosen by the operator for subsequent plotting. The prime factor in deciding which 'slice' to plot was dictated by the requirement to avoid the distortive effects of electromagnetic coupling. For this survey 'slice' 4 was used, equivalent to an integration of the voltage decay curve between 120 mS and 150 mS after the end of each two second transmitted pulse. Transmitter off-time was also two seconds. The IPR-11 displays the running average of the successive integrated values and the measurements are terminated when the operator is satisfied a stable value has been reached.

VLF and magnetic results.

Observations were made at 10 m intervals along all eight survey lines. The results for the VLF are illustrated as in-phase and out-of-phase components in Figure 13; as Fraser filtered in-phase component in Figure 14; and as resistivity and phase angle in Figure 15. The magnetic results (as total field) are illustrated in Figures 16 and 17. Figure 19 is a summary of all the results.

The main VLF magnetic field anomalies are associated with streams that cross the survey area. A wire fence intersecting line 50S at 1300W is indicated by the classic crossover feature seen in the in-phase and out-of-phase data, Figure 13. Other perturbations in the VLF magnetic field data are ascribed to variations in overburden thickness.

The VLF electric field data show high values of resistivity over the zone of alteration inferred from the magnetic survey. Elsewhere, as for the VLF magnetic field, the data are influenced by the variation in thickness of the overburden, although to a lesser extent. Tentative correlations with the zone of brecciation and wet boggy areas can be made.

The magnetic results suggest that a zone of alteration is encountered east of about 600W beneath lines 450S, 550S and probably 750S. The boundary of the magnetic feature is the eastern flank of a southerly trending stream valley, and the topography in the immediate vicinity probably reflects this contact of the alteration and the andesites. The several dyke-like anomalies are best seen in Figure 16 (vertical scale x 2 that of Figure 17, ie 250 nT/cm) but no easy correlations can be made. One such feature (250nT) is coincident with the maximum IP chargeability anomaly (line 550S, 860W) illustrated in Figure 18.

Induced polarisation results.

The induced polarisation results are illustrated as pseudo-sections of chargeability and apparent resistivity in Figures 20 - 23 and the anomalous chargeability zones summarised in plan view as Figure 18. The northern lines over the andesites and trachyandesites are relatively featureless (see Figure 18) but two outcrops of altered lavas coincide with the very good chargeability anomaly between lines 350S and 750S. The lack of a corresponding resistivity (low value) anomaly (see Figure 22, 550S) is significant because it shows the chargeability to be due to a true disseminated conductor, such as pyrite, within the volcanics. From the symmetrical arrangement of the contours illustrating the anomalous chargeability locations in Figures 22 and 23, the disseminated conductor zone is inferred to be bounded by a very steeply dipping or vertical plane, both to the east and

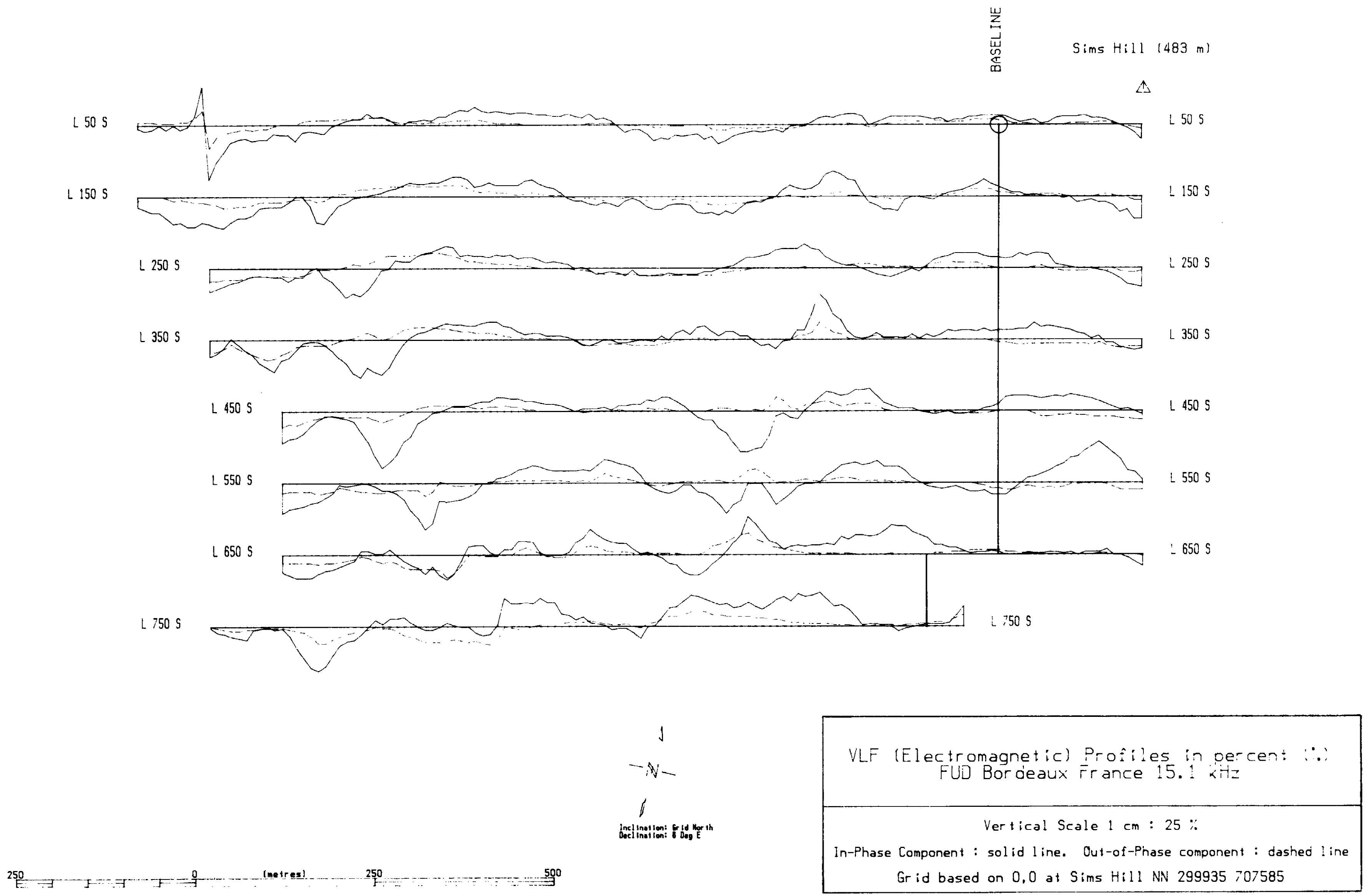

Figure 13 VLF electromagnetic (magnetic field) profiles, Borland Glen.

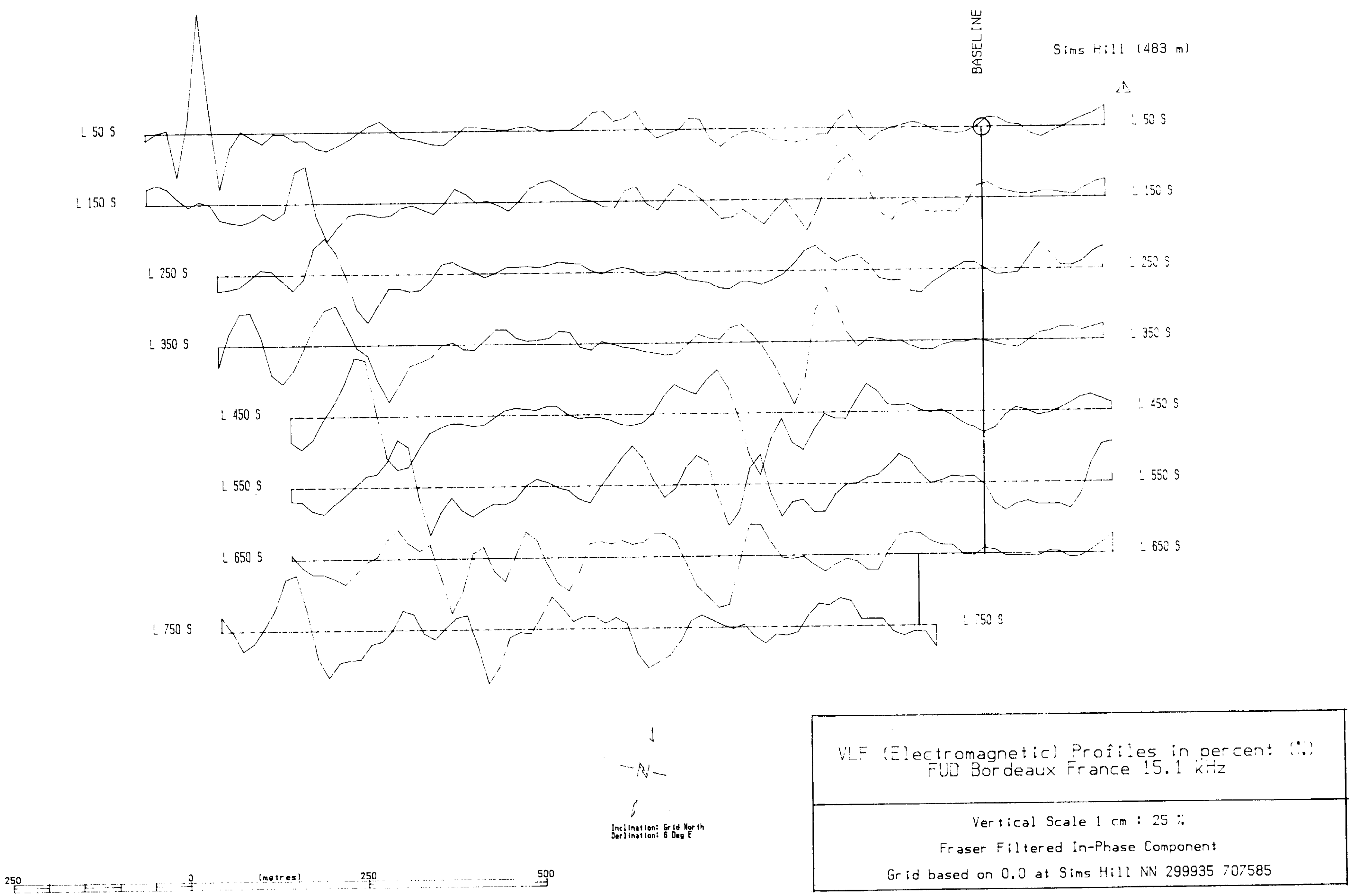

Figure 14 VLF Fraser filter profiles, Borland Glen.

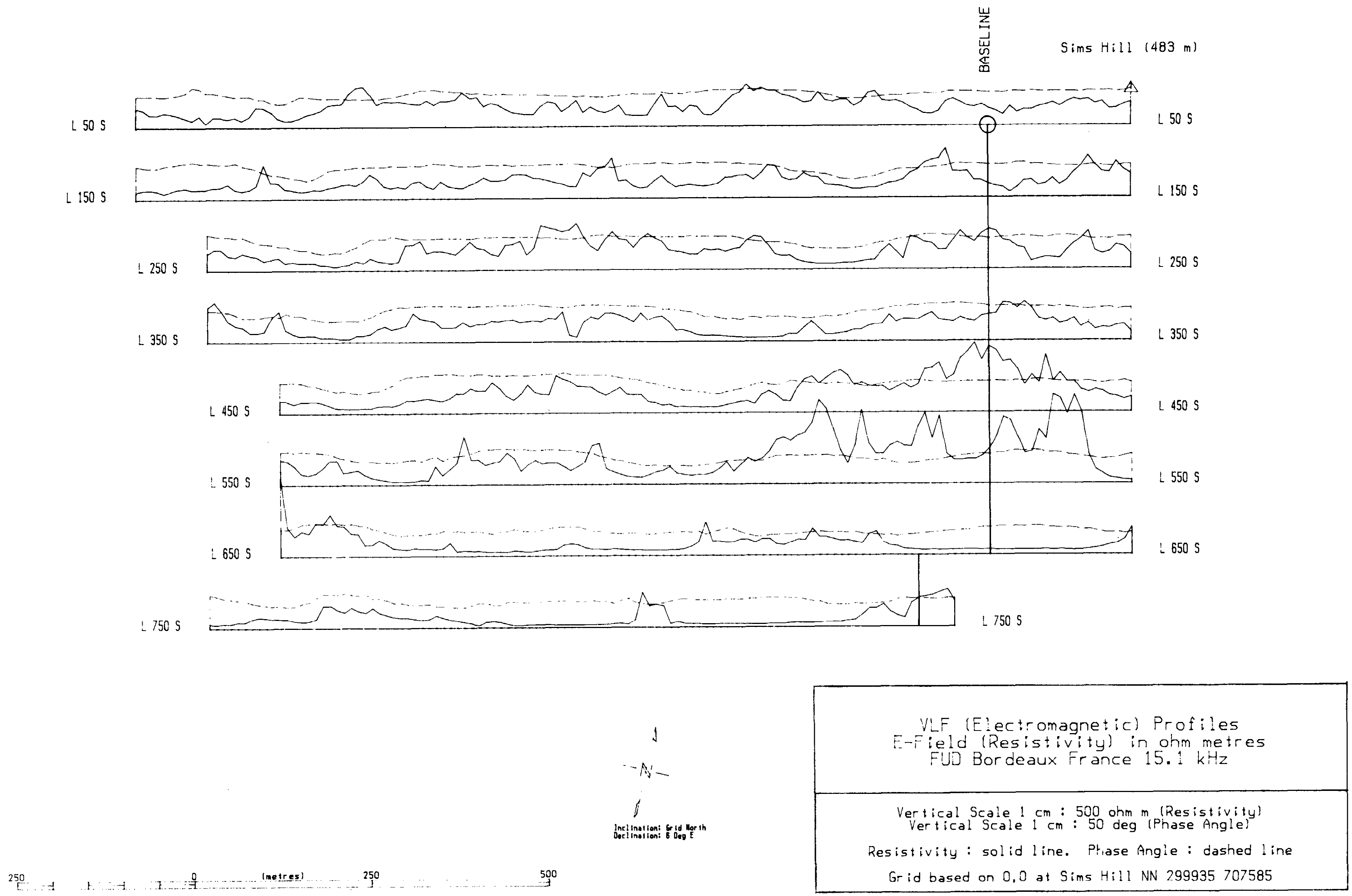

Figure 15 VLF electromagnetic (electric field) profiles, Borland Glen.

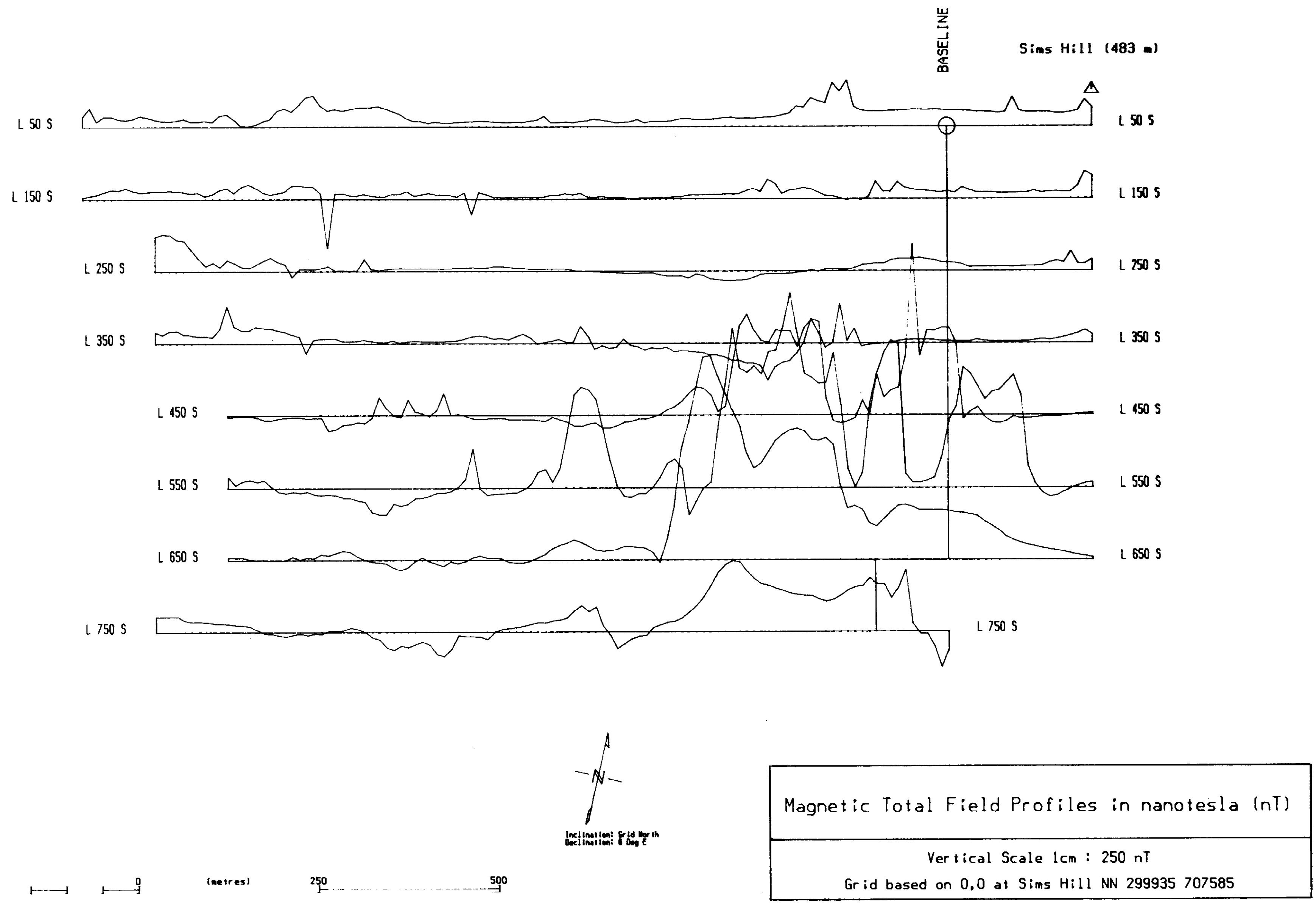

Figure 16 Magnetic total field profiles (250 n/T/cm), Borland Glen.

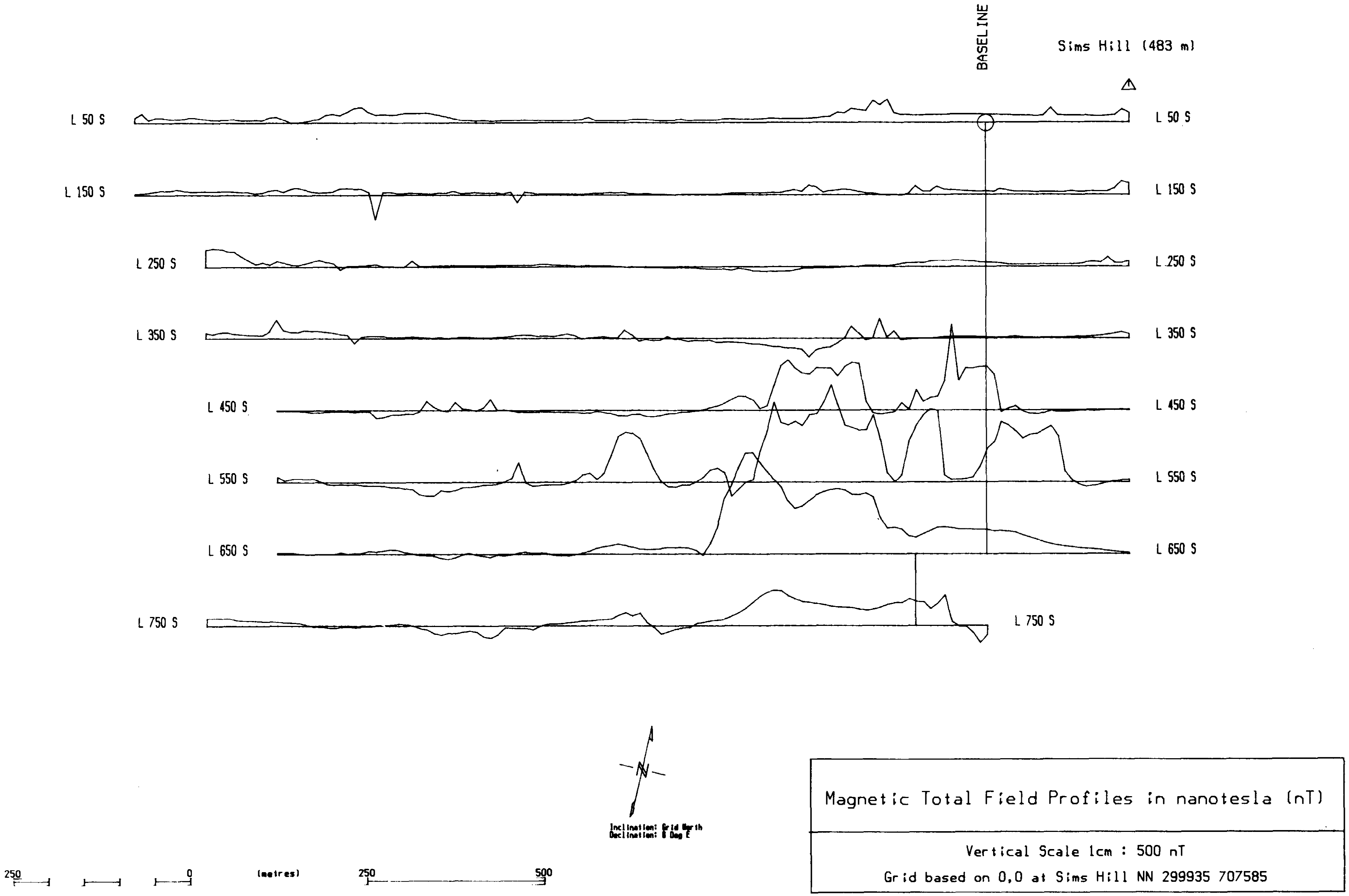

Figure 17 Magnetic total field profiles (500 n/T/cm), Borland Glen.

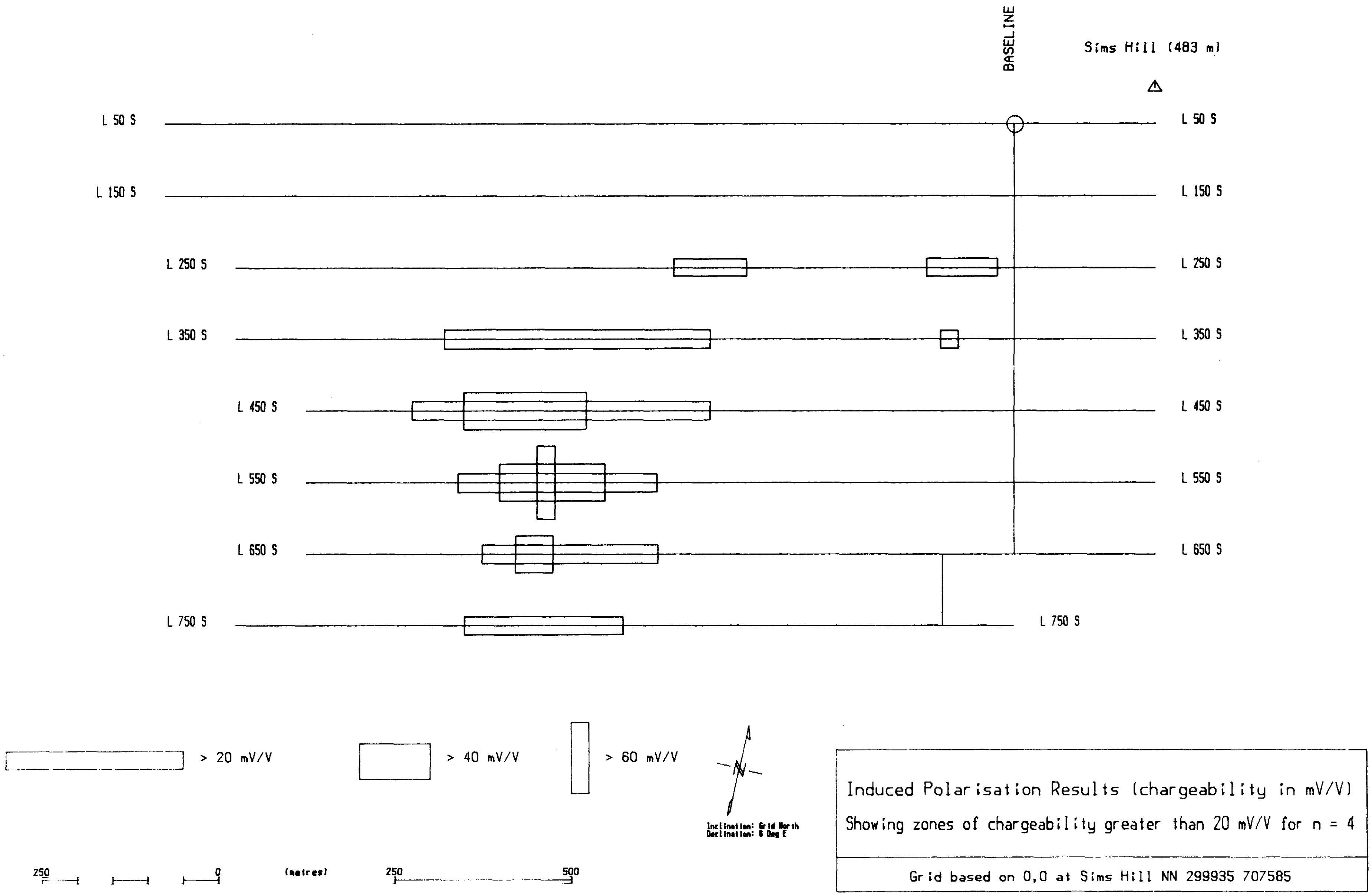

Figure 18 Induced polarisation results, Borland Glen.

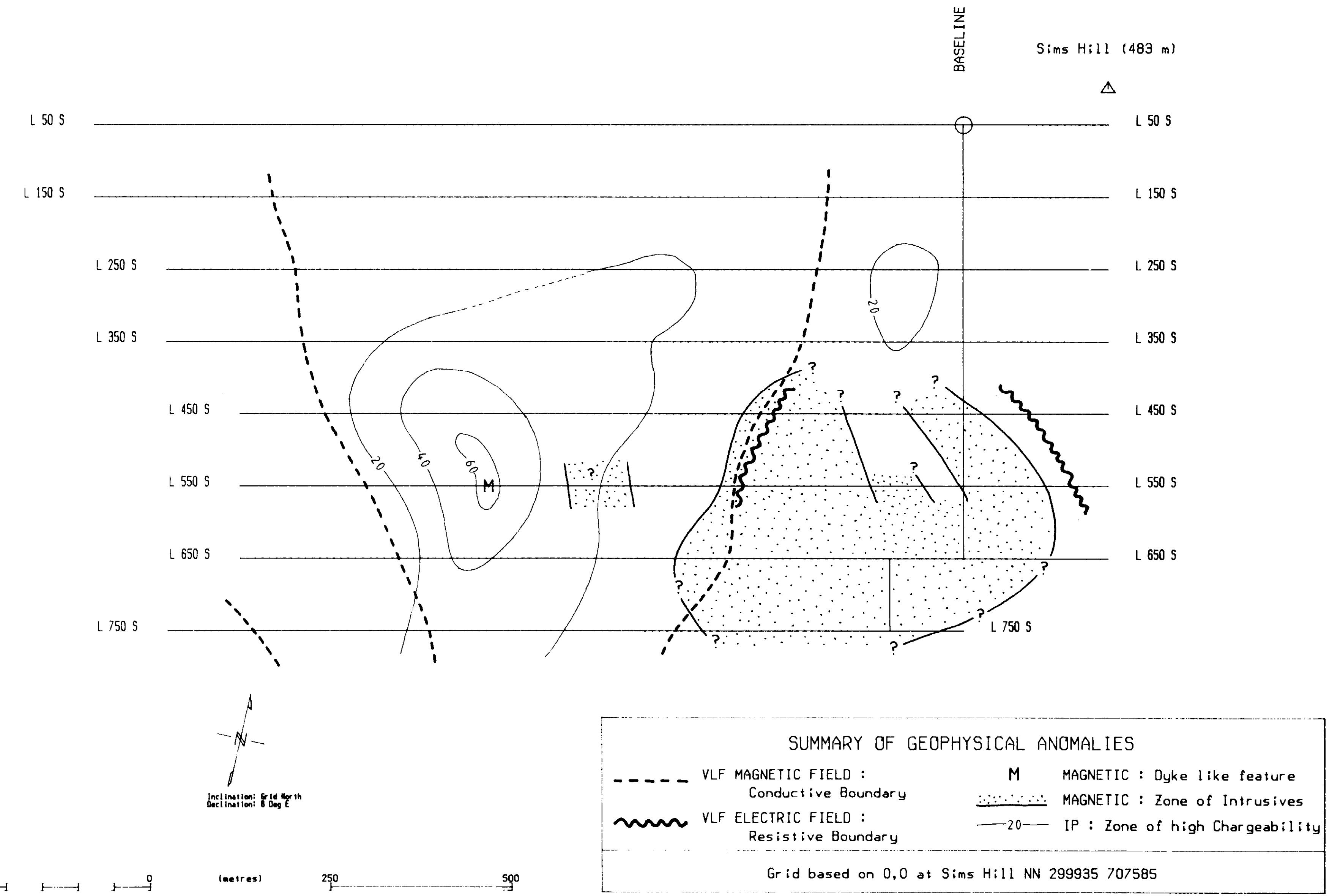

Figure 19 Summary of geophysical anomalies, Borland Glen.

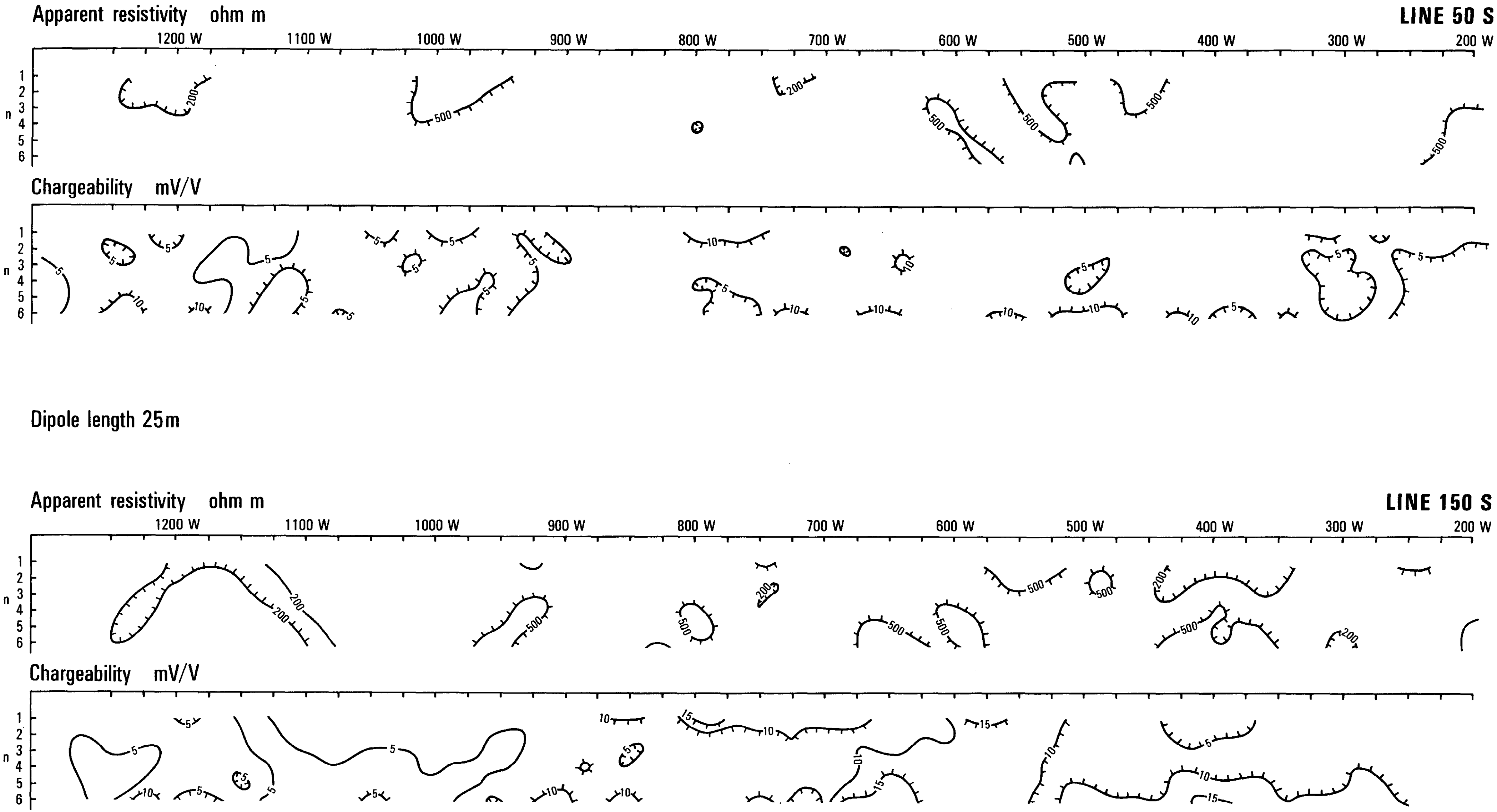

Figure 20 Cross sections of chargeability and apparent resistivity on lines 50S and 150S.

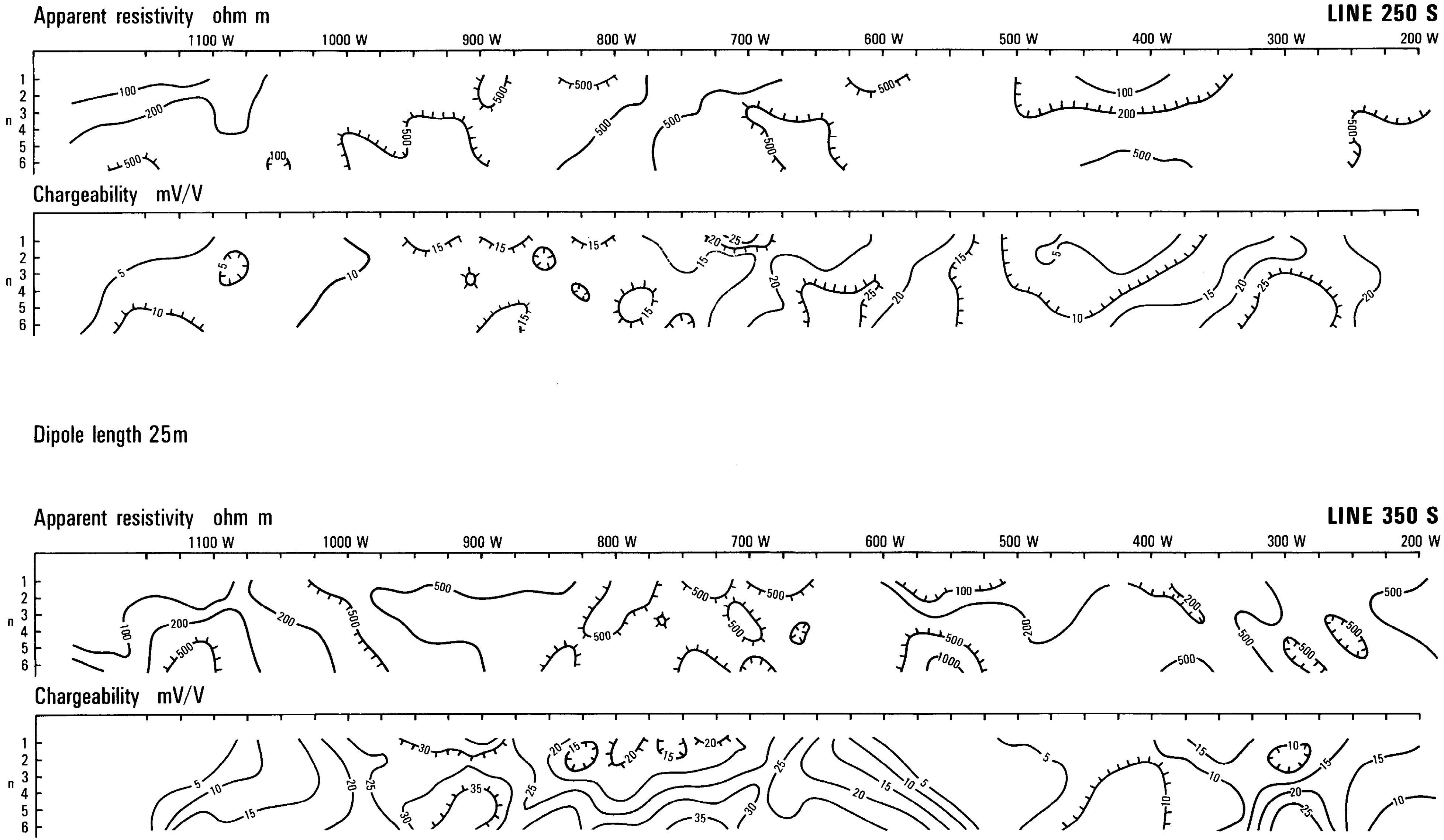

Figure 21 Cross sections of chargeability and apparent resistivity on lines 250S and 350S.

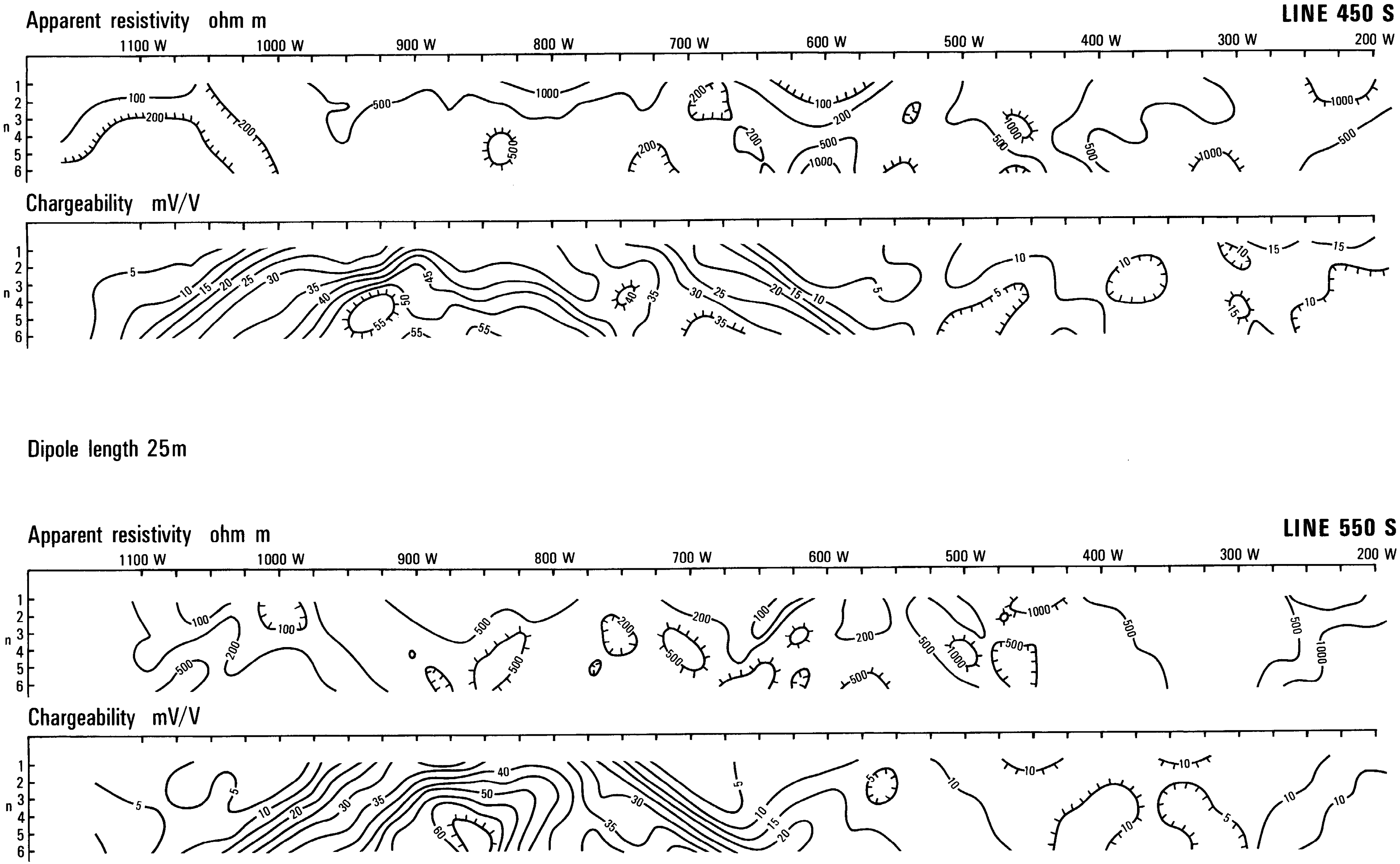

Figure 22 Cross sections of chargeability and apparent resistivity on lines 450S and 550S.

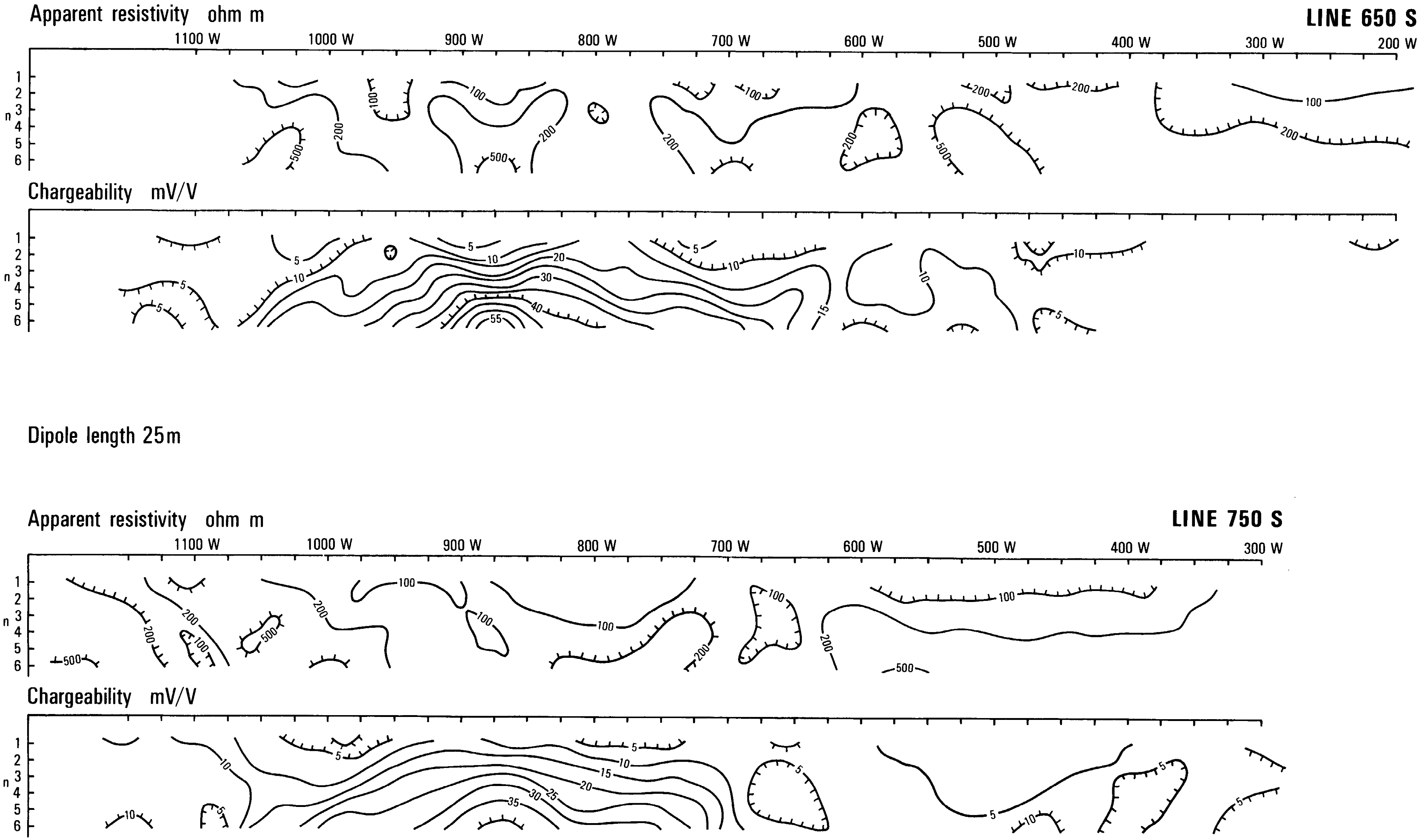

Figure 23 Cross sections of chargeability and apparent resistivity on lines 650S and 750S.

to the west. The northern extent of the zone cannot be determined from the present data; it may terminate north of line 250S or alternatively the top surface may be buried here at a depth greater than approximately 50 m and may thus continue north towards the watershed.

The anomalous zone apparently continues south of line 750S, although chargeabilities are not as high as seen on lines 450S and 550S. Since the electric field associated with the electrode array is three-dimensional (hemispherical for a medium of uniform resistivity) the array 'looks' sideways as well as directly downwards. Thus a plug-like, cylindrical zone could yield the variation in pattern seen between the pseudo-sections illustrated in lines 350S to 750S, as could equally an elongated zone whose northerly and southerly extent continued at depth.

To test the induced polarisation anomalies a series of boreholes was proposed, and the sites listed in order of priority for drilling as follows:

A: Line 550 S @ 850 W	|	
B: Line 450 S @ 900 W	|	
C: Line 650 S @ 875 W	|	Well defined zone
D: Line 750 S @ 875 W	|	
E: Line 350 S @ 900 W	|	
F: Line 250 S @ 300 W		Less clearly defined zone

At sites A and B mineralisation was expected to be very close to the ground surface (<5 m), and to be in excess of 10 m beneath the ground surface at sites C, D and E. Site F was proposed to test for the existence of a zone of mineralisation physically separate from the zone investigated by boreholes A to E. At site F weak mineralisation was suggested at a depth of 20 - 40 m below ground surface.

Boreholes 3, 1, 4, 7 and 6 were subsequently drilled at (or as close as practicable to) sites A, B, C, D and F respectively. The results of the drilling, and the geophysical logging of the boreholes, are described below.

Hodyclach Burn area

Survey methods

A grid of six lines each 2 km long and 200 m apart was established north-west of Sim's Hill (Figure 12) to seek any northward continuation of the anomalous IP zone from Borland Glen, or any other similar zones of sulphidic material.

Similar equipment and methods to those employed in the Borland Glen area were used for the induced polarisation, magnetic and VLF-EM surveys. The dipole length for the IP survey was, however, increased to 50m, providing a corresponding increase in the depth of investigation. A generator-powered 3.5kW transmitter was again used, to ensure an adequate signal-to-noise ratio. The source of the VLF primary field was the transmitter at Medoc, France (FUO, frequency 16.8kHz). This is similar, in terms of power, distance and azimuth to the Bordeaux station, which was not transmitting at the time of the Hodyclach survey.

VLF and magnetic results

Observations for both the magnetic (total field) and VLF (magnetic and electric fields) were made at 10 m intervals along all six survey lines. The results for the magnetic (total field) are illustrated as stacked profiles in Figure 24. The VLF results are illustrated as in-phase and out-of-phase components similarly in Figure 25; as Fraser filtered in-phase component in Figure 26; and as apparent resistivity and phase angle in Figure 27.

The most notable feature of the magnetic results (Figure 24) is the magnetically 'quiet' area in the south-east quadrant of the grid adjacent to Sim's Hill. This is attributed to alteration of the fresh andesite-basalt lavas where magnetite (magnetic) becomes hematite and/or pyrite (both non-magnetic), whilst the introduction of calcite and quartz by hydrothermal fluids has filled the interstitial spaces and cracks, thus displacing the original (electrically conductive) pore fluids. Evidence for the latter process is provided by the VLF (electric field) results of apparent resistivity and phase angle seen in Figure 27 where an area of higher value apparent resistivity coincides with the magnetically 'quiet' area.

Correlations of the magnetic profiles on adjacent survey lines are not readily made in the remaining 'noisy' quadrants of the grid. The pattern and amplitude of the profiles are typical of that seen over a series of volcanic rocks rich in magnetite. In the north-west quadrant three or four major bands trending roughly north - south may correspond to the variation in lava types reported as flow banded rhyolitic, lenses of trachyandesite and andesite-basalt.

Wire fences intersecting lines 0, 200N, 600N, 800N and 1000N are indicated by the classic crossover features seen in the VLF magnetic field in-phase and out-of-phase data (Figure 25). Although of similar construction, the orientation of the wires, the variation in their degree of electrical (galvanic) isolation from the ground and the local topography combine to give the variations in amplitude seen in Figure 25.

Other perturbations in the VLF magnetic field data may be ascribed to variations in the overburden thickness and local topography including several small streams. However, it is possible to correlate the major north - south trending bands inferred from the high magnetic values with the corresponding VLF (magnetic field) results that display a numerically high negative in-phase component. This gross pattern obtains for all lines except due east of the base on lines 800N and 1000N where the in-phase components are markedly positive. These lines lie on the hill of Little Law where andesite agglomerates are reported.

The survey grid is bisected by the Hodyclach Burn which flows north to intersect the baseline over line 600N (see Figure 12). A degree of correlation is seen in both the magnetic and VLF (magnetic field) results with the course of the Hodyclach Burn and in the summary map of geophysical anomalies (Figure 28) as a boundary that may be inferred to lie between the (magnetic) zone of alteration and the (VLF and magnetic) zone of banding. Because the depth of investigation of the IP and magnetic techniques is much greater than that of the VLF (magnetic and electric fields) it is suggested that the course of the burn has been dictated in part by a junction of different rock types.

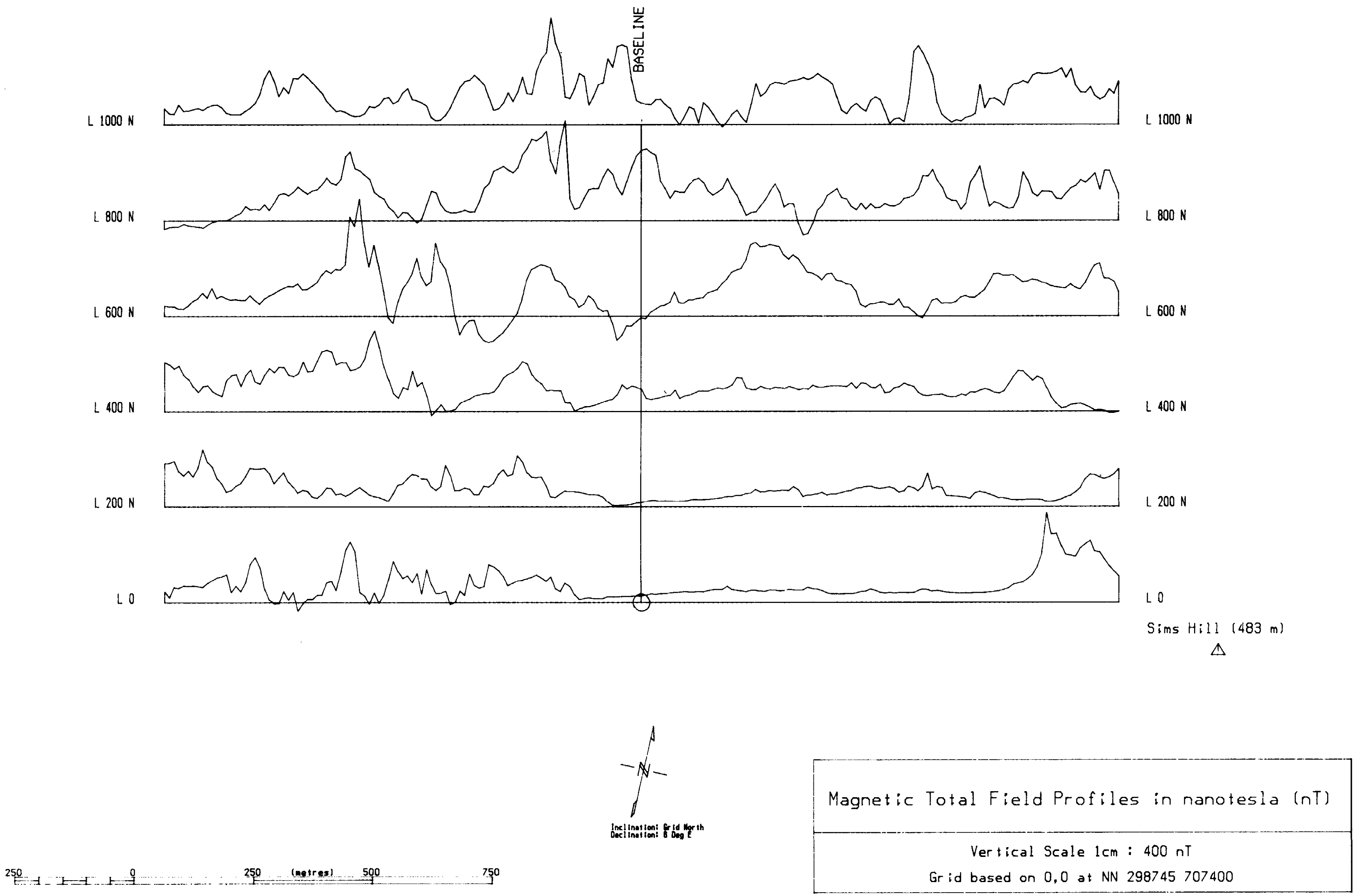

Figure 24 Magnetic total field profiles, Hodyclach Burn.

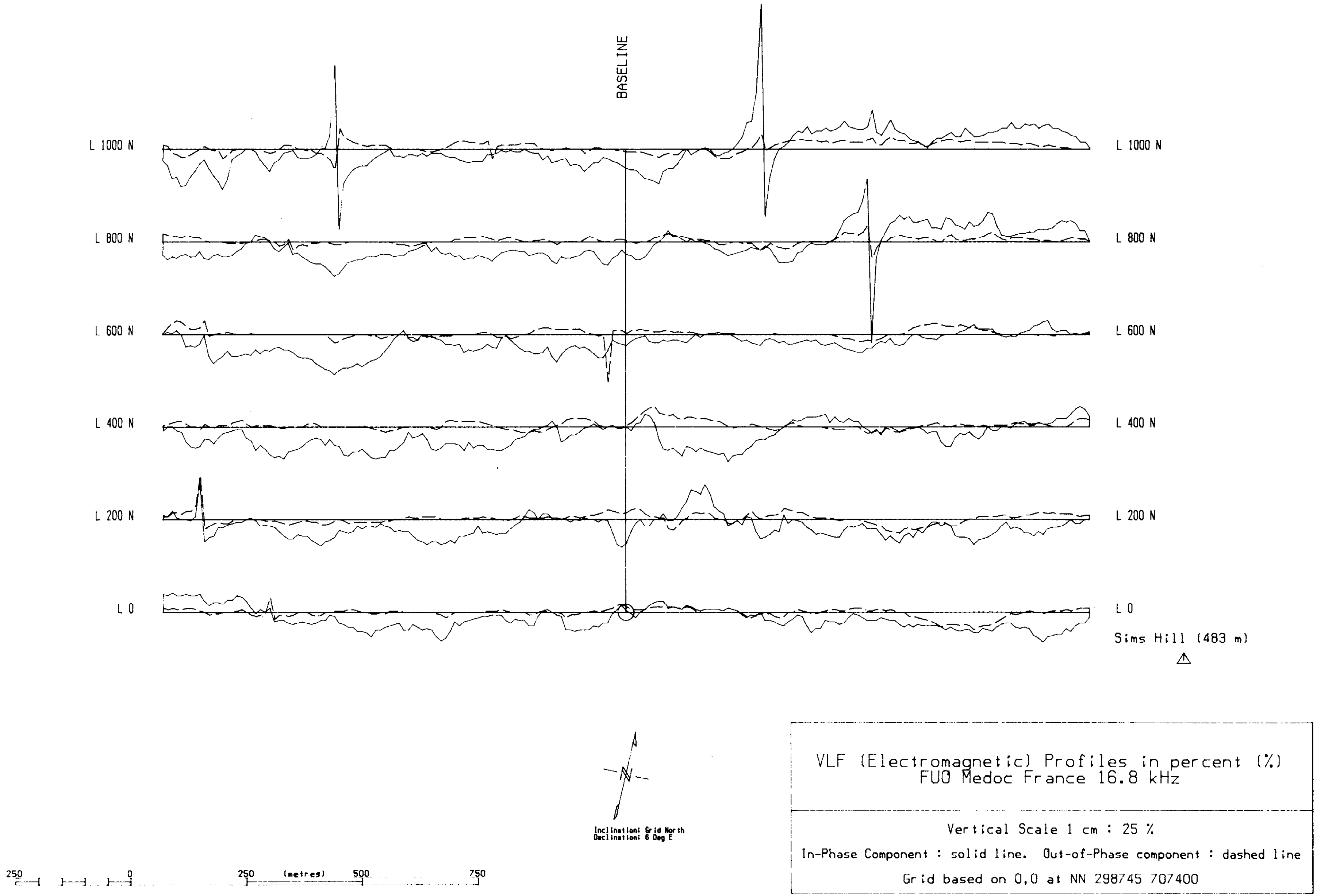

Figure 25 VLF electromagnetic (magnetic field) profiles, Hodyclach Burn.

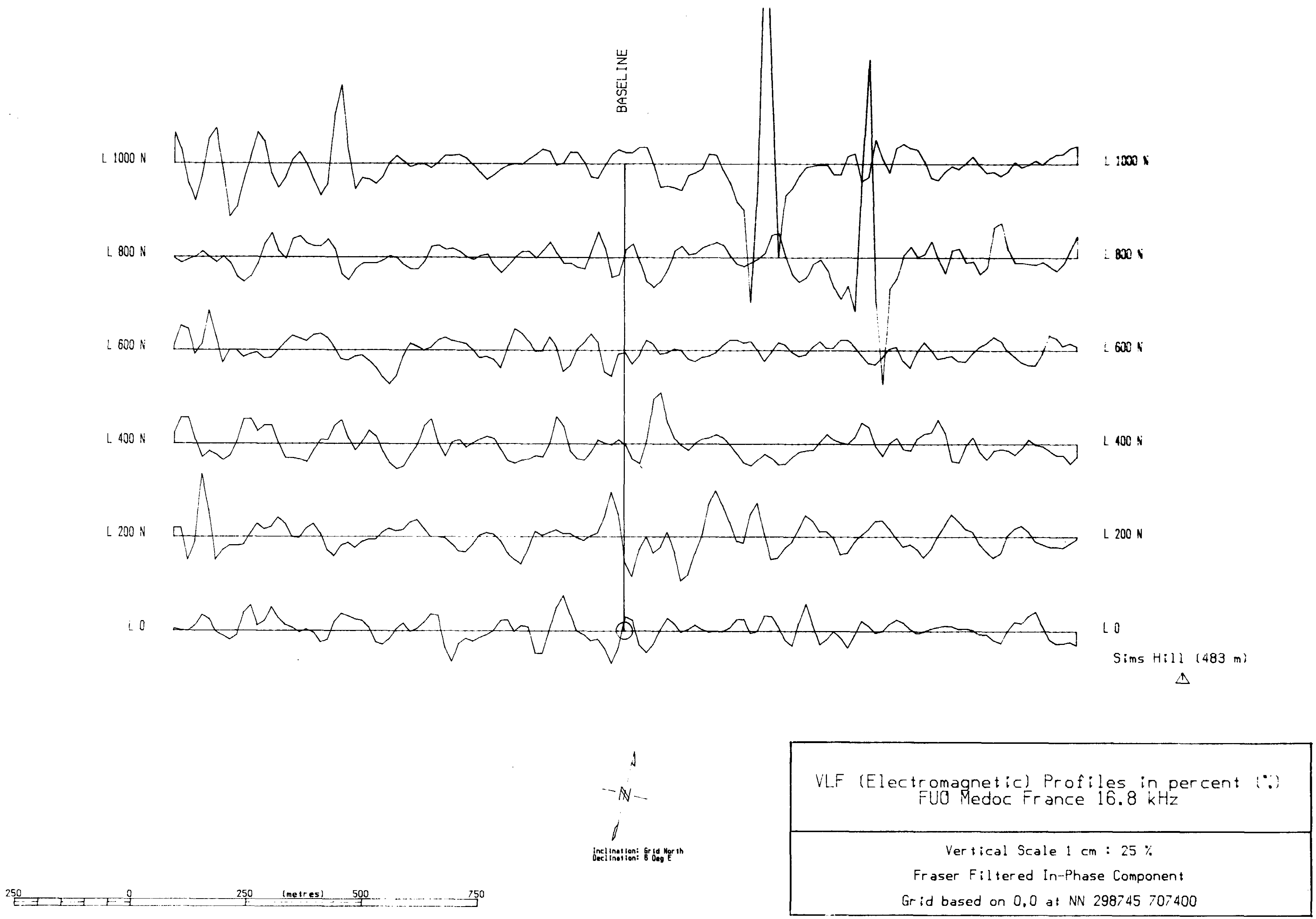

Figure 26 VLF Fraser filter profiles, Hodyclach Burn.

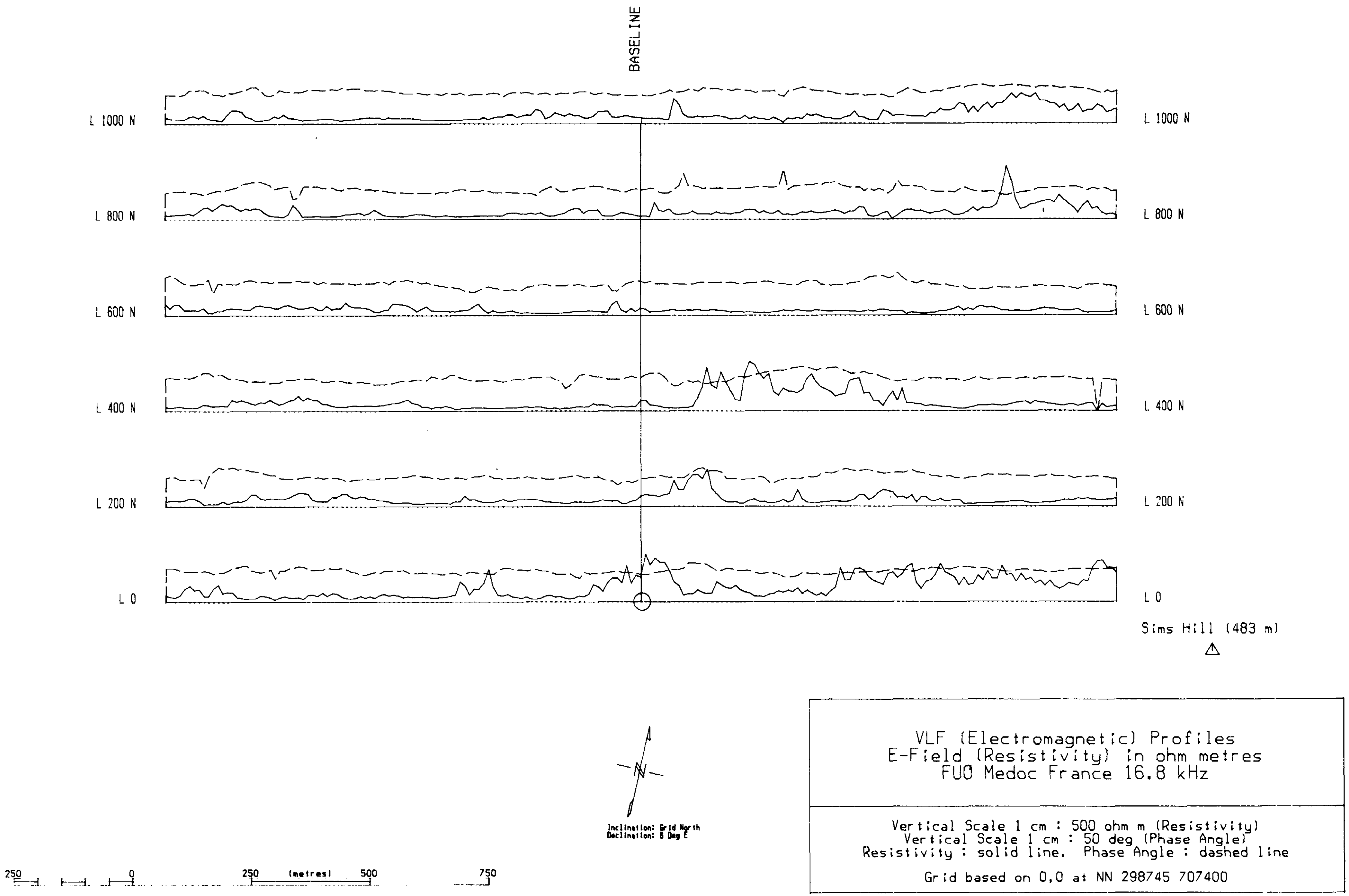

Figure 27 VLF electromagnetic (electric field) profiles, Hodyclach Burn.

Induced polarisation results
The results of the IP survey are illustrated as pseudo-sections of chargeability and apparent resistivity in Figures 29 - 31 and the anomalous chargeability zones summarised in plan view in Figure 28.

The background values for the chargeability of about 5mV/V and the apparent resistivity of between 100 to 400 ohm-m are similar to those obtained in the adjacent Borland Glen area in 1988. But a feature of the data, not seen in the results for Borland Glen, is that on each line of the present survey some negative chargeability was recorded. When this occurred a repeated measurement (or series of measurements) always confirmed the negative value so these values are considered genuine artifacts of the subsurface geological environment. The numerically highest chargeability anomaly is on line 1000N 'beneath' 325E at a depth of about 75 m. The very localised nature of this feature as shown by the pseudo section in Figure 31 provides no clues as to its geometrical form, so drilling is not warranted.

All six lines show at the maximum (depth) 'n' value of 6, one or more isolated locations where the chargeability rises to about twice background (ie 2 x 5 mV/V). These rises may be due to local increases in pyrite or pyrrhotite or are false values due to operating the Rx/Tx array geometry combination at its effective limit (ie the signal to noise ratio is becoming unacceptable at some of the observation stations). In the northern half of the survey area a degree of correlation obtains between these IP features and high values of the magnetic total field suggesting widespread disseminations of pyrrhotite.

Summary

The induced polarisation results for the Borland glen survey area are particularly encouraging as excellent response was obtained over a zone of inferred mineralisation. The VLF method only responded to the linear conductors formed by the two major streams, whilst the magnetic results indicate previously unmapped alteration zones in the Devonian lavas. Neither the VLF nor the magnetic results are a direct guide to mineralisation. The induced polarisation results, however, enabled a series of exploratory boreholes to be sited with confidence.

In the Hodyclach Burn area no significant induced polarisation anomalies were found and it is concluded that within the depth investigated by the present survey the sulphidic material detected to the south is absent. At depth, minor chargeability anomalies may be localised occurences of pyrite or pyrrhotite associated with mineralogical changes within the lavas. In the south-east of the survey grid an extensive area of alteration within the andesite and basalt is indicated from the magnetic data, whilst elsewhere major zones of banding of volcanic rocks is suggested, and both are supported in part by the VLF (magnetic and electric field) data. These results are not considered sufficiently encouraging to justify drilling.

No recommendations are made for any additional geophysics. However, future developments outside the sphere of BGS may dictate further exploratory work in the area, and if so a large scale induced polarisation survey is undoubtedly the preferred geophysical technique.

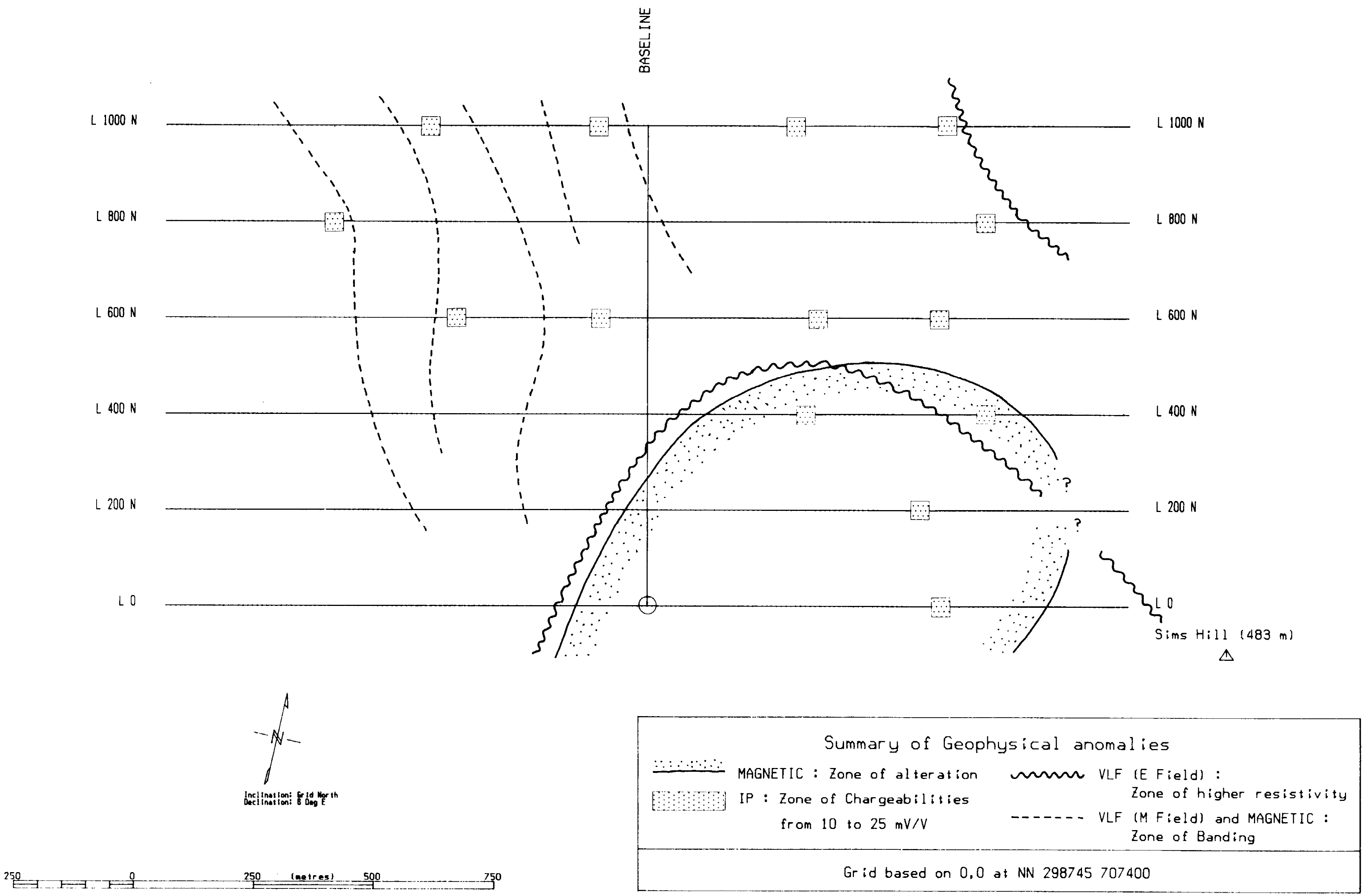

Figure 28 Summary of geophysical results, Hodyclach Burn.

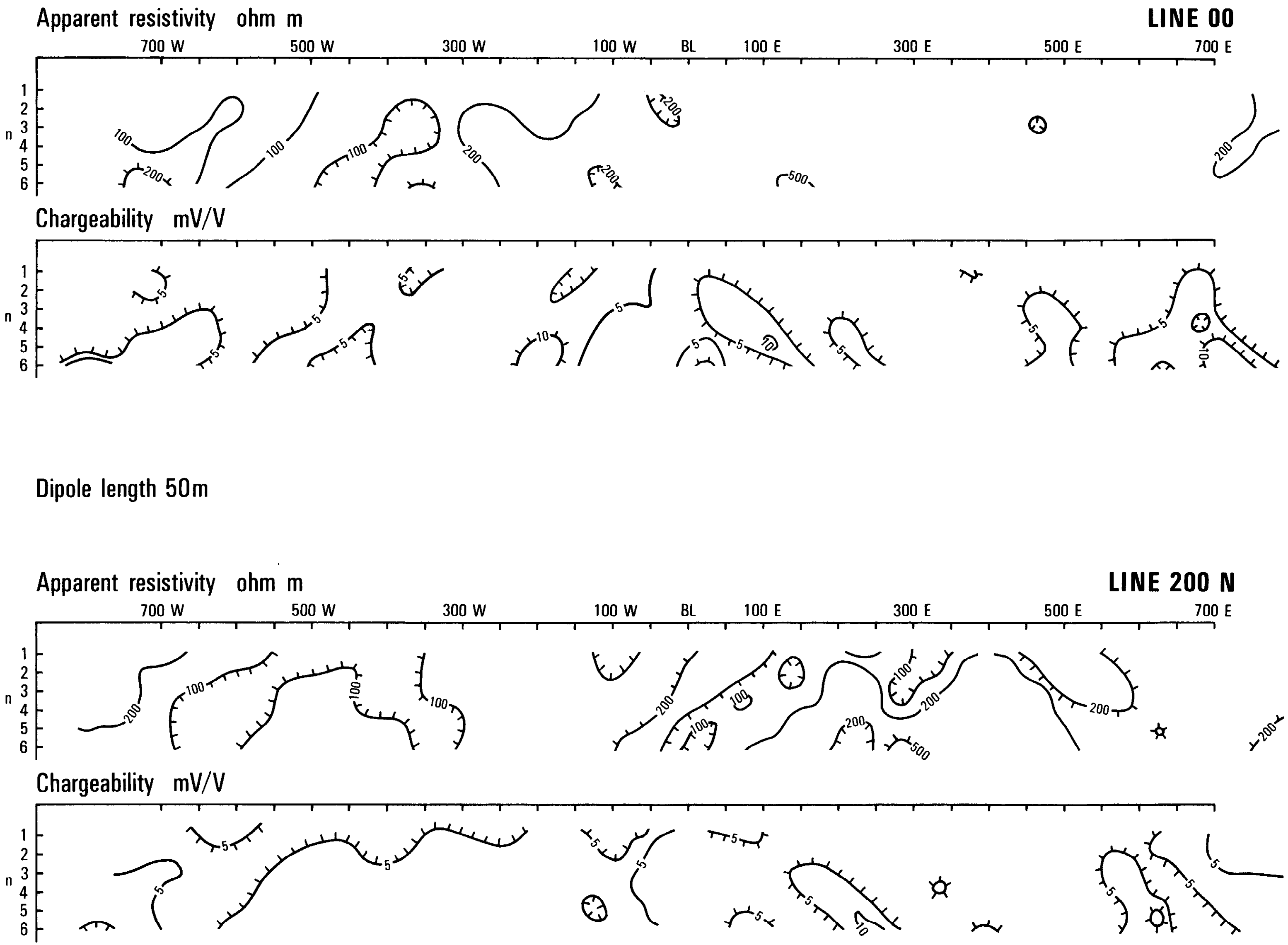

Figure 29 Cross sections of chargeability and apparent resistivity on lines 00 and 200N.

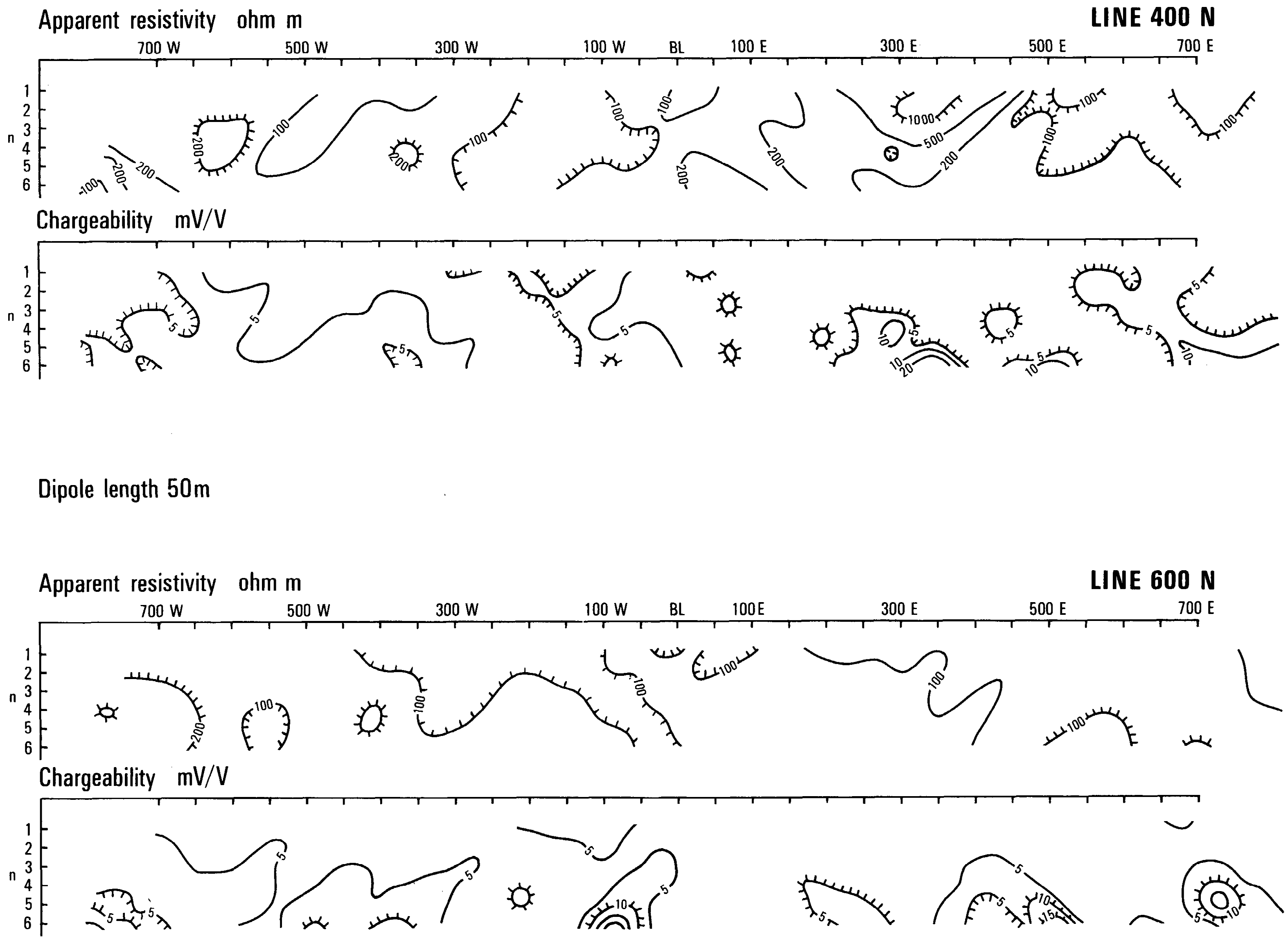

Figure 30 Cross sections of chargeability and apparent resistivity on lines 400N and 600N.

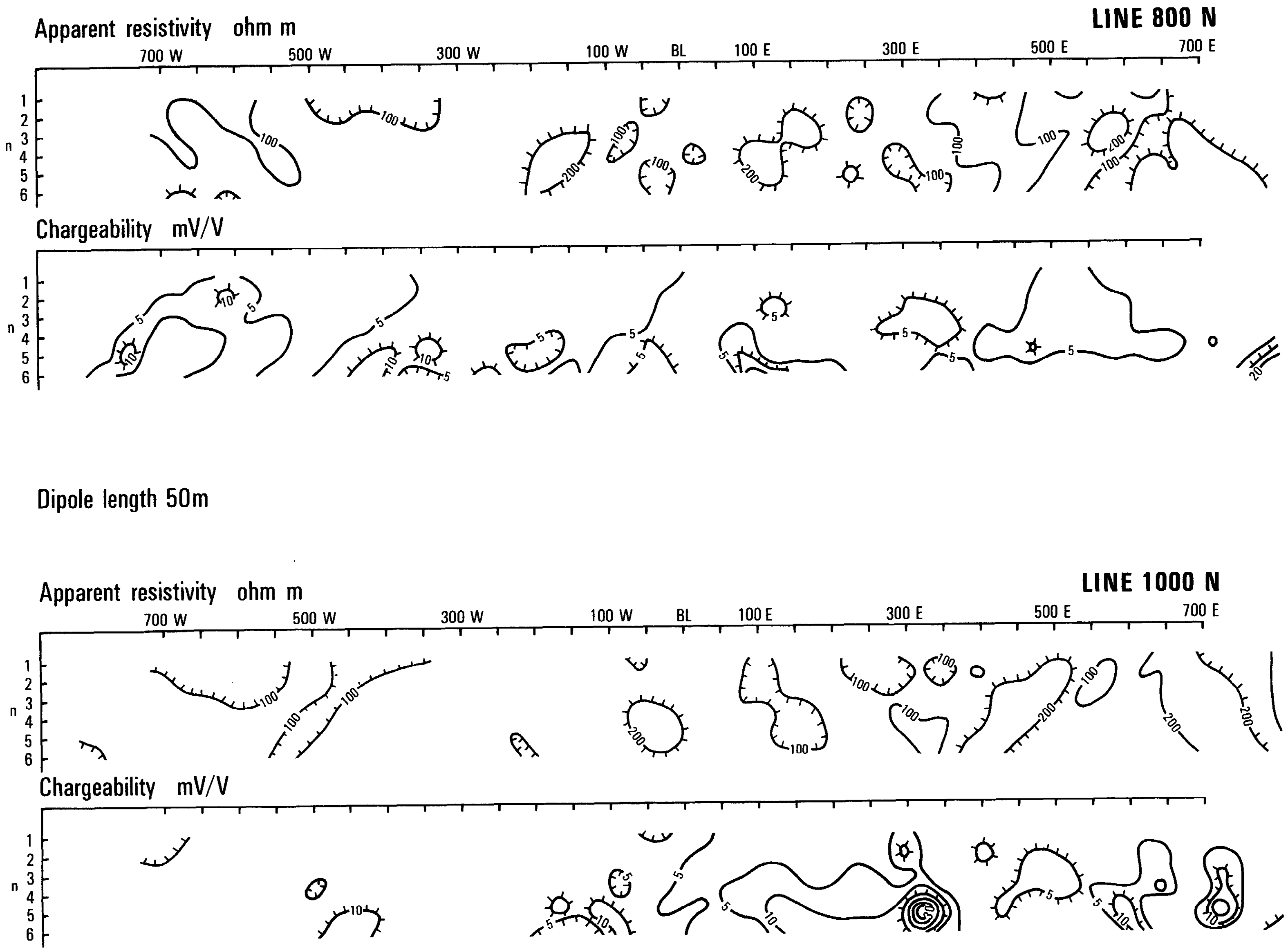

Figure 31 Cross sections of chargeability and apparent resistivity on lines 800N and 1000N.

MINERALOGY AND GEOCHEMISTRY OF SURFACE ROCK SAMPLES

Mineralogy

Introduction

The following notes describe rock samples from surface outcrops collected 1988 - 1990. Most of the work was carried out by optical microscopic examination of covered and polished thin sections.

Rock samples taken from surface exposure in the Borland Glen area were examined petrographically, and full descriptions are given in Fortey (1990). The general geology of the area is of units of basalt and andesite lavas which are interbedded with units of agglomerate and tuff, the sequence being cut by diorite stocks surrounded by a zone of mild contact metamorphism, and also cut by porphyry dykes. The rocks are part of a high-level, calc-alkaline volcanic complex which has not suffered signigicant deformation or regional metamorphism.

The samples under discussion were collected from sites along Borland Glen and the surrounding hill slopes. A small group was also taken from Hodyclach Burn, some 2 km north-north-west of Borland Glen. Locations are shown in Figure 32 on the geological base map and given as National Grid References to the nearest 10 m (Fortey, 1990). Lithologies generally agree with their identities as indicated on this map, and will be considered below, in terms of the geological groupings so defined, into basalt/andesite lavas, pyroclastic rocks, diorite and dyke rocks.

Basalts and andesites

A small suite of samples were examined. They can be divided into those representing lavas exposed in Borland Glen and others stratigraphically higher which are exposed on the upper parts of Ben Thrush and Green Law as well as in the Hodyclach Burn stream section. These two sets of lavas are separated by pyroclastic deposits.

Borland Glen area. Two samples from White Creich Hill (KLM 1011, 1015) are described as porphyritic microgabbro, unmineralised, showing weak alteration. Plagioclase is partially sericitised and pyroxene part made over to carbonate or to actinolite and chlorite. In KLM 1015 basaltic lava is crossed by a pink vein of vuggy biotite microgranite. The site is close to a small exposure of diorite on the south-west side of White Creich Hill (see below).

A sample from Creich Burn in Borland Glen (KLM 1035) just north of the main diorite intrusion is a weakly vesicular andesite with mild sericite-chlorite alteration. South of the diorite, lavas interbedded in a dominantly pyroclastic sequence include a biotitic andesite or dacite whose alteration assemblage includes actinolite and muscovite (KLM 1024). A second sample from this location (KLM 1023) proved to be an agglomeratic pyroclastic rock. Other lavas from this area included andesite with chloritic alteration (KLM 1025) or more complex sericitic alteration (KLM 1031). Grey lava exposed well south of the main diorite (KLM 1046) is a weakly altered augite microgabbro.

On the west side of Borland Glen, samples from a shallow trench included three basalts

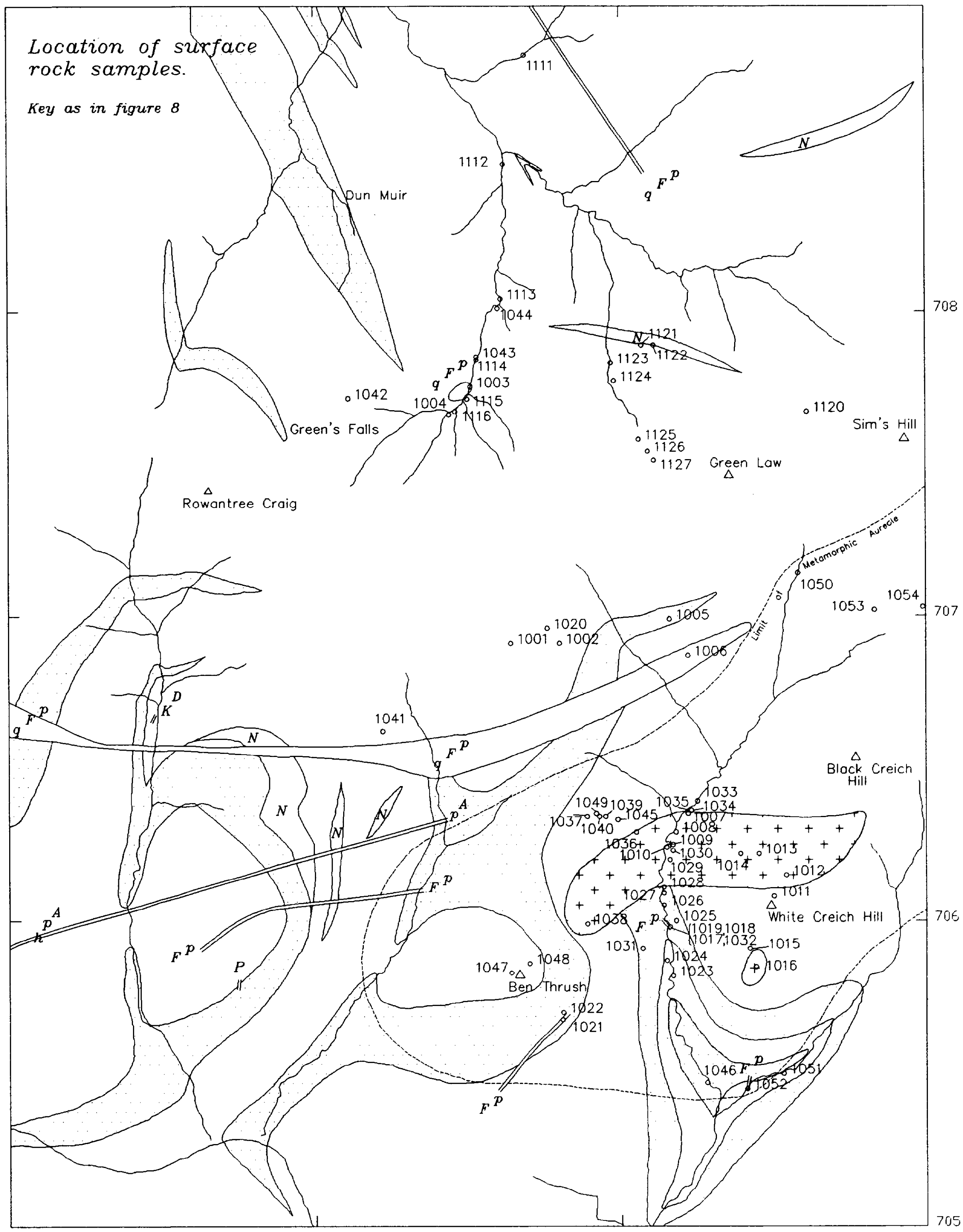

Figure 32 Location of surface rock samples.

(KLM 1037, 1039, 1040). These include porphyritic basalt and/or andesite with only mild sericite-chlorite-carbonate alteration. In KLM 1037 chloritisation is more intense, and the rock carries a network of vuggy quartz-chlorite fracture veinlets.

Green Law and related locations. Two samples from the upper part of Ben Thrush (KLM 1047, 1048) are porphyritic basalt showing partial alteration to sericite-carbonate-chlorite. Pink feldspathic veins cut the hand specimen of KLM 1048 but were not captured in thin section. Exposures on high ground around Green Law (KLM 1001, 1002, 1050) comprise porphyritic basalt and andesite with a moderate degree of carbonate-sericite-chlorite alteration.

Exposures at Hodyclach Burn (KLM 1004, 1042, 1043, 1044) include microporphyritic basalt with very little alteration (KLM 1004) and porphyritic biotite-andesite with weak albitic alteration of plagioclase (KLM 1043) and sericitisation (KLM 1044).

Pyroclastic rocks

A unit of 'agglomerate and tuff' which outcrops around Ben Thrush and extends north-east to Green Law is represented by a single sample (KLM 1005) from the zone of strong alteration and pyritisation which was the focus of follow up diamond drilling. The rock was described in the field as a feldspathic agglomerate. The piece examined was a coherent piece of biotitic andesite or dacite with 'phyllic' alteration involving formation of secondary quartz, sericite and muscovite together with partial dissolution of the 1-2 mm long plagioclase phenocrysts. Original disseminated sulphide, probably pyrite, has been completely oxidised during penetrative weathering. The sample presumably is a single clast from the agglomerate.

Pyroclastic rocks which outcrop in the lower part of Borland Glen, south of the main diorite, were represented by a small group of samples. Some were of solid andesite lavas as already described. Others (KLM 1023, 1026, 1027) are agglomerates in which fragments of andesite and basalt are cemented by a comminuted rock matrix. These rocks show strong hydrothermal alteration. KLM 1023 suffered epidote-hornblende alteration followed by sericitisation accompanied by fine grained secondary biotite. KLM 1026 shows carbonate-chlorite-quartz alteration with seondary quartz common in its vuggy matrix. Grains of probable suphide have been oxidised to goethitic material during weathering.

Diorite

Several samples from the main diorite body exposed in Borland Glen were examined, together with one from the small satellite exposure south of the main mass at White Creich Hill. Taken as a whole, the samples indicate that the intrusion contains areas of gabbro as well as diorite, and varies from coarse grained to medium grained. The gabbro samples (KLM 1008, 1012, 1013, 1014, 1028, 1038) show a quartz-normative, panidiomorphic granular rock with abundant augite. Altered olivine grains are a minor constituent of KLM 1008 and KLM 1029. Alteration is generally weak and deuteric in character. Hydrothermal quartz fracture veinlets carry pyrite and traces of chalcopyrite in KLM 1029.

The diorite samples (KLM 1009, 1016, 1028, 1053) contain biotite and hornblende. Interstitial quartz is accompanied by minor orthoclase. Alteration is again rather weak, including partial sericitisation of plagioclase and chloritisation of mafic silicates. Actinolite and epidote are also minor secondary constituents. Magmatic opaque grains (ilmenite-magnetite intergrowths) are common, but pyrite grains are only a minor component of the rock.

It is apparent that the diorite is a massive body which has escaped strong hydrothermal alteration. Pink feldspar veinlets recorded from the quarry exposure of KLM 1013 indicate local penetration of the intrusion by hydrothermal fluid on joints.

Dyke rocks

Samples representing eleven individual dykes were examined. So far as can be judged, bearing in mind their frequent altered condition, the dykes range from andesite to rhyodacite, and they can be described as pink feldspar porphyry to quartz-feldspar porphyry. Weathering oxidation is frequent, leading to considerable destruction of original pyritic sulphides.

Dykes exposed in Borland Glen south of the diorite (KLM 1017, 1018, 1019, 1032, 1051, 1052) display strong quartz-sericite-carbonate-chlorite alteration accompanied by fine disseminated pyrite. Slender fracture veinlets carrying quartz, carbonate and pyrite are common. Dykes cutting the diorite (KLM 1010, 1030) again show strong sericitic alteration and pyrite disseminations. Dykes exposed in the cutting on the western slope of Borland Glen (KLM 1036, 1045, 1049) show the same pattern of alteration in which plagioclase is sericitised, pyroxene chloritised and biotite replaced by plates of muscovite. Pyrite occurs finely disseminated and grown along hairline fracture veinlets. Comparable features are recorded again in dykes exposed on the south-east side of Ben Thrush (KLM 1021, 1022) and in a dyke south-west of Green Law (KLM 1020) and south-east of Green Law (KLM 1054).

Sample KLM 1006 is from a dyke in the follow up target zone on the southern slope of Green Law. The site is close to that of the dacitic tuff KLM 1005 already discussed. In KLM 1006, the tenor of the pervasive alteration of the dacitic porphyry is lower than in the neighbouring sample, but the rock carries a network of vuggy, chalcedonic fractures. Penetrative weathering has destroyed original sulphides, although such material was probably a major constituent at an earlier stage.

A dyke exposed in Hodyclach Burn (KLM 1003) is a rhyodactic porphyry in which alteration is weak and primary biotite and magnetite are preserved.

Discussion

These results indicate that hydrothermal alteration is not generally strong in the lavas or in the diorite. It becomes more prevalent in the more permeable pyroclastic rocks, and is strongest in the dyke rocks. In addition, alteration of the lavas and diorite typically has a chloritic character, while that in the pyroclastics and dykes is more muscovitic. Analogies with propylitic and phyllic styles of alteration are suggested. Impregnations of fine grained pyrite occur mostly in the muscovitic alteration.

The pattern of alteration and pyritisation was evidently controlled by permeable structures in the form of pyroclastic units and fractured dykes. No major discordant hydrothermal structures have been observed. It is suggested that the hydrothermal activity was intimately related to the volcanism, probably taking place during the late stage of prophyry dyke emplacement. Though emplaced later than the diorite stock, it can be proposed that the concentration of altered, pyritised dykes around this intrusion reflects a degree of centralised control of intrusive activity and hydrothermal processes in the Borland Glen area.

Geochemistry

Basalts and andesites

Twenty seven samples of the andesitic lavas from the area of Figure 32 were analysed by XRF for the range of elements given in Table 4 and for Au by AAS after an aqua regia attack. Median values for the elements (Table 4) compare fairly closely with the mean composition of north Midland Valley lavas (Thirlwall, 1981, Table 4). Elements that are enriched compared to the average are V, Cr, Fe, Mn and Ni, and the elements that are depleted are Ca, Ti, Rb, Y, Zr, Ba, La, Ce and Th. This can be illustrated by spidergram plots (Figure 33) which show that the Borland Glen andesites are slightly more primitive and closer to the MORB in composition than the mean given by Thirlwall, though they are not as primitive as his high Ni group.

Some samples show evidence of mineralisation as well as the mineralogical alteration. The two samples with detectable Au, KLR 1050 with 20 ppb and KLR 1051 with 10 ppb, are both located near the limit of the metamorphic aureole of the diorite intrusion but at these extremely low levels too much should not be read into these isolated occurrences.

KLR 1039, which was collected from a small stream section on the west side of Borland Glen, has a high barium content of 2632 ppm indicating addition of baryte. A neighbouring sample, KLR 1040, has 1580 ppm Ba, also indicating baryte mineralisation. KLR 1022, which is a sample of andesite lava adjacent to a feldspar-porphyry dyke, is also slightly enriched in barium (1056 ppm).

One andesite (KLR 1035) near the main diorite outcrop is 0enriched in lead (85 ppm). This sample shows evidence of mild sericite-chlorite alteration and possibly contains small amounts of galena. Lavas enriched in zinc are KLR 1007 and 1034, both adjacent to the diorite body, and KLR 1037 from the west side of Borland Glen, which mineralogically shows intense chloritic alteration. An isolated sample KLR 1127 is also slightly anomalous in zinc. Minor base metal enrichment of barium, lead or zinc is indicated in Borland Glen adjacent to small porphyry dykes and the diorite.

Pyroclastic rocks

Eight samples of pyroclastic rocks were analysed. Their chemistry is similar to the andesites for the incompatible elements such as Ba, La, Ce, and Rb but is noticeably depleted in elements such as Ca, Fe, Co, Ni, Cu, and Sr. This is probably the result of leaching and subaerial weathering soon after deposition. Some samples show evidence of mineralisation, with KLR 1027 and 1028 having high levels of Sr (indicating calcite addition), As and Sb. These two samples of agglomerate were collected from the Borland Glen stream section adjacent to the diorite and show strong hydrothermal alteration. KLR 1028 also has a lower Ba content than expected and this feature is shown by samples KLR 1126 and 1127 from the north side of Green Law (Figure 32) which have some of the lowest Ba and Sr contents of all the rocks.

Table 4 Comparison of median compositions of lava, pyroclastic, porphyry and diorite with average north Midland Valley lava.

	Andesite (N=27)	Pyroclastic (N=8)	Porphyry (N=11)	Diorite (N=14)	NMV lava (N=44)
Element					
Ca	19400	3600	14500	39150	26660
Ti	4020	2365	2700	5680	5216
V	90	51	51	124	82
Cr	164	154	119	147	31
Mn	1030	860	1150	1200	620
Fe	43700	24100	27700	50250	37370
Co	20	8	12	27	
Ni	28	12	9	45	19
Cu	18	3	17	35	16
Zn	73	74	82	87	74
As	16	27	26	11	
Rb	53	77	60	32	78
Sr	459	240	287	609	490
Y	16	16	16	19	27
Zr	163	140	171	195	305
Mo	6	6	4	3	
Ag	1	0	0	1	
Sb	1	4	4	1	
Ba	571	501	580	449	760
La	27	23	23	24	38
Ce	31	33	32	35	82
Pb	20	20	16	24	
Th	6	7	5	5	12
U	3	2	4	2	

Notes

1. All elements in ppm and determined by XRF.
2. Au and Bi have median contents less then detection limit.
3. Cr levels may be enhanced by contamination from Cr steel used in sample preparation.
3. NMV lavas are mean values of north Midland Valley intermediate lavas (Thirlwall, 1981, Table 4).

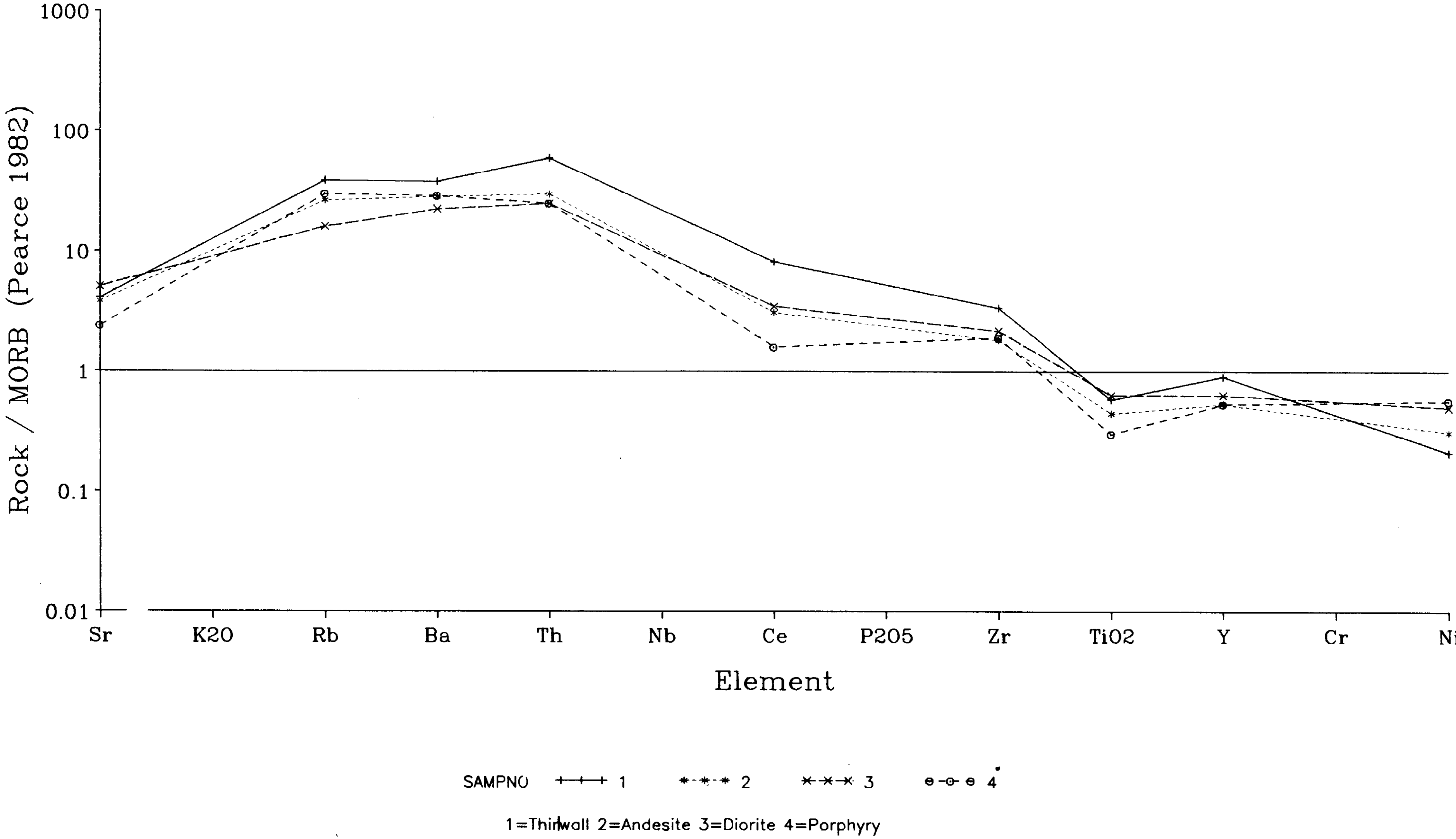

Figure 33 Spidergram plots of the main rock types in Borland Glen compared with average north Midland Valley lava, all normalised to MORB.

Diorite

Thirteen samples of the main diorite mass and one of the subsidiary body were analysed. The chemical character of the diorite is very similar to that of the andesites as shown by the spidergram (Figure 33), and the two suites are obviously consanguineous. The diorite is more basic in character with higher Ca, Sr, Ti, Mn, Fe, Co, Ni, Cu,

Zn, Y and Zr and lower Rb and Ba. None of the diorite samples show strong evidence of mineralisation except for slightly elevated Cu values up to 76 ppm in KLR 1029, a sample containing hydrothermal quartz veinlets with pyrite and chalcopyrite. The lack of high values of elements such as As, Sb or Ba shows that the hydrothermal alteration is generally weak.

Dyke rocks

The dyke rocks are more fractionated than the andesites, with lower contents of most elements except for Ba, Rb, Zn and As (Table 4). The dykes are also much more mineralised than the other rock units. The small porphyry dyke exposed in Borland Glen to the south of the diorite has elevated As and Sb levels and its possible extension to the north-west is similarly high (samples KLR 1040 and 1049). The dyke south-east of Ben Thrush has a similar enrichment in Cu, As and Sb. The one sample from the main east - west dyke KLR 1006 is also high in As and Sb. The intrusion in Hodyclach Burn is enriched only in Zn and Cu, confirming its lower degree of alteration as shown by the mineralogy.

The barium levels in the dykes are variable, KLR 1006, 1052 and 1115 being depleted in barium, whereas KLR 1022 and 1045 are enriched. The hydrothermal alteration probably redistributes the barium by breakdown of K-felspar and the formation of baryte. Some of the dykes will therefore be leached and have low barium levels.

DRILLING

Introduction

Seven holes were drilled to investigate the source of the gold anomalies in the drainage and overburden and to ascertain the cause of the IP anomalies. The locations of the holes are given in Table 5 and abbreviated logs in Appendix 2. Full descriptive logs and the borehole cores are lodged in the National Geosciences Data Centre at BGS Keyworth.

Boreholes 1, 2, 3 and 4 were drilled to investigate the main induced polarisation anomaly and associated gold anomaly in the overburden. Borehole 5 was drilled to locate the source of the high gold in overburden (up to 119 ppb Au) near the watershed between Borland and Cloan Glens. Borehole 6 was drilled to investigate the smaller IP anomaly (site F, page 40) to the east of the main anomaly. Borehole 7 was added at the end of the drilling programme to study the southern extension of the IP zone and any possible effects of the metamorphic aureole of the diorite. The boreholes were drilled with the BGS Diamec 260 rig producing core of 57 mm diameter . Drilling conditions were normally excellent with nearly total recovery of core except in the near surface weathering zones beneath the overburden which itself was often recovered intact.

Table 5 Locations of boreholes

Borehole Number	National Grid Easting	Northing	Collar Ht (m)	Depth (m)	Inclination	Azimuth
1	299170	706930	397	101.86	90	
2	299250	706950	414	95.31	70	256
3	299280	706850	383	82.32	70	256
4	299240	706740	356	57.50	90	
5	299400	707450	475	51.46	70	256
6	299710	707260	424	50.35	90	
7	299289	706645	345	88.91	90	

Geophysical logging

Boreholes 1, 2, 3 and 7 were logged for natural gamma activity, chargeability and apparent resistivity. The gamma log was run with a Mt. Sopris 1000-C hand-winched logger; the electrical logs were recorded by deploying two electrodes of a conventional array downhole. These electrodes (cuurent and potential) were maintained at a 2 m spacing, with observations made at 1 m intervals. The remaining two electrodes were sited at surface, remote from the borehole. The observations were made with a Huntec Mk III IP transmitter and receiver. The receiver was set up to record chargeability as the area under the secondary voltage decay curve between times of 240 milliseconds and 1140 milliseconds after transmitter switch-off. Thus the chargeability values are not equivalent to those presented in the pseudo-sections for the surface IP profiles. The logs and the pseudo-sections can, however, be compared qualitively. Note that the plastic casing prevented acquisation of electrical log data in the uppermost parts of boreholes 3 and 7.

Borehole 1 was cased throughout its depth, so only a gamma log could be recorded (Figure 34). The most notable feature on this log is the sharp fall in activity from about 320 to 140 counts per second, which occurs at 40 m depth. The higher activity above this depth appears to be correlated with pink K-feldspar alteration. Similar alteration is seen where the log again records high gamma activity from 77-81 m and 85-100 m depth.

Borehole 2 was logged from 2 to 80 m for chargeability and apparent resistivity, and from 19-80 m for gamma activity (the gamma sonde snagged at 19 m, so the run above that point was abandoned). The gamma log (Figure 34) shows high activity levels from 280-480 cps throughout the logged depth and this is correlated with strong sericite alteration and the feldspar-porphyry intrusion. There is little feldspathic alteration recorded in this borehole. The chargeability log (Figure 35) shows a steady increase from 20 msecs to over 50 msecs. The peak chargeabilities correlate approximately with the estimated pyrite content, and the lower peak at 80 m to high Au. The resistivity log shows high values at the top and base of the log (Figure 36). After the initial high

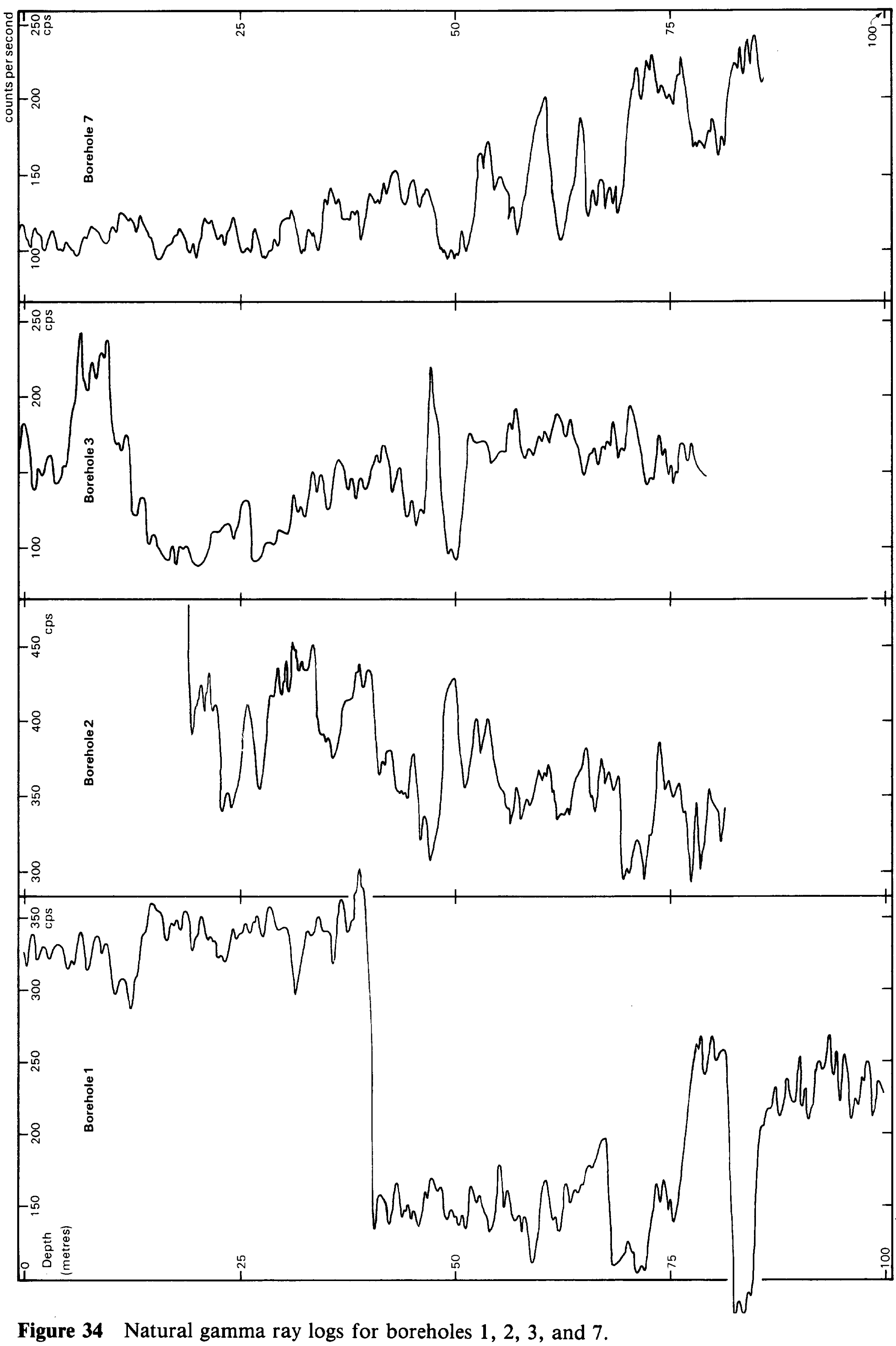

Figure 34 Natural gamma ray logs for boreholes 1, 2, 3, and 7.

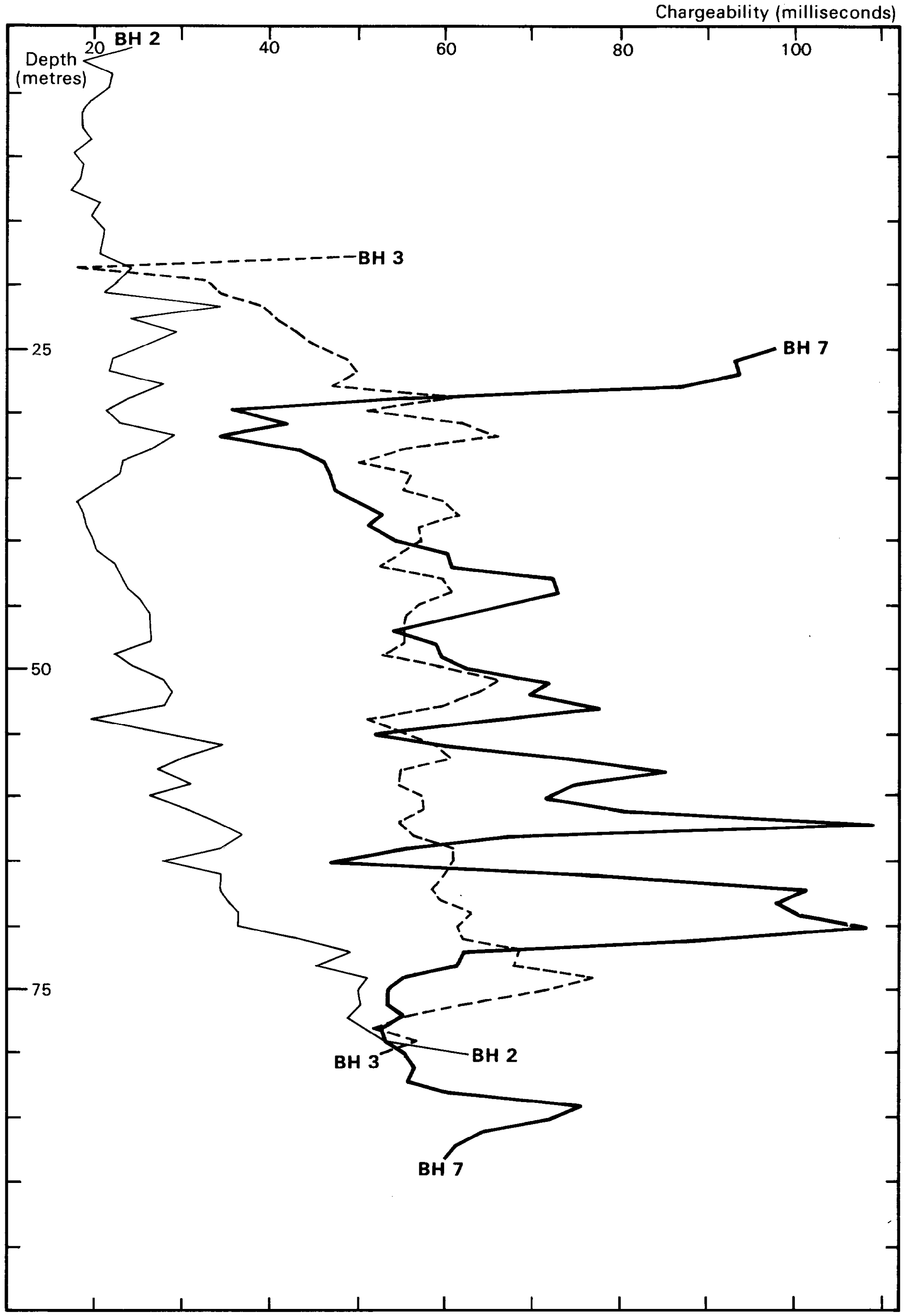

Figure 35 Chargeability logs for bores 2, 3, and 7.

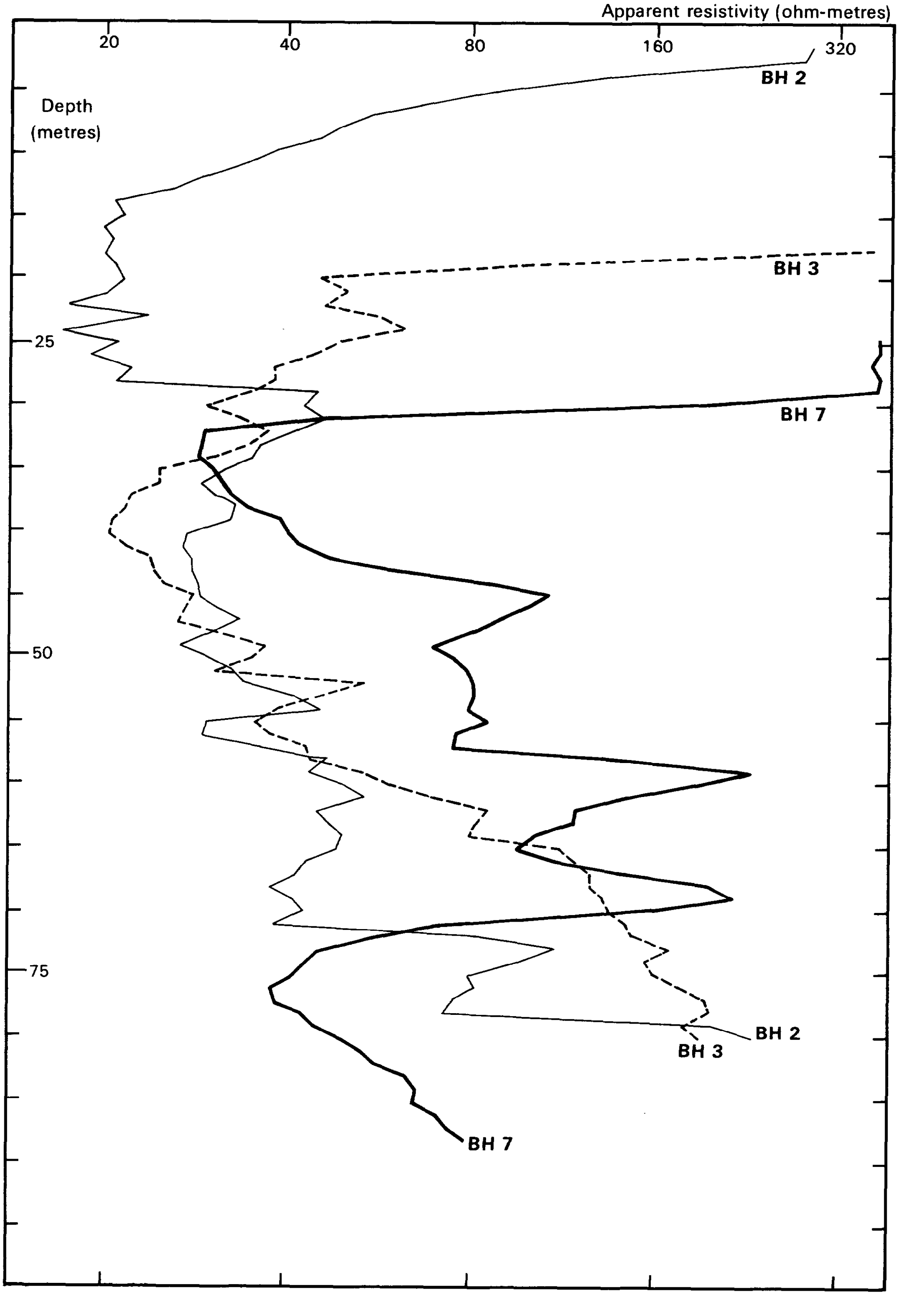

Figure 36 Apparent resistivity logs for boreholes 2, 3 and 7.

values, logged as a silicified trachyte, the resistivity is correlated to the chargeability, indicating that the degree of alteration, particularly silicification, is closely related to the sulphide content.

Borehole 3 has two obvious peaks on the gamma log from 7 to 11 m and 44 to 48 m, and again these can be correlated with the degree of K-feldspar alteration. The chargeability log shows a broad correlation with the observed pyrite content except that the chargeability peak at 74 m does not have a very high observed sulphide content. The resistivity log shows a similar pattern to that of borehole 2, with values exceeding 200 ohm-m at the top and base of the logs, and is correlated with quartz-sericite rather than chloritic alteration.

Borehole 7 exhibits levels of gamma activity similar to those of borehole 3, rising from 100-150 cps to over 200 cps (Figure 34), again closely following the extent of reddening and K-feldspar alteration. The chargeability log shows large variations from less than 40 to over 100 msecs (Figure 35). The peaks at 62 and 70 m are correlated with calcite veins; the latter has a high pyrite content (up to 40%). Resistivity (Figure 36) tracks the chargeability indicating that the intensity of the quartz-sericite alteration follows the sulphide mineralisation.

Mineralogy of drillcore samples

Introduction
After visual logging of cores from the seven drillholes, samples were selected for mineralogical examination by microscopic study of thin sections and X-ray diffractometry. The results are set out formally by Fortey (1990). The following notes give summaries of the borehole logs supplemented where appropriate by the more detailed mineralogical data. Certain limitations of this work should be borne in mind. Identification of lava type from visual hand specimen examination of hydrothermally altered rocks is prone to uncertainties. It is difficult to distinguish with confidence between andesite and basalt. Perhaps more controversially, salmon pink microporphyritic lavas are logged as trachyte or trachyandesite on the basis of what is interpreted as a primary K-feldspar content. Confirmation of this by major element analysis and systematic petrography would have been advisable had it been feasible within the limited project budget.

Examination of the thin sections indicates that the secondary minerals are very fine grained and thus difficult to identify optically. Examination by bulk XRD suffers from the limitations that minor phases may not produce interpretable peak patterns, and also that the results say nothing about how many minerals occur or which are primary and which are secondary. Electron microscopy can overcome many of these problems but is too time consuming on a routine basis.

Borehole 1
The visual log of this borehole records a series of andesite lavas showing variable degrees of hydrothermal alteration. Changes in the pattern of alteration are reflected by the colour of the rock from grey (quartz-sericite) to grey with dark green patches (chlorite a major constituent) or pink (K-feldspar a major constituent). Sulphide, mostly as fine disseminations of pyrite, varies from traces up to about 15% by volume. Several thin agglomerate bands were also intersected. These typically display strong pink feldspathic alteration and high contents of disseminated pyrite. Non-porphyritic pink lava intersected between 79.54 m and 84.03 m is described as trachyte.

Mineralogical examination added the following information. Grey vein material at 30.10 m proved to be quartz, tourmaline and muscovite with minor pyrite. A patch of soft grey sulphide at 39.87 m was mixed galena and sphalerite. Minute patches of probable tourmaline were recorded in strong calcite-sericite alteration of andesitic rock at 59.43 m. Sphalerite was confirmed at 66.53 m. Minute sprays of tourmaline prisms were again recorded at 70.88 m. At 81.93 m pink 'trachyte' is described in thin section as more probably andesitic rock made up to closely spaced agglomeratic clasts and a minor amount of comminuted matrix. Despite sericite-calcite-quartz alteration much albite and K-feldspar remain. The rock is also notable for a network of dissolution cavities developed along quartzose fractures. In addition to traces of sphalerite and galena, traces of chalcopyrite are present and molybdenite was tentatively identified in four samples (KLD 3264, 3285, 3292, 3294).

Borehole 2

Buff-coloured lavas logged visually as trachytes at the top of this borehole are succeeded at 10.99 m by argillised andesites cut by zones of grey siliceous hydrothermal brecciation which carry abundant disseminated and veinlet pyrite. Below about 20 m the andesites become grey with sericitic alteration although clay-rich areas persist to considerably below this depth. Limonitised tuff was intersected from 35.43 m to 38.64 m. Below this depth further andesites with strong argillic alteration,probably superimposed on early pyritic, sericitic alteration, continue to 53.43 m. Grey siliceous hydrothermal breccia at 48.40-50.18 m carries ca 20% disseminated pyrite and traces of molybdenite and bornite.

From 53.43 m to 70.73 m is an acute intersection through a grey to pink feldspar-porphyry dyke with strong quartz-sericite alteration and minor disseminated pyrite. A locally epidotic zone at ca 56-57 m contains fractures carrying clay gouge with pyrite, sphalerite and baryte. Minor quantities of sphalerite and molybdenite were recorded locally in this dyke section.

Below 70.73 m the core is dominantly of andesitic agglomerate to the base of the hole at 95.31 m. Short intersections with solid lava occur at 70.73-71.95 (?basalt), 75.75-80.20 (three thin dacite units) and 87.00-91.84 m (andesite). Alteration in these rocks is mostly grey quartz-sericite, locally with clay, feldspar, chlorite, hematite or calcite. Disseminated pyrite runs at 10-20% through much of these rocks though contents are lower in calcitic and chloritic rock towards the base of the hole. Chalcopyrite is recorded locally as a trace constituent; molybdenite occurs at ca 78 m and ca 82 m; baryte occurs in a vein with pyrite at ca 76 m.

Mineralogical examination by microscopy and X-ray diffractometry added the following details. At 17.10 m the secondary alteration assemblage in fine grained agglomerate comprises quartz, kaolinite, muscovite, pyrite, K-feldspar and dravitic tourmaline. A similar alteration was described at 20.70 m with the additional presence of dolomite, smectite and chalcopyrite; tourmaline was not identified here. This argillic style of alteration was again described at 22.30 m, here with the addition of minor pyrophyllite. Alteration of dacitic porphyry at 27.58 m has a more phyllic character reminiscent of alteration described in dykes at surface exposures in the area. Muscovite flakes, probably pseudomorphous after biotite, are conspicuous. Fine tourmaline prisms occur on the margins of a carbonate veinlet. Phyllic alteration was again described in brecciated rock at 49.21 m. Pyrite is abundantly disseminated but occurs only sparsely in quartz-carbonate veining. Molybdenite was recorded during the visual logging. Phyllic alteration was again described in the feldspar-porphyry dyke at 57.88 m. Andesite at 71.21 m shows weaker sericitic alteration, but is cut by a local crackly network of slender pyrite veinlets. Quartz-carbonate-'clay' alteration in agglomerate at 72.07 m is accompanied by minute sprays of prisms of tourmaline or actinolite. Patches of chlorite are a significant component of the alteration of vesicular andesite at 87.66 m. Disseminated pyrite is accompanied by very minor chalcopyrite.

Borehole 3

Andesite and agglomerate intersected to a depth of 14.20 m have suffered intense penetrative limonitic and argillaceous alteration due to weathering. Below this, the remainder of the hole to its base at 82.32 m consists dominantly of andesites. Thin agglomerate units were intersected at 42.13-43.93 m, 48.87-49.50 m and forming the brecciated top of an andesite unit at 50.75-52.94 m. The borehole also intersected a grey-brown 'trachyandesite' intrusion, probably a sill, at 54.86-63.64 m. Alteration below the weathered rock is mostly strong to intense, varying from chloritic with minor disseminated pyrite (and locally sphalerite) to sericitic-feldspathic with abundant disseminated pyrite. In addition to pyrite, other minerals occuring in veins or zones of local hydrothermal brecciation include pyrrhotite, sphalerite, baryte and galena.

XRD investigations added the following details. Greyish blue material at 41.80 m in altered andesite at 41.80 m consists of quartz and tourmaline. Galena was confirmed on a narrow fracture veinlet at 72.75 m.

Borehole 4

Beneath a thick cover of overburden to 6.89 m, argillic alteration occurs in agglomerate and andesite to 11.72 m, below which it gives way over some 3 m to pervasive hydrothermal alteration in agglomerate and, below 18.56 m, in andesite. The rocks are grey to pinkish brown, with sericite-chlorite-feldspar-calcite alteration and very minor pyrite through most of the borehole. Contents of disseminated pyrite reach 10% or more only locally in association with concentrations of calcitic veining or in a unit of pink, strongly altered 'trachyte' at 35.80-38.65 m. Chalcopyrite was recorded very sparsely, and at ca 48 m is accompanied by baryte in a calcite vein.

Mineralogical investigations added the following details. At 25.45 m, intense hydrothermal alteration takes the form of branching vein-like zones of cryptogranular silicification. Strong pyrite enrichment is spatially associated with the development of dilational quartz and carbonate veinlets and pockets after the main stage of silicification. A very similar pattern of anastomosing zones of silicification is also described at 30.63 m. A sample of 'trachyte' at 36.74 m with vivid salmon pink body colour proved to be plagiophyric and unlikely to be a true trachyte. Its colour may relate to a prominent component of disseminated carbonate. XRD confirmed the presence of chalcopyrite at 47.82 m and at 47.98 m. At 50.30 m altered andesite is crossed by zones of silicification very similar to those encountered higher in the borehole. Pyrite in this sample is accompanied by very minor chalcopyrite. At 57.18 m XRD examination of a clay-bearing veinlet indicated the presence of corrensite (mixed layer chlorite-smectite or chlorite-vermiculite) and chlorite, presumably representing a minor stage of retrograde argillisation.

Borehole 5

This borehole was logged entirely as andesite lavas. To 17.19 m the rocks show moderate clay-chlorite alteration with minor calcite veining. Chlorite-sericite alteration was encountered from 17.19 m to 37.07 m, beneath which mixed argillic and sericitic types of chloritic alteration are found to the base of the hole at 51.46 m. The andesites are locally conspicuously amygdaloidal, 3-5 mm calcite amygdales being surrounded by pink feldspar rims. The only mineralisation recorded was local trace amounts of dissmeninated pyrite, and traces of baryte in a calcitic vein at 44.0 m.

A sample of xenolithic andesite at 28.02 m proved on mineralogical examination to comprise microporphyritic quartz-andesite with weak calcite-chlorite-muscovite alteration, in which occur fragments of gabbro with strong chlorite-calcite-quartz alteration. Chloritised pyroxene xenocrysts also occur in the host lava.

Borehole 6

All 50.35 m of this borehole is logged as feldspar-porphyry save for the topmost 3.18 m of overburden. The porphyry is broken and weathered to 12.11 m, below which mild sericitic alteration is succeeded downwards at 26.89 m by moderate sericite and K-feldspar alteration which persists to the base of the hole. The porphyry locally shows auto-brecciation, flow-banding and the presence of pink to red iron-stained feldspathic rock. Hematite staining is conspicuous, for instance from 28.12 m to 34.60 m. Calcite veins with pink feldspathic rims are present at some points. Sulphide mineralisation is restricted to very minor pyrite disseminations particularly in the lower part of the hole below 39.48 m. A sample from 25.03 m showed an internal contact between porphyritic andesite and porphyritic rhyodacite with prominent apatite phenocrysts. XRD showed that a reddish-brown grain from this rock consists of hematite with traces of quartz, feldspar and calcite.

Borehole 7

Overburden down to 11.71 m is followed by agglomerate to 40.64 m. The pink to grey pyroclastic rocks show quartz-sericite-feldspar alteration patchily superseded by argillaceous alteration. Where clays are absent the rocks carry about 10% of disseminated pyrite on average although the distribution can be very uneven. At 23.00-23.30 m a calcite vein running parallel to the core carries chalcopyrite and molybdenite. The agglomerates are made up to clasts of porphyritic andesite and locally of pink 'trachyte'.

From 40.64 m to 50.16 m the borehole intersected andesite lava with moderate chlorite-quartz-sericite alteration and minor disseminated pyrite. Multiple sets of pyritic veins are recorded at 48.67-50.16 m. Two short intersections with trachyandesite lavas occur at 50.16-54.44 m and 59.11-59.62 m, carrying moderate to strong alteration and disseminated pyrite with traces in veins of chalcopyrite and molybdenite. Between and below these units are andesites similar to those higher up the borehole. At 64.34-64.68 m is a thin dacite dyke with minor quartz-sericite-chlorite alteration and minor disseminated pyrite. Below 71.35 m the borehole intersected alternating agglomerate and andesite with moderate to strong quartz-sericite-chlorite alteration locally accompanied by feldspar or clay. Disseminated pyrite frequently forms 10% or more and is very locally accompanied by trace amounts of chalcopyrite and molybdenite. Below 83.83 m to the base of the hole at 88.91 m alteration in andesite is weak and disseminated pyrite is only a minor component. Chalcopyrite and baryte were recorded from a calcite vein at ca 86m.

Mineralogical examination added the following details. Alteration of andesite clasts in agglomerate at 20.04 m is intense, passing into zones of concentracted silicification which carry muscovite flakes and pockets of chlorite which include conspicuous pseudomorphs after mafic phenocrysts, probably of augite. Andesite at 53.16 m shows moderate alteration which includes clasts of intergrown blue tourmaline and pyrite. The presence of biotite recorded in the visual log was not confirmed.

Discussion

With the exception of boreholes 5 and 6, the logs indicate a zone of strong hydrothermal alteration and pyritisation. The tenor of these is considerably higher than that of the area as a whole in so far as can be judged from the surface exposure sampling.

The boreholes transected andesitic lavas and interbedded agglomerates cut by feldspar-porphyry and 'trachyte' dykes and sills. There is some tendency for lavas to show relatively chloritic alteration whereas the more permeable agglomerates show more sericitic alteration of greater intensity. Contents of disseminated pyrite are commonly 10% or more in the latter rocks but somewhat lower in the lavas. The sericitic alteration is accompanied by minor but widespread dravitic tourmaline.

Hydrothermal effects are seen most strongly in zones of hydrothermal brecciation and attendant feldspathisation and silicification, together with locally high pyrite concentrations. Examples include zones in borehole 2 in which pyrite contents range up to 35% in breccia showing evidence of fluidisation and intrusive transport of entrained rock fragments. Between 26.12 m and 29.71 m in this borehole is a zone in which hydrothermally brecciated andesite has been intruded by an unbrecciated sheet of dacitic porphyry; the implication is that the intrusion followed on and was controlled by the brecciation. Alternatively the hydrothermal alteration is only affecting the agglomeratic andesite rather than the less permeable dacite intrusion.

In addition to the pervasive alteration, thin fracture veinlets of quartz and/or calcite are common. Minor quantities of chalcopyrite occur widely in association with the pyritisation. Sphalerite, galena and molybdenite were recorded locally, mostly in or close to veinlets. Vuggy veins of sparry calcite and quartz also carry minor amounts of baryte. Fibrous gypsum was recorded on a joint surface at one point (borehole 3 at 41.80 m). The boreholes also show an argillic style of alteration. In borehole 5 clay is recorded at points down to the base of the hole at 51.46 m. Clay-rich alteration in the upper part of borehole 2 was shown by XRD to be kaolinite-rich. Moreover, it is possible to suggest that this alteration was superimposed on earlier sericitic alteration, and may be associated with the gypsum occurrence and the late stage of baryte-bearing calcitic veins.

Geochemistry

Sampling methods

The drillcore was visually logged after slicing or splitting the core and sample intervals were chosen at lithological contacts or alteration changes. The half core was coarse crushed in a jaw crusher to <2 mm and then passed through a disc mill which produces a predominantly <0.5 mm particle size. This material was riffle split to produce a 250 g subsample for Tema swing mill grinding. A 35 g subsample of the ground material, split by cone and quartering, was sent to Acme Analytical Laboratories in Vancouver for analysis for Au by fire assay concentration followed by an ICP finish on the bead. A second split was taken for XRF analysis by the BGS laboratories. Precision of the Au analysis was monitored by analysing random subsamples from the Tema material. Preliminary studies indicate that there is still considerable subsampling error, which has probably occurred in the selection of the 35 g subsample from the 250 g tema material rather than in the analysis. Long term monitoring of the precision of the analytical method indicates that the overall precision is around 20% in the range 30-1000 ppb Au .

Results

Only Au, As, W and Bi results are available at the present time, so that conclusions about the chemistry of the mineralisation and alteration can only be tentative. The summary statistics for these elements are given in Table 6. Full details of the geochemistry will be available from the MRP database by the time of publication of this report. The Au results are relatively low,as shown by this table and the log-probability graph (Figure 37). The median content of the borehole samples is 6 ppb Au, which is closely comparable with the average level (6.8 ppb Au) in intermediate extrusive rocks given by Boyle (1979). The background population probably extends to 15 ppb and samples above this threshold show limited enrichment in Au up to 100 ppb, where there is another population break. The samples in the highly anomalous group above 100 ppb Au are from boreholes 1, 2 and 5.

Table 6 Summary statistics of borehole samples (n=349)

Element	Median	Percentiles		Maximum	Minimum
		25th	75th		
Au (ppb)	6	2	21	505	1
As	24	18	33	301	3
W	0	0	1	57	0
Bi	1	1	2	9	0

Notes

1. All elements in ppm except Au.
2. As, W, and Bi determined by XRF.

In borehole 1 the maximum Au content is 163 ppb and the anomalous samples are rather scattered through the hole at 43.10-43.99, 52.55-54.03, 66.53-67.42 and 81.50-82.75 m.There are no anomalous levels of As, W or Bi near these intervals.

In borehole 2 the anomalous Au values, which range up to 130-295 ppb Au, are grouped in samples KLD 3058-3069 from 78.75 m to the base of the hole at 95.31 m. Within this range there are samples with low Au content, such as KLD 3066 with only 1 ppb Au, but these and neighbouring samples are often anomalous in W and Bi.

Levels of Au in borehole 3 reach a maximum of 66 ppb near the top where the core is also enriched in As reaching 301 ppm. This sample range from 5.26-14.20 m is a zone of intense limonitic and argillaceous alteration due to weathering, and the enhanced As is probably a secondary weathering effect.

Borehole 4 also has generally low levels of Au, up to a maximum of 34 ppb, and As, W and Bi are only at background levels.

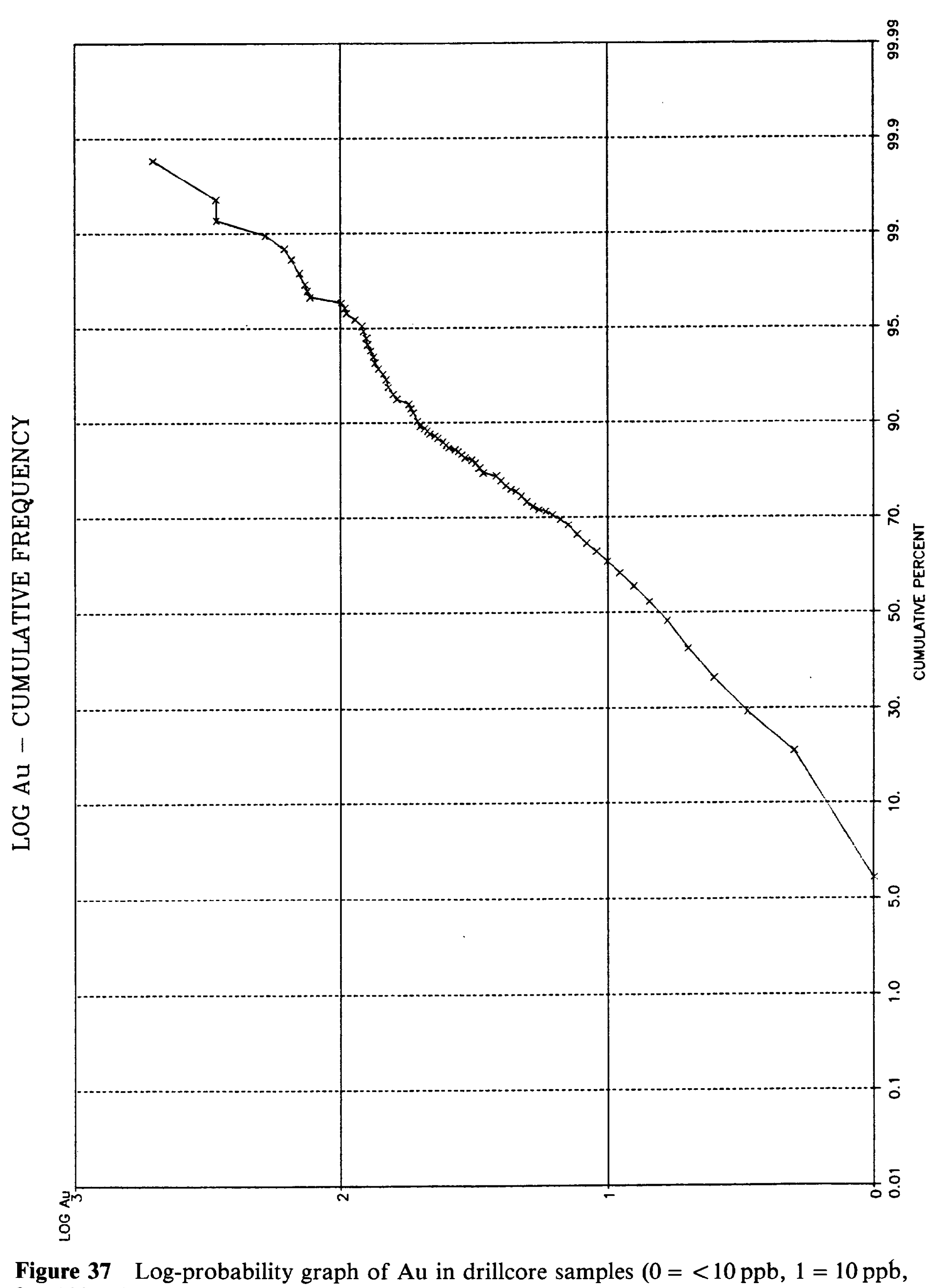

Figure 37 Log-probability graph of Au in drillcore samples (0 = <10 ppb, 1 = 10 ppb, 2 = 100 ppb, 3 = 1000 ppb).

Borehole 5 yielded two anomalous samples, KLD 3160 with 505 ppb and KLD 3174 with 143 ppb Au at 25.14-26.22 m and 46.91-48.21 m respectively. Both these intervals are iron stained, with the higher interval possibly being a small fault zone. It also shows anomalous As (135 ppm). The lower sample from the base of the borehole is also anomalous for W (57 ppm).

Borehole 6 reaches slightly higher levels of Au, up to 96 ppb in KLD 3137 at 36.22-38.28 m. This sample does not contain pyrite and only exhibits propylitic alteration with chlorite and hematite.

Borehole 7 has a similar maximum level of 95 ppb Au but there is a broad enrichment near the top of the hole (13.17 m-40.64 m) coinciding with the upper agglomerate unit (Appendix 2). The lower agglomerate conversely has very low levels of Au. The only element which seems to follow Au is W which is around 3-4 ppm in the top unit.

Discussion

The borehole cores are not strongly enriched in Au but there is evidence for the addition of Au coupled with the pyrite mineralisation and locally intense hydrothermal alteration. There are good prospects for finding other zones with higher levels of Au. The Au does not appear to be closely controlled by the lithology, with the exception of the agglomerate unit in borehole 7, nor is there any distinct association with one alteration type. The highest Au content is associated with a fault zone and secondary weathering in borehole 5. This hole was drilled well away from the hydrothermal centre as shown by the geophysical investigations and confirmed by the quantity of disseminated pyrite in boreholes 1-4. Because the drilling was centred on the main IP geophysical anomaly it is possible that further drilling may best be concentrated at the margins of the pyritic zone.

CONCLUSIONS

An overall model of the mineralisation can be envisaged in which the Borland Glen area is a locus of Lower Devonian intrusive and hydrothermal processes within an evolving calc-alkaline volcanic complex in the Ochil Hills. Control of porphyry dyke emplacement by zones of hydrothermal brecciation, and the presence also of such dykes (with hydrothermal alteration) cutting the substantially unaltered diorite intrusive, point to genetic and chronological inter-relationships between hydrothermal and magmatic activities. Thus, hydrothermal activity is seen as having consisted of convective movement of meteoric waters driven by the cooling magmas during the period of active volcanism. The main channelways for this fluid were the faults which also guided the porphyry dyke intrusions. The local control on the hydrothermal alteration was probably the porosity of the rocks; thus agglomerates are much more extensively altered than lavas.

The location of the alteration in the cogenetic pile of subaerial lavas and pyroclastics suggests a high, almost epithermal setting. There is, however, no evidence for surface hot spring activity such as recently described from the Devonian lavas in the Rhynie area (Rice and Trewin, 1989). The mineralisation is closest to that described from the porphyry intrusions at Kilmelford (Ellis et al., 1977) and Lagalochan (Harris et al., 1988) and, as at these localities, the Borland Glen mineralisation may be at too low a level in the volcanic pile to contain economic porphyry style gold mineralisation. The mineralisation does not fall into the quartz-alunite high-sulphide class of epithermal gold deposits but is better classified into the sericite-adularia low-sulphide class (Sillitoe, 1990). The subalkaline andesite subgroup of this class accurately describes the Borland Glen mineralisation, alteration pattern and host lithologies. The absence of fluorite and alunite and the presence of carbonates and base metal sulphides with the K-feldspar and sericite alteration of andesitic host rocks are the key features of this subgroup.

Despite these findings, the work has not, with certainty, determined the source rock of the gold concentrated in stream courses. Gold which is present at low concentrations in the pyritic or other altered rocks could have been leached and concentrated during the deep weathering recorded in the surface and drillcore samples. However, it is also possible that some more concentrated source exists, such as a particularly fertile breccia zone or vein, which has so far remained concealed. More detailed overburden sampling at closer intervals than 25 m, followed by trenching and drilling, will be required to locate any such breccia zones or thin veins. The exceptional quantity of gold in the stream sediments and alluvial terraces in Borland Glen indicates that such a rich source is concealed beneath the glacial overburden.

The drainage geochemical data indicate that other areas of the Ochil Hills, studied in much less detail than Borland Glen, have potential for gold, and it is recommended that they are investigated for evidence of hydrothermal alteration and auriferous bedrock. Remarkably, gold had not been reported from the Ochil Hills in the post-war phase of Scottish mineral exploration, prior to the geochemical survey carried out by the Mineral Reconnaissance Programme which initiated the detailed work described in this report. The value of well-documented regional geochemical surveys, properly archived, is demonstrated.

ACKNOWLEDGEMENTS

The cooperation and assistance of all the landowners in the area covered by this report are gratefully acknowledged. In particular, Mr J Paterson at Borland Farm, Mr R Haldane at Cloan Estate and Mr G Macrae at Coulshill are specially thanked for their interest in the work, their valuable assistance and their tolerance of our activities. Amateur prospectors are also thanked for donating alluvial gold grains at an early stage of the study.

REFERENCES

ADAMSON, G F S. 1979. *At the End of the Rainbow. The Occurrence of Gold in Scotland.* (Haddington: Albyn Press.)

ARMSTRONG, M. and PATERSON, I.B. 1970. The Lower Old Red Sandstone of the Strathmore Region. *Report of the Institute of Geological Sciences,* No. 70/12.

BOYLE, R W. 1979. The geochemistry of gold and its deposits (together with a chapter on geochemical prospecting for the element). *Bulletin of the Geological Survey of Canada, No. 280,* 1-584.

BUTTS, A, and COXE, C D (editors). 1967. *Silver - Economics, Metallurgy, and Use.* (Princetown: Van Nostrand.)

COCHRAN-PATRICK, R W. 1878. *Early Records Related to Mining in Scotland.* (Edinburgh: David Douglas.)

COLLINS, R S (compiler). 1976. Gold. *Mineral Dossier Mineral Resources Consultative Committee,* No. 14.

DICKIE, D M AND FORSTER, C W. (editors) 1974. *Mines and Minerals of the Ochils.* (Clackmannanshire Field Studies Society.)

ELLIS, R A, COATS, J S, HASLAM, H W, MICHIE, U McL, FORTEY, N J, JOHNSON, C E, and PARKER, M E. 1977. Investigation of disseminated copper mineralisation near Kilmelford, Argyllshire, Scotland. *Mineral Reconnaissance Programme Report, British Geological Survey,* No. 9.

ELLIS, R A, MARSDEN, G R, and FORTEY, N J. 1978. Disseminated sulphide mineralisation at Garbh Achadh, Argyllshire, Scotland. *Mineral Reconnaissance Programme Report, British Geological Survey,* No. 23.

FORTEY, N J. 1980. Hydrothermal mineralization associated with minor late Caledonian intrusions in northern Britain: preliminary comments. Transactions of the *Institution of Mining and Metallurgy (Section B: Applied Earth Sciences),* Vol. 89, B173-176.

FORTEY, N J. 1990. Mineralogy and petrography of rock samples and drillcore from the Borland Glen area, Ochil Hills, Scotland. *British Geological Survey Technical Report WG/90/7R.*

FRANCIS, E H, FORSYTH, I H, READ, W A, and ARMSTRONG, M. 1970. The geology of the Stirling district. *Memoir of the Geological Survey of Great Britain,* Sheet 39 (Scotland.)

GROEN, J C, CRAIG, J R, and RIMSTIDT, J D. 1990. Gold-rich rim formation on electrum grains in placers. *Canadian Mineralogist,* Vol. 28, 207-228.

GUNN, A G. 1989. Drainage and overburden geochemistry in exploration for platinum-group element mineralisation in the Unst ophiolite, Shetland, *U.K. Journal of Geochemical Exploration,* Vol. 31, 209-236.

HALL, I H S, GALLAGHER, M J, SKILTON, B R H, and JOHNSON, C E. 1982. Investigation of polymetallic mineralisation in Lower Devonian volcanics near Alva, central Scotland. *Mineral Reconnaissance Programme Report, British Geological Survey,* No. 53.

HARRIS, M, KAY, E A, WIDNALL, M A, JONES, E M, and STEELE, G B. 1988. Geology and mineralization of the Lagalochan intrusive complex, western Argyll, Scotland. *Transactions of the Institution of Mining and Metallurgy (Section B: Applied Earth Sciences),* Vol. 92, B213-216.

HASLAM, H W, and CAMERON, D G. 1985. Disseminated molybdenum mineralisation in the Etive plutonic complex in the western Highlands of Scotland. *Mineral Reconnaissance Programme Report, British Geological Survey,* No. 76.

HASLAM, H W, and KIMBELL, G S. 1981. Disseminated copper-molybdenum mineralisation near Ballachulish, Highland Region. *Mineral Reconnaissance Programme Report, British Geological Survey,* No. 43.

JASSIM, R Z, PATTRICK, R A D, and RUSSELL, M J. 1983. On the origin of the silver + copper + cobalt + baryte mineralization of Ochil Hills, Scotland: a sulphur isotope study. *Transactions of the Institution of Mining and Metallurgy (Section B: Applied Earth Sciences),* Vol. 92, B213-216.

PARNELL, J. 1988. Mercury and silver-bismuth selenides at Alva, Scotland. *Mineralogical Magazine,* Vol. 52, 719-720.

RICE, C M, and TREWIN, N H. 1989. A Lower Devonian gold-bearing hot-spring system, Rhynie, Scotland. *Transactions of the Institution of Mining and Metallurgy (Section B: Applied Earth Sciences),* Vol. 97, B141-144.

ROBINSON, N, PARNELL, J, and BRASSELL, S. 1989. Hydrocarbon compositions of bitumens from mineralized Devonian lavas and Carboniferous sedimentary rocks, central Scotland. *Marine and Petroleum Geology,* Vol.6, 316-323.

SILLITOE, R H. 1990 Exploration applications of epithermal models. *8th IAGOD Symposium, Ottawa, Canada, Program with Abstracts,* A131.

SMITHELLS, C J. (editor) 1976. *Metals Reference Book* (5th edition). (London: Butterworths.)

THIRLWALL, M F, 1981. Implications for Caledonian plate tectonic models of chemical data from volcanic rocks of the British Old Red Sandstone. *Journal of the Geological Society of London,* Vol. 138, 123-138.

ZHOU, J -X. 1988. A gold and silver-bearing subvolcanic centre in the Scottish Caledonides near Lagalochan, Argyllshire. *Journal of the Geological Society of London,* Vol. 145, 225-234.

APPENDIX 1 Locations of Gold-bearing Panned Concentrates 1978 Survey

Sample Grid Reference Location

CXP 156 299390 0705410 1st tributary of stream from Glendevon to Borland Glen 100 m from confluence.
Pan magnetite hematite zircon. Several specks of gold seen in pan.
CXP 213 288300 0698680 10 m from junction with Alva Burn (Glenwinnel Burn).
Pan magnetite hematite gold?. Contamination tin cans.
CXP 250 298940 0713070 2nd stream west of Rossie Dunning 20 m above edge of wood.
Pan magnetite hematite, 1 grain gold and 1 grain opaque white mineral.
CXP 254 296004 0711070 Stream opposite Cloan Hatcheries 5 m up from entrance.
Pan magnetite 1 grain of gold.
CXP 285 304380 0714050 Stream east of Woodhead 10 m above confluence with tributary.
Pan Fe oxides gold.
CXP 413 307200 0709780 On Chapel Burn 10 m above confluence. Burn down from Baulk of Struie.
Pan magnetite + gold.
CXP 447 310990 0712600 Most easterly of 3 tributaries from Berry Hill to resevoir. 30 m above confluence.
Considerable drift. Pan gold.
CXP 480 310390 0713400 Kelty Burn S tributary 1 km upstream of confuence.
Pan magnetite + gold + barytes.
CXP 484 309500 0714110 N tributary of Kelty Burn 1st minor tributary 20 m from confluence.
Pan magnetite hematite gold.
CXP 595 302730 0701610 Stream passing Newbigging 500 m below A91. 5 m below small bridge.
Pan magnetite haemetite + gold one grain.
CXP 605 319150 0716130 50 m upstream of Water Works 200 m N of quarry 1-2 km SW of Aberne.
Pan Fe oxides garnet zircon gold.
CXP 607 325270 0712880 1-2 km upstream of Rossie.
Pan magnetite zircon gold.
CXP 608 325660 0713220 200 m east of Lochieheads.
Pan magnetite + gold.
CXP 609 326280 0712500 100 m upstream of A91 1-2 km NW of Rossie House.
Pan Fe oxides + gold.
CXP 631 327580 0713060 1-2 km downstream of Kinloch House.
Pan magnetite + gold(1 grain).
CXP 635 299120 0699400 1-2 km N of Cowden Farm N Tributary 5 m from confluence.
Pan Fe oxides barytes zircon garnet 1 gold.
CXP 680 336700 0722470 Stream running past Grange 8 m above confluence with stream from Fincraigs.
Rusty wire. Pan gold + magnetite + zircon. Exotic schist pebbles common.
CXP 681 336750 0722060 Stream from Ballindean 1 m above junction with Mottray

Water.

Much fluvioglacial drift. Pan 1 grain gold + magnetite + zircon.

CXP 697 335150 0724290 20 m upstream from Tay 1-2 km West of Byres Farm.

Pan 1 grain of gold Fe oxides zircon.

CXP 699 333180 0723230 35 m upstream from Tay Estuary in Flisk wood.

Contamination tin cans. Pan Fe oxides gold.

CXP 734 340130 0720840 Stream draining NW from Logie 5 m above wood.

Contamination rusty Fe. Exotic quartz pebbles. Pan oxides zircon 3 grains gold.

CXP 754 335900 0724760 Balmarino 10 m upstream of road 200 m from Abbey.

Pan 1 grain of gold magnetite.

CXP 756 337930 0725400 400 m NE of Kilburns.

Pan magnetite 1 gold zircon.

CXP 766 333210 0717470 Stream draining North to Bankfoot Cottage : 300 m N of A913.

Pan Fe oxides + zircon 3 grains gold.

CXP 767 332860 0717280 Stream draining N between Hopetoun + Mount Hill: 50 m up from road (A91).

Pan Fe oxides + zircon + 2 specks gold.

CXP 788 333760 0715760 1-2 km SW of the Mount.

Pan Fe oxides 2 grains of gold.

CXP 906 323910 0707200 200 m SE of Westfield Maspie Burn 5 m upstream of farm road.

Pan Fe oxides 1 grain of gold.

CXP 908 323090 0703250 Lothrie Burn 400 m downstream of Water Works.

Contamination Water Works upstream. Pan Fe oxides 1 grain of gold.

CXP 918 324820 0704180 Conland Burn 20 m downstream of confluence 3 km ENE of Rhind Hill.

Pan Magnetite + several specks of gold? Contamination? lead swarf

APPENDIX 2 Summary Borehole Logs and Sample Intervals

Borehole: 1 Logged by: J S Coats

Sample No.	Depth From	Depth To	Lithology	Mineralisation	
	0.00	2.20	Overburden, loose cobbles of weathered and fresh andesite		
3227	2.20	3.60	Andesite, weathered, porphyritic brown lava, phenocrysts plagioclase and, chlorite after Femags. Goethite and limonite stained.		
3228	3.60	4.53	Andesite, grey brown colour, fractured, as above.		
3229	4.53	6.60	Andesite, pink/brown colour, weathered, broken and stained on joints. Phenocrysts altered to clay and chlorite.	Py	tr
3230	6.60	8.75	Andesite, weathered, brown porphyritic lava with chlorite phenocrysts with goethite rim after pyroxene in groundmass of quartz-sericite.		
3231	8.75	10.56	Andesite, altered, grey brown, porphyritic lava with chlorite and sericite phenocrysts in fine grained purple-brown of groundmass.	Py	0.5
3232	10.56	12.05	Andesite, altered, as above, slightly browner, weathered.		
3233	12.05	13.95	Andesite, altered, brown porphyritic lava. Chlorite after pyroxene and clay after plagioclase phenocrysts. Groundmass altered to quartz-sericite.	Py	1
3234	13.95	15.25	Andesite, altered, as above but more feldspar phenocrysts. Fe-stained with no pyrite visible, black stained fractures. Quartz-sericite alteration.		
3235	15.25	16.20	Andesite, much paler grey than above, more intense alteration to quartz-sericite, remnant chlorite, lower part is weathered.	Py	tr
3236	16.20	17.58	Andesite, leached and altered, pale brown rock, very light and porous. Limonite stained but relict intense quartz-sericite alteration.	Py	1
3237	17.58	18.48	Andesite, as above.	Py	1
3238	18.48	18.99	Andesite, light grey, intensely altered lava. Strong quartz-sericite alteration of grey plagioclase. Abundant pyrite in groundmass (10-20%). [KLM 3238 at 18.63m].	Py	10
3239	18.99	20.35	Andesite, dark grey, slightly porphyritic lava with chlorite after pyroxene, and clay-altered plagioclase.		
3240	20.35	21.83	Andesite, as above, little altered except chlorite.	Py	tr
3241	21.83	23.04	Andesite, altered, pink/pale grey colour, same flow as above but rapid increase in alteration to quartz-sericite replacing chlorite.	Py	10
3242	23.04	24.76	Andesite, altered as above with possibly new alkali feldspar in pinkish patches.	Py	10
3243	24.76	26.01	Andesite, altered, pale grey as above, quartz-sericite alteration.	Py	10
3244	26.01	26.90	Andesite, as above. Top half of unit heavily iron stained	Py	10
3245	26.90	27.46	Andesite, grey, altered, porphyritic lava. Rapid change from above, chlorite still present with pyrite rims, clay alteration of sericite.	Py	10
3246	27.46	28.18	Agglomerate, pink, altered clast-supported pyroclastic rock. Feldspars in clasts altered to bright pink K-feldspar.	Py	15
3247	28.18	30.02	Andesite, dark grey altered lava. Alteration is transitional to agglomerate above, with K-feldspar rich,then quartz-sericite, before going into normal dark grey andesite with chlorite and calcite porphyroblasts.	Py	tr
3248	30.02	32.29	Andesite, dark grey slightly porphyritic lava with chlorite after pyroxene phenocysts. Groundmass fine grained dark grey with fresh feldspar.	Py	tr
3249	32.29	33.18	Andesite, as above, but top 28 cm altered to pink feldspar near a quartz vein. Remainder has grey, chloritic alteration.	Py	tr
3250	33.18	33.79	Andesite, grey altered rock with pink feldspar porphyroblasts. Relict chlorite after pyroxene in quartz-sericite-pyrite groundmass.	Py	10
3251	33.79	35.03	Andesite, grey altered lava similar to above with pink patches of strong quartz-K-feldspar alteration. Grey zones are quartz-sericite alteration.	Py	15

3252	35.03	36.32	Andesite, altered brownish grey lava with chlorite after mafics. Groundmass variably altered to quartz- sericite.	Py	3
3253	36.32	37.42	Andesite, pink and grey patchily altered lava. Pink areas with new feldspar growth, overprinted by ?later grey alteration of quartz-sericite.	Py	15
3254	37.42	39.04	Andesite, grey lava with rare pink feldspathic patches, grey quartz-sericite intergrowth with lighter zones around thin vuggy calcite veins.	Py Cpy	15 tr
3255	39.04	40.59	Andesite, light grey altered lava with 1-2 cm pink K-feldspar altered bands. Top of unit shows strong alteration to white quartz-sericite cut by pale grey mineral + pyrite vein [KLM 3255 at 39.10m, tourmaline identified by XRD]. [KLM 3255A at 39.87 m grey sulphide]	Py	15
3256	40.59	41.75	Andesite, grey altered lava with rare white clay replacing plagiocase in quartz-sericite-calcite-pyrite groundmass.	Py	15
3257	41.75	43.10	Andesite, uniform grey, slightly porphyritic, altered lava as above. More chlorite. Less pyrite which decreases with the sericite alteration.	Py	3
3258	43.10	43.99	Andesite, variable unit with dark grey, slightly porphyritic lava. Darker areas show chlorite alteration and grey areas quartz-sericite sericite.	Py	0.5
3259	43.99	44.89	Andesite, medium/pale grey altered lava, as above. Matrix lighter grey with quartz-sericite-calcite-hematite.	Py	tr
3260	44.89	45.72	Andesite, ?autobrecciated lava, strong hydrothermal alteration overprinting breccia texture. Grey sericite areas rich in pyrite.	Py	15
3261	45.72	46.74	Andesite, as above, patches due to alteration rather than original	Py	15
3262	46.74	48.34	Andesite, hydrothermally brecciated altered lava. Grey quartz-sericite and pink K-feldspar alteration.	Py	10
3263	48.34	49.64	<u>Breccia/agglomerate</u>, similar to the above, but clasts differ in alteration and composition. Some clasts vuggy, pink K-feldspar and sericite-bearing, others darker.	Py	15
3264	49.64	50.85	Breccia/agglomerate as above, K-feldspar and quartz-sericite alteration.	Py Cpy MoS_2	15 tr tr
3265	50.85	52.55	Agglomerate, grey, patchily altered pyroclastic. Clasts 1-10 cm of porphyritic lava in grey matrix with quartz-sericite-calcite-pyrite-chlorite.	Py	3
3266	52.55	54.03	<u>Andesite</u>, pinkish grey-brown vesicular lava, rarely porphyritic with chlorite after pyroxene, indistinct quartz-sericite hydrothermal alteration bands.	Py	5
3267	54.03	54.83	Andesite, grey, slightly porphyritic, lava with white clay altered phenocrysts and less chlorite after pyroxene set in a grey-brown matrix.	Py	2
3268	54.83	55.49	Andesite, as above, some hematite in groundmass.	Py	1
3269	55.49	56.24	Andesite, dark grey, less altered, magnetic variety of above with fresh feldspar, hematite and magnetite.	Py	tr
3270	56.24	57.94	Andesite, grey, then pale pinkish brown, altered lava. Gradational to unit above over 10-40cm. Grey top is rich in pyrite 15% then new brown feldspar in groundmass.	Py	10
3271	57.94	58.70	Andesite, greyer variety of above, groundmass more silicified	Py	10
3272	58.70	59.71	<u>Agglomerate</u>, hydrothermally altered pyroclastic with indistinct subrounded clast boundaries. Some clasts have new alkali-feldspar with matrix more quartz-sericite-pyrite altered [KLM 3272 at 59.43 m]	Py	15
3273	59.71	61.05	Agglomerate, altered, as above,	Py	15
3274	61.05	62.13	Agglomerate, very variable unit, top part dark green (?basalt clast) with many alteration veins, then grey with irregular sericite altered zones.	Py	5
3275	62.13	63.36	<u>Andesite</u>, uniform grey brown, slightly porphyritic lava with pink sections. Pervasive quartz-sericite alteration with little chlorite left.	Py	5
3276	63.36	64.20	Andesite, dark grey, slightly porphyritic lava with fresh brown-grey groundmass with rare chlorite and white clay after plagioclase.	Py	tr
3277	64.20	65.10	Andesite, as above, more calcite-pyrite vein network.	Py	tr

3278	65.10	66.53	<u>Agglomerate/Breccia</u>, grey-brown altered matrix with indistinct altered clasts. Top may be hydrothermally altered lava, base shows agglomeratic texture. Sphalerite in open calcite-pyrite veins.	Py Sph	10 tr
3279	66.53	67.42	Agglomerate, brecciated as above but of more uniform texture and pervasive netveined quartz-sericite alteration.	Py	10
3280	67.42	68.29	Agglomerate, brecciated as above with clasts up to 18 cm. Hydrothermally brecciated in parts to quartz-sericite and K-feldspar.	Py	15
3281	68.29	69.31	Agglomerate, as above, volcanic agglomerate with varied, 1 cm clasts.	Py	10
3282	69.31	70.10	Agglomerate, as above but grey in colour with little pink feldspar. Sharp contact to unit below with blocks of lava.	Py	10
3283	70.10	71.08	<u>Andesite</u>, grey-white, fine grained lava with prominent phenocrysts of pale green chlorite + pyrite. Hydrothermal crackle breccia in parts with pyrite + calcite veins. [KLM 3283 at 70.88 m].	Py	5
3284	71.08	72.23	Andesite, as above, phenocrysts to 6 mm. Calcite veining with zoned sphalerite (honey coloured core, dark rim).	Py Sph	8 tr
3285	72.23	73.44	Andesite, as above, more massive, less broken, groundmass quartz-sericite alteration.	Py MoS_2	5 tr
3286	73.44	74.64	Andesite, as above, much browner matrix with 3 cm mafic xenolith at 73.54 m (chlorite-dolomite-quartz-sericite-pyrite).	Py	3
3287	74.64	75.38	<u>Agglomerate</u>, top similar to above units before basal section of agglomerate. Tuffaceous section more sericite altered and pyrite to 10%.	Py	2
3288	75.38	76.33	<u>Andesite</u>, altered, grey brown, vesicular lava with slighly flattened spherical cavities lined with calcite and pyrite in pale brown quartz-sericite-pyrite-calcite groundmass.	Py	5
3289	76.33	77.60	Andesite, as above, pinker feldspar in groundmass, little chlorite, crackle breccia.	Py	10
3290	77.60	78.70	Andesite, 24 cm of grey, fine grained, slightly porphyritic chilled lava, then sharp contact to vesicular lava below.	Py	8
3291	78.70	79.54	<u>Andesite</u>, vesicular lava, core broken, patchy feldspathisation.	Py	10
3292	79.54	80.67	<u>Trachyte</u>, (or altered trachyandesite) non-porphyritic pink lava with irregular flow banding. Pink feldspar alteration with ?later bands of quartz-sericite alteration.	Py MoS_2	5 tr
3293	80.67	81.50	Trachyte, as above, partly vesicular. Hydrothermal brecciation and quartz alteration.	Py	5
3294	81.50	82.76	Trachyte, as above, crackle breccia in parts. [KLM 3294 at 81.93 m] Trace of molybdenite on joints.	Py MoS_2	3 tr
3295	82.76	84.03	Trachyte, as above, grey towards base which shows a sharp flow contact to unit below, increase in hematite near boundary and pyrite below.	Py	3
3296	84.03	85.30	<u>Andesite</u>, mid-grey, altered porphyritic lava with chlorite phenocrysts after pyroxene, rare white clay-altered plagioclase. Grey matrix with slight ?quartz-sericite alteration.	Py	1
3297	85.30	86.37	Andesite, as above.	Py	1
3298	86.37	87.50	Andesite, as above, more altered and browner, pyrite more abundant [KLM 3298 at 86.80 m pale green mineral in vein with calcite and pyrite].	Py	3
3299	87.50	88.44	Andesite, as above, core very shattered.	Py	2
3300	88.44	89.32	Andesite, as above, brownish grey with later feldspar alteration adjacent to common calcite-pyrite veins.	Py	2
3301	89.32	90.50	Andesite, as above but top 20 cm very feldspathised and red with 5 mm, coarse calcite-pyrite-chlorite vein.	Py	1
3302	90.50	91.32	Andesite, same flow as above but browner alteration, little chlorite left. Pyrite in fine dissemination and veins less broken than above units.	Py	2
3303	91.32	92.41	Andesite, red-brown altered lava, same flow as above but hydrothermally brecciated to brownish red K-feldspar cut by irregular boxwork of pyrite and calcite veins with crackle breccia.	Py	10
3304	92.41	93.56	Andesite, same flow as above but greyer and less hydrothermally	Py	1

			brecciated.		
3305	93.56	94.58	Andesite, same slightly porphyritic lava, brown-red colour. Feldspars in groundmass altered to brick red K-feldspar.	Py	5
3306	94.58	95.70	Andesite, as above, but browner alteration (of groundmass feldspar). Disseminated pyrite and in cavities and veins.	Py	10
3307	95.70	97.34	Andesite, as above but white sericite after plagioclase phenocrysts.	Py	1
3308	97.34	99.25	Andesite, brown, slightly porphyritic, altered lava. Patchy alteration from chlorite to red brown feldspathic. Pyrite variable.	Py	1
3309	99.25	100.50	Andesite, as above, brown to reddish brown, sericite alteration but some areas of reddish feldspar. Brecciated at base with lining of calcite-baryte crystals in cavity. [KLM 3309 at 100.32 m] Baryte vein.	Py	1
3310	100.50	101.86	Andesite, as above, chlorite on joint faces Moderate sericite alteration.	Py	1

Base of hole at 101.86

Borehole: 2 Logged by: J S Coats, N J Fortey

Sample No.	Depth From	Depth To	Lithology	Mineralisation
	0.00	3.14	Overburden, till and partly broken bedrock.	
	3.14	5.97	Trachyte, feldspar porphyritic lava weathered.	
3001	5.97	6.85	Trachyte, buff, feldspar porphyritic lava, minor clay alteration.	Py 0.5
3002	6.85	7.98	Trachyte, pyrite more variable 1-10% moderate silicification.	Py 2
3003	7.98	9.85	Trachyte, 10% disseminated pyrite Sericite alteration.	Py 10
3004	9.85	10.99	Trachy-andesite(?), grey brown white, altered feldspar phenocrysts, moderate clay alteration.	Py 20
3005	10.99	12.42	Andesite, purple brown porphyritic lava, weathered with rare fresh sections, clay alteration.	Py 5
3006	12.42	13.62	Andesite, grey brown, porphyritic altered lava, minor chlorite alteration.	Py 10
3007	13.62	15.30	Andesite, pale purplish-grey, porphyritic lava, strong clay alteration.	Py 3
3008	15.30	16.69	Andesite, white feldspar phenocrysts and green chlorite patches with quartzose hydrothermal breccia. Argillic alteration.	Py 10
3009	16.69	17.38	Hydrothermal breccia, leaden grey, siliceous with andesite fragments 1-5 mm, intense argillic alteration [KLM 3009 at 17.10-17.18 m].	Py 35
3010	17.38	18.10	Andesite, pale grey, porphyritic lava, soft argillic alteration.	Py 4
3011	18.10	19.23	Andesite, olive green lava, strong chlorite alteration.	Py 5
3012	19.23	20.30	Andesite, olive green,strong clay-chlorite alteration.	Py 2
3013	20.30	21.25	Hydrothermal breccia, grey, fragments of altered andesite in silicified pyritic matrix [KLM 3013 at 20.70-20.80 m].	Py 15 Sph tr
3014	21.25	22.71	Hydrothermal breccia, as above, strong sericite alteration. [KLM 3014 22.30-22.40 m].	Py 20
3015	22.71	24.26	Hydrothermal breccia, as above, strong sericite alteration.	Py 10
3016	24.26	25.30	Andesite, mid-grey mottled lava, strong sericite-chlorite alteration.	Py 2
3017	25.30	26.12	Andesite, grey-brown, altered, porphyritic lava fine sericite + carbonate alteration.	Py 5
3018	26.12	27.04	Andesite, brecciated, pale brown/buff colour, strong silicification.	Py 10
3019	27.04	28.40	Dacitic porphyry, pale pinkish grey, moderately silicified [KLM 3019 at 27.58-27.70 m].	Py 3
3020	28.40	29.71	Andesite, brecciated, grey, quartz-sericite alteration.	Py 10
3021	29.71	32.03	Andesite, pinkish grey lava, strong sericite alteration.	Py 5
3022	32.03	34.50	Andesite, grey lava, sericite and quartz alteration.	Py 3 Sph tr
3023	34.50	35.43	Andesite, as above, with a sericitised groundmass.	Py 3

3024	35.43	36.45	Tuff-breccia, angular 5-10 mm white clasts, core weathered.		
			Sericite and clay alteration.		
3025	36.45	37.53	Tuff, fine grained pyroclastic,		
			clay and hematite alteration.		
3026	37.53	38.64	Tuff, as above.		
3027	38.64	39.89	Andesite, pale grey lava,	Py	5
			sericite alteration.		
3028	39.89	41.35	Andesite, massive, pale grey altered lava	Py	5
			sericite alteration.		
3029	41.35	42.91	Andesite, as above.	Py	5
3030	42.91	44.35	Breccia, weathered, clay alteration.		
3031	44.35	45.57	Andesite, altered, pale grey porphyritic lava,		
			clay alteration.		
3032	45.57	46.66	Andesite, as above,	Py	10
			sericite and clay alteration.		
3033	46.66	47.40	Andesite, grey, porphyritic, altered lava,	Py	5
			strong sericite alteration.		
3034	47.40	48.40	Andesite, grey, strongly porphyritic lava,	Py	8
			feldspars altered to sericite.		
			Trace of MoS_2 at 48.35 m and ? bornite at 48.55 m.		
3035	48.40	49.45	Hydrothermal breccia,	Py	20
			sericite and quartz net veining.		
			Traces of molybdenite [KLM 3035 at 49.21-49.33 m].		
3036	49.45	50.18	Hydrothermal breccia, as above, sericite and	Py	20
			quartz alteration. Bornite in very small crystals.		
3037	50.18	51.50	Andesite, grey porphyritic lava	Py	5
			strong sericite alteration.		
3038	51.50	52.67	Andesite, pale pinkish grey,	Py	5
			strongly sericitised.		
3039	52.67	53.43	Andesite, altered lava with crackle texture of	Py	20
			intense quartz-sericite alteration.		
3040	53.43	54.32	Feldspar-porphyry, grey, marginal facies of dyke,	Py	5
			strong sericite alteration.		
3041	54.32	55.84	Feldspar-porphyry, as above.	Py	3
3042	55.84	57.23	Feldspar-porphyry, as above.	Py	3
			sphalerite on fracture at 55.95-56.00 m and		
			baryte at 56.60m on a similar vein.		
3043	57.23	58.33	Feldspar-porphyry, pink, gradational to above.	Py	5
			Sparse tenuous crackly pyrite veinlets		
			and disseminated pyrite. [KLM 3043 at 57.88-57.98 m]		
3044	58.33	59.22	Feldspar-porphyry, pink, siliceous rock cut by	Py	5
			pale sericitic zones.	Sph	tr
3045	59.22	60.68	Feldspar-porphyry, pale pink, massive as above.	Py	3
			Quartzose zones centred on veinlets of sericite	Sph	tr
			Trace MoS_2 in pink siliceous zone [KLM3045 59.72-59.8 m].		
3046	60.68	61.84	Feldspar-porphyry, pink, massive, as above,	Py	5
			quartz-sericite alteration.		
3047	61.84	62.87	Feldspar-porphyry, grey pink, similar to above,	Py	5
			quartz-sericite alteration.		
3048	62.87	65.03	Feldspar-porphyry, grey-brown,	Py	5
			quartz-sericite alteration.	Sph	tr
3049	65.03	67.48	Feldspar-porphyry, grey brown, as above.	Py	5
			Traces of chalcopyrite and MoS_2.		
3050	67.48	69.30	Feldspar-porphyry, brown-pink,	Py	5
			traces of chalcopyrite in fractures,	Cpy	tr

			strong quartz-sericite alteration.		
3051	69.30	70.73	Feldspar-porphyry, basal unit of dyke,	Py	8
			moderate argillic alteration.		
3052	70.73	71.95	Andesite, (?basalt) grey porphyritic lava	Py	5
			moderate quartz-sericite alteration,		
			pyrite veinlets cut by later quartz [KLM3052 71.21-71.31 m].		
3053	71.95	73.38	Agglomerate, altered, grey pyroclastic.	Py	20
			Groundmass extensively altered to sericite.	Cpy	tr
			Rare white calcite veins and pyrite stringers		
			[KLM 3053 at 72.07-72.19 m].		
3054	73.38	74.62	Agglomerate, as above,	Py	20
			strong quartz-sericite alteration.		
3055	74.62	76.18	Agglomerate, grey, altered, as above,	Py	15
			Fractures with pyrite, baryte and cavities after carbonate.		
3056	76.18	77.53	Agglomerate, grey altered as above,	Py	10
			silicified and hydrothermally brecciated.	Sph	tr
3057	77.53	78.75	Agglomerate, dark grey, silicified,	Py	10
			veinlets of pyrite-quartz-baryte-MoS_2 (tr) and		
			baryte+brown sphalerite.		
3058	75.75	80.20	Dacite, three, thin lava flows.	Py	10
			Silicified, feldspar and sericite alteration.		
3059	80.20	81.34	Agglomerate, brown, silicifed pyroclastic.	Py	10
3060	81.34	82.31	Agglomerate, as above,	Py	10
			Strong quartz-sericite alteration.		
			MoS_2 traces disseminated with pyrite.		
3061	82.31	83.25	Agglomerate, grey, strongly argillic altered.	Py	5
3062	83.25	84.49	Agglomerate, grey, as above	Py	10
				Sph	tr
3063	84.49	84.98	Andesite, clast in agglomerate,	Py	2
			altered to pale sericite with feldspar tabulae.		
3064	84.98	87.00	Agglomerate, grey, andesite clasts to 20 cm,	Py	15
3065	87.00	89.10	Andesite, grey, massive, vesicular lava.	Py	5
			Pink siliceous alteration 87.00-87.35 m and then calcite-hematite-chlorite alteration.		
			Bleached zone with pyrite [KLM 3065 at 87.66-87.78 m].		
3066	89.10	90.10	Andesite, brown-grey lava, calcite occurs	Py	5
			in veinlets and abundant hematite spots. Late veinlets.		
			of calcite-baryte-chalcopyrite.		
3067	90.10	91.84	Andesite, dark grey, sparsely vesicular lava	Py	1
			Moderate calcite alteration.		
3068	91.84	93.38	Agglomerate, pink pyroclastic.	Py	3
			Intense feldspar alteration with minute solution holes.		
3069	93.38	95.31	Agglomerate, pink-grey similar to above.	Py	20
			Grey argillic fracture zones.		

Base of hole at 95.31 m

Borehole: 3 Logged by: J S Coats, N J Fortey

Sample No.	Depth From	To	Lithology	Mineralisation	
	0.00	3.30	Overburden.		
	3.30	5.26	Agglomerate, weathered.		
3070	5.26	7.18	Agglomerate, weathered, as above.		
3071	7.18	8.57	Agglomerate, as above.		
3072	8.57	12.63	Agglomerate, as above, pale grey argillic zone.		
3073	12.63	14.20	Agglomerate, as above, weathered.	Py	20
3074	14.20	16.30	Andesite, weathered, porphyritic lava.	Py	20
3075	16.30	17.87	Andesite, green porphyritic lava with abundant chlorite spots.	Py	2
3076	17.87	19.58	Andesite, pale green, porphyritic lava as above.	Py	tr
3077	19.58	22.06	Andesite, green lava, as above.	Py	tr
3078	22.06	23.00	Andesite, grey, altered lava, quartz sericite alteration.	Py	0.5
3079	23.00	24.70	Andesite, altered pale green lava with chlorite spots.	Py	10
3080	24.70	25.94	Andesite, grey and pink altered lava.	Py	10
			K-feldspar-quartz-pyrite breccia.	Sph	tr
3081	25.94	27.51	Andesite, grey pink lava, quartz-sericite and K-feldspar alteration.	Py	15
3082	27.51	28.64	Andesite, pink-grey, K-feldspar alteration.	Py	15
3083	28.64	30.02	Andesite, grey green, slightly porphyritic, chlorite-quartz-sericite-pyrite alteration.	Py	2
3084	30.02	31.27	Andesite, pink-grey altered lava with chlorite-sericite-quartz-pyrite alteration	Py	5
3085	31.27	32.90	Andesite, pink altered lava with	Py	15
			quartz-sericite alteration.	Sph	tr
3086	32.90	33.91	Andesite, salmon pink altered lava, quartz-feldspar-sericite alteration.	Py	20
3087	33.91	34.98	Andesite, salmon pink lava, as above. Pink bladed baryte with quartz in vugs.	Py	20
3088	34.98	35.85	Andesite, grey, vesicular lava, quartz-sericite alteration. [KLM 3088 at 35.60m grey sulphide = pyrite on XRD examination].	Py	25
3089	35.85	36.57	Andesite, yellow, limonitic/jarositic, weathered lava.		
3090	36.57	37.80	Andesite, creamy grey lava. chlorite-quartz alteration.	Py	tr
			[KLM 3090 at 37.41m grey sulphide = pyrite on XRD examination].	Sph	tr
3091	37.80	39.09	Andesite, pink, vesicular lava, extensive quartz-feldspar-pyrite alteration.	Py	10
3092	39.09	40.27	Andesite, pink, altered, vesicular lava, as above.	Py	10
3093	40.27	42.13	Andesite, as above. K-feldspar alteration. [KLM 3093 at 41.80 white fibrous mineral = gypsum]	Py	10
3094	42.13	42.93	Agglomerate, pink, vesicular, altered pyroclastic also with grey agglomerate with quartz-sericite alteration.	Py	15
3095	42.93	44.66	Andesite, pink, slightly vesicular, quartz-K-feldspar alteration.	Py	10
3096	44.66	45.83	Andesite, pink, altered lava as above but some silicification.	Py	15
3097	45.83	47.48	Andesite, grey pink, slightly vesicular lava as above.	Py	15
3098	47.48	48.87	Andesite, as above but intensity of hydrothermal brecciation increases.	Py	15
3099	48.87	49.50	Agglomerate, grey, pyroclastic altered to quartz-sericite in groundmass.	Py	15
3100	49.50	50.75	Andesite, pink, vesicular lava altered to quartz-K-feldspar in groundmass.	Py	15
3101	50.75	52.94	Andesite/agglomerate, grey fine grained lava and agglomerate,	Py	15
			altered, brecciated.	Sph	tr

3102	52.94	54.07	Andesite, pink altered lava, quartz-K-feldspar intergrowth, brecciated.	Py Sph	20 tr
3103	54.07	54.86	Andesite, flow banded, pinkish grey, lava quartz-sericite alteration, sharp, sheared contact to unit below.	Py	15
3104	54.86	55.93	Trachyandesite, grey, fine grained sill, quartz-sericite-calcite-pyrite alteration.	Py	10
3105	55.93	58.23	Trachyandesite, grey brown, quartz-sericite brecciation.	Py	10
3106	58.23	60.25	Trachyandesite, as above.	Py	5
3107	60.25	63.37	Trachyandesite, as above, but chlorite in matrix.	Py	3
	63.37	63.64	Contact zone, not sampled.		
3108	63.64	65.56	Andesite, grey-brown, porphyritic, lava with quartz-sericite and chlorite alteration.	Py Cpy	2 tr
3109	65.56	66.14	Andesite, brecciated, altered lava, quartz-sericite -K-feldspar hydrothermal breccia matrix.	Py Sph	8 tr
3110	66.14	67.45	Andesite, grey brown, porphyritic lava quartz-sericite alteration and chlorite after mafics.	Py Sph Cpy	2 tr tr
3111	67.45	69.42	Andesite, as above, with pink zones of hydrothermal brecciation and K-feldspar.	Py Sph Cpy	3 tr tr
3112	69.42	71.38	Andesite, as above, hydrothermal breccia zones.	Py	3
3113	71.38	72.36	Andesite, grey brown lava, quartz-sericite alteration.	Py	1
3114	72.36	73.22	Andesite, as above, increasingly hydrothermally altered to quartz-K-feldspar. [KLM 3114 at 72.75 m pyrite with galena in calcite vein].	Py Gal	5 tr
3115	73.22	75.97	Andesite, grey brown, porphyritic lava, altered to quartz-sericite-K-feldspar.	Py	3
3116	75.97	77.43	Andesite, similar to above, quartz-sericite alteration.	Py	1
3117	77.43	78.55	Andesite, as above, little veining.	Py	1
3118	78.55	80.57	Andesite, paler brown with more quartz-sericite alteration.	Py	2
3119	80.57	82.32	Andesite, darker grey with quartz-sericite-chlorite alteration. Little veining or brecciation.	Py	2

Base of hole at 82.32 m

Borehole: 4 Logged by: J S Coats

Sample No.	Depth From	To	Lithology	Mineralisation
	0.00	3.60	Overburden.	
3311	3.60	4.32	Overburden, stony, clast-rich, glacial till purple.	
3312	4.32	5.30	Overburden, as above.	
3313	5.30	6.30	Overburden, as above.	
3314	6.30	6.89	Overburden, basal till becoming yellow over lower 10 cm.	
3315	6.89	8.80	Agglomerate, weathered, argillic alteration of andesite clasts.	
3316	8.80	9.68	Andesite, fragmental core with clasts of argillised andesite.	
3317	9.68	11.72	Andesite, weathered core of argillised andesite.	
3318	11.72	13.65	Andesite, weathered, pale grey, sericitic altered lava.	
3319	13.65	14.60	Andesite, flow-banded, pale to mid grey, altered lava with argillic alteration.	
3320	14.60	16.22	Agglomerate, mid grey, quartz-sericite altered pyroclastic.	Py tr
3321	16.22	17.50	Agglomerate, grey, agglomeratic andesite and sericitic alteration.	Py 5
3322	17.50	18.56	Agglomerate, as above.	Py 5
3323	18.56	19.52	Andesite, pinkish grey, flow banded lava with Sericite-chlorite alteration.	Py 5 Cpy tr
3324	19.52	20.56	Andesite, pink, altered lava with sericite-chlorite-hematite alteration.	Py 0.5
3325	20.56	22.60	Andesite, pinkish brown, slightly flow banded lava. Chlorite-sericite-calcite alteration.	Py 0.5
3326	22.60	23.86	Andesite, dark pinkish brown, massive altered lava with chlorite-calcite-pyrite veinlets.	Py 0.5
3327	23.86	25.35	Andesite, dark pinkish brown lava as above, alteration similar with some pink feldspar.	Py 2
3328	25.35	26.40	Andesite, pink, altered lava with calcitic veins and hydrothermal sericitic brecciation veins. [KLM 3328 at 25.48-25.57 m]	Py 10
3329	26.40	27.57	Andesite, pinkish-brown, altered lava with argillised andesite and chloritic alteration.	Py 0.5
3330	27.57	29.02	Andesite, as above, some pinker sericitic and feldspathic zones	Py 2
3331	29.02	30.30	Andesite, pink, as above, but more sericite-feldspar alteration.	Py 8
3332	30.30	31.56	Andesite,pink feldspathised lava [KLM 3332 at 30.63-30.74 m]	Py 10
3333	31.56	32.90	Andesite, pink, as above but less feldspathic.	Py 5
3334	32.90	33.72	Andesite, steel-grey, less porphyritic lava with minor calcite-sericite-chlorite alteration.	Py 0.2
3335	33.72	34.45	Andesite, brown, porphyritic, massive lava with sparse chlorite and calcite hairline veinlets	Py 0.1
3336	34.45	35.80	Andesite, pinkish brown, massive, porphyritic lava becoming more sericitic and pyritic.	Py 1
3337	35.80	37.32	Trachyte, pink, slightly porphyritic intrusion Calcite-sericite-chlorite alteration. [KLM 3337 at 36.4-36.84 m].	Py 10
3338	37.32	38.65	Trachyte, as above, basal contact is irregular.	Py 10
3339	38.65	40.03	Andesite, pinkish grey, porphyritic lava with chlorite and sericite alteration.	Py 2
3340	40.03	41.39	Andesite, as above, numerous white calcite-pyrite veinlets.	Py 5
3341	41.39	42.32	Andesite, as above, but less coarse phenocrysts. Alteration variable from grey calcite to pink sericite-feldspar-pyrite.	Py 4

3342	42.32	43.80	Andesite, as above, most sulphide in white calcite veinlets associated with pink feldspathic alteration.	Py 3
3343	43.80	45.34	Andesite, grey, sparsely porphyritic, chlorite-sericite-calcite alteration.	Py 0.5
3344	45.34	46.30	Andesite, pinkish grey, porphyritic lava with chlorite after mafic phenocrysts and sericite-chlorite-feldspar alteration.	Py 4
3345	46.30	47.30	Andesite, grey, porphyritic lava with sericite-chlorite-calcite alteration. Later white calcite + baryte veinlet.	Py 3
3346	47.30	48.04	Andesite, pink, strongly altered, porphyritic lava with sericite-calcite alteration then K-feldspathic [KLM 3346A & B XRD confirms chalcopyrite].	Py 15 Cpy tr
3347	48.04	49.42	Andesite, grey, porphyritic lava, weakly flow foliated. Chlorite-calcite-hematite replace mafics.	Py 1
3348	49.42	50.05	Andesite, brown, altered porphyritic lava, calcite-chlorite-pyrite veinlets. Thicker 1 cm veins carry late pink calcite-baryte [KLM 3348 at 49.70-49.80 m].	Py 3
3349	50.05	50.95	Andesite, massive brown porphyritic lava with chlorite-sericite alteration and grey calcite cemented hydrothermal brecciation [KLM 3349 at 50.30-50.40 m].	Py 0.1 Py 15
3350	50.95	52.20	Andesite, as above, chlorite-calcite-sericite alteration.	Py 0.1
3351	52.20	53.18	Andesite, massive, pinkish brown, porphyritic lava, weak chlorite-sericite-calcite alteration.	Py 0.5
3352	53.18	54.40	Andesite, as above, also with chlorite-pyrite-hematite stringers.	Py 0.2
3353	54.40	55.36	Andesite, pinkish brown, porphyritic lava, moderate chlorite-calcite-sericite alteration.	Py 0.5
3354	55.36	56.30	Andesite, as above.	Py 0.5
3355	56.30	57.50	Andesite, grey, massive, porphyritic lava moderately altered near veins of soft ?clay-calcite-pyrite [KLM 3355 57.18-57.26 m complex phyllo-silicate assemblage by XRD].	Py 0.5

Base of hole at 57.50 m

Borehole: 5 Logged by: J S Coats

Sample No.	Depth From	To	Lithology	Mineralisation	
	0.00	1.00	Overburden.		
3145	1.00	2.30	Andesite, broken and weathered. Slightly porphyritic grey andesite with clay alteration.		
3146	2.30	3.23	Andesite, light brown, porphyritic weathered with altered plagioclase, and chlorite after pyroxene.		
3147	3.23	4.35	Andesite, as above but more highly fractured. Minor clay alteration.		
3148	4.35	5.89	Andesite, as above but less broken and grey in colour, altered to clay and chlorite.		
3149	5.89	8.03	Andesite, relatively fresh, light brown porphyritic lava with phenocrysts of chlorite after pyroxene and lesser clay alteration.		
3150	8.03	9.88	Andesite, as above. Xenoliths up to 6 cm long, rare calcite veins. Clay and chlorite alteration.		
3151	9.88	11.33	Andesite, as above with some pink banding.		
3152	11.33	13.17	Andesite, as above but highly broken.		
3153	13.17	15.09	Andesite, light brown, chlorite phenocrysts after pyroxene up to 2 mm chlorite and clay alteration.		
3154	15.09	16.25	Andesite, as above but groundmass is pinker in parts (? alteration to albite). Elsewhere alteration is to clay and chlorite.		
3155	16.25	17.19	Andesite, as above but finer grained and less porphyritic. Chlorite and clay alteration.		
3156	17.19	19.49	Andesite, lighter grey-brown, with white feldspar phenocrysts (sericitised), hematite about 1-2%. Sericite and chlorite alteration.		
3157	19.49	21.46	Andesite, as above. Sericitisation is patchy in places intense, flooding out chlorite alteration. Hematite variable 0-3%, average 1%.		
3158	21.46	22.49	Andesite, as above, finer grained. Sericite alteration less intense. Hematite 1%.		
3159	22.49	25.14	Andesite, as above, becoming paler towards base. Irregular reddening fronts separate brown from pale sericite alteration. Trace hematite.		
3160	25.14	26.22	Andesite, core very shattered and iron stained below 25.4 m.		
3161	26.22	27.35	Amygdaloidal andesite, grey with calcite amygdales of 3-5 mm diameter in groundmass of chlorite-pink feldspar (albite?).		
3162	27.35	28.37	Andesite, pale brown, porphyritic with chlorite phenocrysts after pyroxene and sericite after plagioclase. Trace hematite.		
3163	28.37	29.43	Andesite, homogeneous brown with no alteration of feldspars. Moderate chlorite alteration.		
3164	29.43	31.00	Andesite, as above but more heavily veined.		
3165	31.00	32.72	Andesite, pinkish brown with spots of white sericitic plagioclase. Trace hematite and pyrite in paler zones.	Py	tr
3166	32.72	33.56	Andesite, xenolithic broken and slightly weathered on joints with Chlorite alteration. Hematite 1-2%.		
3167	33.56	35.84	Amygdaloidal andesite, grey fine grained lava with irregular 3-4 mm white calcite filled amygdales and pink feldspathic rim. Groundmass of chlorite-feldspar-hematite (1%), with trace of disseminated pyrite near quartz vein. [KLM 3167 at 34.65 m, grey sulphide in calcite vein]. Fine grained chilled base to flow.	Py	tr
3168	35.84	37.07	Andesite, light brown porphyritic. Some sericitisation of feldspar and chloritisation of pyroxene phenocrysts, set in brown groundmass with trace hematite.		

3169	37.07	38.71	Andesite, as above but lacks white feldspar alteration. Chlorite and clay alteration. Trace hematite and calcite.		
3170	38.71	40.78	Andesite, as above but groundmass finer and paler brown		
3171	40.78	42.70	Andesite, normal brown. Some chlorite altered to pale greenish clay with chlorite rim. Minor hematite.		
3172	42.70	44.32	Andesite, as above with 43.70 m progressive sericite alteration of phenocrysts and groundmass. Quartz-calcite-baryte vein at 44.00 m, with marginal disseminated pyrite	Py	tr
3173	44.32	46.91	Andesite, progressive reduction in groundmass and phenocryst alteration, although feldspars still sericitised at base of section.		
3174	46.91	48.21	Andesite, brown as above with incipient white sericite alteration. Moderate chlorite alteration.		
3175	48.21	51.46	Andesite, as above but most feldspars are pink. Disseminated calcite. Chlorite and clay alteration.		

Base of hole at 51.46 m

Borehole: 6 Logged by: J S Coats

Sample No.	Depth From	Depth To	Lithology	Mineralisation
	0.00	3.18	Overburden, cobbles of purple porphyritic andesite	
3120	3.18	4.48	Feldspar porphyry, weathered with black staining on fractures.	
3121	4.48	6.00	Feldspar porphyry, less broken than above. Xenoliths and flow-banding still visible, weathered.	
3122	6.00	7.45	Feldspar porphyry, loose rubble, weathered.	
3123	7.45	8.62	Feldspar porphyry, less broken, primary fine banding visible.	
3124	8.62	10.66	Feldspar porphyry, broken and limonitic, weathered.	
3125	10.66	12.11	Feldspar porphyry, less broken, primary textures visible.	
3126	12.11	14.98	Feldspar porphyry, xenolithic, phenocrysts of plagioclase. in quartz-K-feldspar groundmass. Minor sericite alteration.	
3127	14.98	17.75	Feldspar porphyry, more fractured than above, flow banded, sericitised, weathered calcite veins.	Py tr
3128	17.75	19.68	Feldspar porphyry, partly weathered, xenolithic, sericitised plagioclase phenocrysts, in quartz-K feldspar-plagioclase groundmass.	Py tr
3129	19.68	22.40	Feldspar porphyry, slightly weathered. Autobrecciated and flowbanded. Minor sericite alteration with trace hematite.	
3130	22.40	25.15	Feldspar porphyry, as above. A few sections contain fresh disseminated pyrite (2%). Minor sericite alteration. [KLM 3130 red mineral at 25.03 m].	Py 0.5
3131	25.15	26.89	Feldspar porphyry, homogeneous and less xenolithic, clay-altered plagioclase phenocrysts in sericitic groundmass.	
3132	26.89	28.12	Feldspar porphyry, grey-pink feldspar phenocrysts in pink K-feldspar-plagioclase-quartz-hematite groundmass. K-feldspar alteration marginal to calcite-pyrite veins, elsewhere minor sericite alteration.	Py tr
3133	28.12	30.35	Feldspar porphyry, as above. Some xenoliths are K-feldspar altered. Moderate sericitisation and (1-2%) hematite in groundmass.	
3134	30.35	32.35	Feldspar porphyry, grey-pink, as above, K-feldspar and sericite alteration. Hematite 3% in groundmass.	
3135	32.35	34.60	Feldspar-porphyry, uniformly pink, only one xenolith. Moderate K-feldspar and sericite altered pink groundmass. 2% hematite.	
3136	34.60	36.22	Feldspar-porphyry, xenolithic down to 35.35 m. Reddened K-feldspathised xenoliths up to 4 cm in size. Hint of flow-banding. Sericite and K-feldspar alteration. Hematite 2%	
3137	36.22	38.28	Feldspar-porphyry, similar to above but less xenolithic. Moderate K-feldspar and sericite alteration. Hematite 2%.	
3138	38.28	39.48	Feldspar-porphyry, greyish pink, finer grained. Sericite alteration with rare reddened xenoliths.	
3139	39.48	41.12	Feldspar-porphyry, "smoked salmon" pink uniform colour. Growth of new K-feldspar in groundmass of K-feldspar-sericite-quartz, with 1.5% disseminated pyrite adjacent to veins. Calcite vein with clay margins at shallow angle to core axis contains fine-grained pyrite and chalcopyrite disseminated through clays.	Py 1 Cpy tr
3140	41.12	42.88	Feldspar-porphyry, greyer in colour becoming pink. Moderate K-feldspar and sericite alteration. Hematite is disseminated throughout groundmass.	Py tr
3141	42.88	44.94	Feldspar-porphyry, pink colour as 3139. Moderate new K-feldspar in groundmass and relict sericite after plagioclase plus trace hematite. Pyrite present only near calcite-clay veins.	Py tr
3142	44.94	46.78	Feldspar-porphyry, as above but no hematite. K-feldspar	Py tr

			and minor sericite alteration.		
3143	46.78	47.81	Feldspar-porphyry, as above with clay-calcite-pyrite vein containing pyrite-rich disrupted fragments. Adjacent marginal sericite-clay alteration.	Py	2
3144	47.81	50.35	Feldspar-porphyry, pale brown. Dominantly sericitised plagioclase phenocrysts in pale brown K-feldspar-quartz-plagioclase-hematite (2%) groundmass. Slight K-feldspar alteration near base. Minor calcite veining.		

Base of hole at 50.35 m

Borehole: 7 Logged by: J S Coats

Sample No.	Depth From	To	Lithology	Mineralisation
	0.00	5.60	Overburden, loose cobbles.	
3176	5.60	7.09	Overburden, glacial till. Clasts of andesite in chocolate brown clay matrix.	
3177	7.09	10.21	Overburden, as above.	
	10.21	11.71	Core lost.	
3178	11.71	13.17	Agglomerate, weathered and iron stained.	
3179	13.17	16.05	Agglomerate, clasts of porphyritic andesite set in grey quartz-sericite-calcite-pyrite groundmass. Some feldspathic alteration.	Py 10
3180	16.05	17.73	Agglomerate, as above but more weathered with limonite.	Py 10
3181	17.73	19.50	Agglomerate, as above but fresher. Volcanic clasts altered to intense quartz-sericite-calcite-pyrite intergrowth.	Py 10
3182	19.50	21.93	Agglomerate, as above. Clast at 20.04 m is altered, with alteration terminating at clast boundary [KLM 3182].	Py 10
3183	21.93	23.90	Agglomerate, as above. Intense quartz-sericite alteration. Thick calcite vein parallel to core axis from 23.00 to 23.30m contains coarse pyrite and molybdenite.	Py 10 MoS_2tr Cpy tr
3184	23.90	26.05	Agglomerate, as above, dark to pale grey with intense quartz-sericite alteration. Clasts preferentially enriched in pyrite, with variable alteration to quartz , sericite or pink alkali feldspar.	Py 10
3185	26.05	26.99	Agglomerate, two large clasts with minor matrix. Pale grey porphyritic lava with quartz-sericite alteration and pyrite.	Py 8
3186	26.99	28.48	Agglomerate, as above, but clasts have a pink feldpathic rim set in grey quartz-sericite groundmass.	Py 8
3187	28.48	30.28	Agglomerate, as above but less pink. Intense quartz-sericite alteration, less feldspathic.	Py 10
3188	30.28	31.41	Agglomerate, pink clasts in grey matrix , with intense quartz-sericite groundmass containing abundant calcite and pyrite. Some clasts have 2-3 mm pink feldspathised rims.	Py 10
3189	31.41	32.94	Agglomerate, as above, lacking pink feldspathic rims but with intense quartz-sericite alteration.	Py 10
3190	32.94	34.45	Agglomerate, as above with some hydrothermal brecciation. Strong quartz-sericite alteration slightly richer in pyrite.	Py 12
3191	34.45	35.95	Agglomerate, as above but more intense pink/brown feldspar alteration of clasts and rims.	Py 12
3192	35.95	37.48	Agglomerate, clasts increasingly abundant towards base. Strong quartz-sericite and moderate feldspar alteration.	Py 12
3193	37.48	39.29	Agglomerate, as above but distinctive pink alkali feldspar rim alteration of clasts. Groundmass is quartz with pyrite (20%) with clay-baryte in late vugs and few fracture surfaces.	Py 12
3194	39.29	40.64	Agglomerate, brecciated and hydrothermally altered. Strong quartz-sericite alteration. Pyrite in matrix (20%) and clasts (5%).	Py 8
3195	40.64	41.61	Andesite, top of flow indistinct hydrothermal brecciation and quartz-sericite alteration. Red alkali feldspar alteration at top, proximal to quartz-pyrite vein.	Py 5
3196	41.61	42.78	Andesite, slightly porphyritic, homogeneous, with subtle alteration variations of chlorite and quartz-sericite.	Py 2
3197	42.78	44.71	Andesite, as above but more grey in colour. Chlorite and irregular, patchy quartz-sericite alteration away from a network of quartz veins.	Py 2
3198	44.71	46.61	Andesite, slightly less altered than above. Chlorite alteration greater than quartz-sericite. Increase in hematite over pyrite	Py 1

			towards base.	
3199	46.61	48.67	Andesite, variably altered with paler quartz-sericite rich zones and chloritic with hematite and little pyrite.	Py 1
3200	48.67	50.16	Andesite, mid grey, slightly porphyritic lava with white plagioclase phenocrysts and spots of chlorite set in a groundmass of pale grey quartz-sericite-?albite-calcite.	Py 2
3201	50.16	52.31	Trachyandesite, pale brown, porphyritic lava with chlorite spots after mafics. Feldspars altered to quartz-sericite-chlorite-pyrite-calcite.	Py 2
3202	52.31	54.44	Trachyandesite, as above, more altered to quartz-sericite. Pools of calcite with ?biotite + pyrite + chalcopyrite + MoS_2. Base chilled at low angle to core axis but tectonised [KLM 3202 53.00 m].	Py 2 Cpy tr MoS_2 tr
3203	54.44	56.44	Andesite, pale grey, porphyritic lava, agglomeratic top to flow with reddened patches and grey hydrothermal breccia with quartz-sericite. Network of interlocking pyrite-calcite-quartz veins and quartz-pyrite (50%).	Py 10
3204	56.44	57.41	Andesite (?basalt), dark grey, fine grained, chilled facies of above flow. Rare chlorite phenocrysts after mafics.	Py 0.5
3205	57.41	59.11	Andesite, mid grey, slightly porphyritic lava gradational to above but more altered to chlorite-quartz.	Py tr
3206	59.11	59.62	Trachyandesite, thin pink intrusion with chilled grey margins. Phenocrysts and matrix altered to K-feldspar and quartz.	Py 10
3207	59.62	61.46	Andesite, mid grey unit similar to KLD 3205 with sericite-quartz alteration and veins.	Py 1
3208	61.46	63.28	Andesite, pink-brown colour, slightly porphyritic lava with white sericitic feldspars and rarer chlorite phenocrysts. Coarse red K-feldspar zone at 62.38 m adjacent to 2.5 cm thick sparry calcite vein.	Py 2
3209	63.28	64.34	Andesite similar to KLD 3207, grey coloured lava. Groundmass chlorite-quartz-hematite-calcite-sericite. No pyrite except near veins where more sericite alteration.	Py tr
3210	64.34	64.68	Dacite, grey-brown, intrusive dyke with grey chilled contacts. Small feldspar and chlorite phenocrysts. Pyrite in chlorite pseudomorphs.	Py 0.5
3211	64.68	66.42	Andesite, mid-grey, slightly porphyritic lava as 3209. Common calcite-hematite-pyrite veins to 1 cm thickness near top. Chlorite-sericite alteration.	Py 0.5
3212	66.42	67.14	Andesite, browner than above unit with reddish feldspar alteration, and lack of chlorite except in phenocrysts. Grey quartz-sericite groundmass.	Py 2
3213	67.14	68.63	Andesite, dark grey, slightly porphyritic lava with chlorite after pyroxene in fine grained chloritic groundmass.	Py 0.5
3214	68.63	70.00	Andesite, as above. Plagioclase still fresh and core is slightly magnetic. Calcite-chlorite-pyrite veins, occasionally with hematite.	Py tr
3214A	70.00	71.35	Andesite, agglomeratic top to a new flow unit. Top of unit reddened, very feldspathic altered and abundant pyrite to 40% passing downwards into grey patchy rock with quartz-sericite alteration with cavities lined with calcite and pyrite. Trace dark grey sulphide [KLM 3214 at 71.08 m].	Py 8
3215	71.35	72.80	Agglomerate, pink and grey, indistinct, K-feldspar altered clasts in quartz-sericite-pyrite groundmass (10-15%). Some clasts vuggy 10% holes. Porphyroblastic chlorite spots to 5 mm which overgrow clast boundaries begin at 71.90 m.	Py 15
3216	72.80	73.64	Agglomerate, as above but grey quartz-sericite alteration dominant and few porphyroblasts of chlorite. Vuggy core 10% holes.	Py 10
3217	73.64	74.40	Andesite, pale brown to grey, porphyritic lava with sericitic feldspar phenocrysts. Groundmass quartz-sericite near top, then chlorite-calcite-hematite dominant.	Py 5

3218	74.40	75.15	Agglomerate, pale brown, altered pyroclastic with clasts in grey matrix. Feldspar altered to K-feldspar in paler quartz-sericite groundmass. Spotty porphyro-blastic chlorite.	Py 10 MoS_2tr
3219	75.15	76.62	Andesite, interbedded lava and agglomerate. Vesicular grey lava and fragmental agglomerate. Chlorite porphyroblasts and quartz-sericite alteration. Vesicules filled with calcite-hematite-MoS_2.	Py Cpy tr
3220	76.62	78.43	Agglomerate, grey-brown pyroclastic with 3-4 mm chlorite porphyroblasts overprinting altered 1-10 cm size clasts of porphyritic lava with amygdaloidal calcite [KLM 3220 at 77.12 m].	Py 5
3221	78.43	79.90	Agglomerate, as above but larger (to 40 cm) clasts. Matrix has large chlorite porphyroblasts and quartz-sericite alteration.	Py 10 MoS_2tr
3222	79.90	81.54	Agglomerate, as above. One melanocratic clasts with less pyrite and feldspathised pink rim. Matrix comminuted lithic frags and minor crystals	Py 15
3223	81.54	83.83	Agglomerate, as above, brown clasts predominate over grey groundmass. Irregular chlorite porphyroblasts suggest pyroxene in outline and are concentrated in some clasts.	Py 15
3224	83.83	85.28	Andesite, massive, brown grey, slightly porphyritic lava. Quartz-sericite-chlorite-calcite alteration. Spotted by chlorite porphyroblasts. Rare calcite-pyrite-baryte veins	Py 2
3225	85.28	87.27	Andesite, as above but slightly vesicular with plagioclase and calcite filled vesicles. Chlorite porphyroblasts rare. Calcite vein with pyrite, baryte and trace of chalcopyrite. Increase in quartz-pyrite hydrothermal alteration at lower boundary.	Py 1 Cpy tr
3226	87.27	88.91	Andesite, as above, irregular calcite veining.	Py 3

Base of hole at 88.91 m